EFFECTS OF INDUCED MYOPIA AND HYPEROPIA ON DOPAMINERGIC AND SEROTONERGIC AMACRINE NEURONS IN CHICK RETINA

by

Sharon Tsau-Yuen Wong

A thesis
presented to the University of Waterloo
in fulfilment of the
thesis requirement for the degree of
Doctor of Philosophy
in
Vision Science and Biology

Waterloo, Ontario, Canada, 1998

The University of Waterloo requires the signature of all persons using or photocopying this thesis. Please sign below, and give address and date.

ABSTRACT

EFFECTS OF INDUCED MYOPIA AND HYPEROPIA ON DOPAMINERGIC AND SEROTONERGIC AMACRINE NEURONS IN CHICK RETINA

The ametropias, myopia and hyperopia, are refractive errors which can be experimentally induced in young animals by manipulating their early visual experience. Myopia and hyperopia result from abnormal ocular growth mechanisms, and the control signals are believed to originate from within the eye itself.

In this study, unilateral application of convex lenses, concave lenses, and translucent goggles over the eyes of newly-hatched chicks respectively produced defocus-induced hyperopia (DIH), defocus-induced myopia (DIM), and form deprivation myopia (FDM). Treatment rapidly produced refractive errors and changes in eye size within 6 to 10 days. The effects of induced ametropias on retinal serotonergic and dopaminergic amacrine neurons were assessed on a quantitative and qualitative basis. Cell distributions and morphology in immunohistochemically labelled wholemount retinae were examined using confocal laser scanning microscopy. Neurochemical levels were measured using high pressure liquid chromatography (HPLC).

Induced ametropias produced changes in: (1) serotonergic amacrine cell distribution, (2) dopaminergic amacrine cell morphology, and (3) levels of dopamine and 3,4-dihydroxyphenylacetic acid (DOPAC). With respect to serotonergic amacrine cell numbers, there was evidence of redistribution within the retina. In the central retina, FDM produced significant decreases in serotonergic cell numbers, while DIH provoked significant localized increases. These

changes in serotonergic cell number appeared to be correlated with the magnitude of the induced refractive error. There were no changes in dopaminergic amacrine cell numbers. Dendritic morphology was assessed by recording optical sections across individual dopaminergic amacrine cells, then stacking these confocal images into composite overlays. FDM provoked increases in dendritic field spreads and dendritic branching in treated dopaminergic amacrines relative to control. Conversely, DIH produced consistent decreases in field size, staining intensity, and dendritic branching. HPLC analysis showed that both FDM and DIH caused significant decreases in retinal dopamine and DOPAC levels in treated eyes relative to controls. These changes were mainly localized within the central retina. There were no conclusive changes in the levels of serotonin and its metabolite 5-hydroxyindoleacetic acid, although slight decreases were noted in FDM, while DIH caused slight increases.

There is a high degree of neural plasticity within the young eye. Results from this study suggest that dopamine and serotonin may contribute, in a localized manner, to the ocular growth mechanisms which regulate the development of refractive errors.

ACKNOWLEDGEMENTS

This work was made possible by the combined efforts of many people to whom I am grateful. I wish to extend sincere thanks to my supervisor, Dr. Jacob Sivak, for the opportunity to work in his laboratory at the School of Optometry, University of Waterloo. I appreciate his support, sense of humour, and one-word motto which serves as a great explanation for everything: "serendipity!" I would like to thank my committee members, Dr. Murchison Callender and Dr. Niels Bols, for their encouragement and advice during my studies and research endeavours. I also thank Dr. James Frank and Dr. Howard Howland for reviewing this thesis, and for acting as internal and external examiners respectively at my thesis defence.

Thank you to Dr. Alexander Ball at McMaster University for generously arranging my use of the confocal microscope facilities, and also for providing guidance in many aspects of this research. Ernest Spitzer, Dr. Larry Arsenault, and Marie of the confocal microscopy unit at McMaster University helped with the use and scheduling of the equipment. Dr. Candace Gibson at The University of Western Ontario deserves special recognition for her help and advice with the HPLC portion of this study. I appreciate the assistance of Amy Bakelaar during the preliminary stages of this research. Chris Mathers and Vivian Choh provided help with the computer hardware and software. Derivations of the ellipsoid formulae were obtained from Dr. David Matthews in the Department of Statistics and Actuarial Science, University of Waterloo, and from Ms. Denise King at the School of Optometry. Nancy Gibson provided expert animal care throughout the duration of my experiments. I appreciate the friendship and support of all past and present graduate students, faculty, and staff at the School of Optometry.

This research was funded by grants from the Natural Sciences and Engineering Research Council of Canada (NSERC) awarded to Dr. Jacob Sivak, and by various other financial sources including the Ontario Graduate Scholarship program, and the Science Incentive Fund at the University of Waterloo.

For my loving family

TABLE OF CONTENTS

LIST OF ABBREVIATIONS

ACh	acetylcholine
ANOVA	analysis of variance
°C	degrees in Celsius
CD-R	recordable compact disc
CNS	central nervous system
$CO_{2(g)}$	gaseous carbon dioxide
$CO_{2(s)}$	solid carbon dioxide (dry ice)
COMT	catechol-O-methyltransferase
D	dioptre
DA	dopamine
DHBA	dihydroxybenzylamine
DIH	defocus-induced hyperopia
DIM	defocus-induced myopia
DOPA	dihydroxyphenylalanine
DOPAC	3,4-dihydroxyphenylacetic acid
EDTA	ethylenediamine-tetraacetic acid
FDM	form deprivation myopia
GABA	gamma-aminobutyric acid
g	grams
g	gravity
5-HIAA	5-hydroxyindoleacetic acid
HPLC-EC	high pressure liquid chromatography, coupled with electrochemical detection
5-HT	5-hydroxytryptamine (synonym=serotonin)
5-HTP	5-hydroxytryptophan
HVA	homovanillic acid
IBM-PC	International Business Machine™, Personal Computer
INL	inner nuclear layer (of the retina)
IPL	inner plexiform layer (of the retina)
L	litre
LSM	laser scanning monitor
M	molar
MAO	monoamine oxidase
MHz	megahertz
µg	microgram
µL	microlitre
µm	micrometre
μm^2	square-micrometre
mg	milligram
mL	millilitre
mm	millimetre
mm^2	square-millimetre

LIST OF ABBREVIATIONS, CONTINUED

mM	millimolar
N	normal
NAT	N-acetyltransferase
NIH	National Institute of Health (USA)
nm	nanometre
nM	nanomolar
NMDA	N-methyl-D-aspartate
6-OHDA	6-hydroxydopamine
OPL	outer plexiform layer
pg	picogram
PIC	picture file format (Zeiss confocal image)
pmol	picomolar
QA	quisqualic acid
RPE	retinal pigment epithelium
SEM	standard error of the mean
TIFF	tagged image file format
TTX	tetrodotoxin
V	volt
VIP	vasoactive intestinal polypeptide

LIST OF TABLES

LIST OF FIGURES

1.0 INTRODUCTION AND LITERATURE REVIEW

The purpose of this thesis is to study how specific neurons in the chick retina may participate in ocular growth mechanisms associated with refractive error development of the eye. The major contribution of this dissertation is the novel use of confocal microscopy to examine how myopia and hyperopia affect particular retinal neurons: the dopaminergic and serotonergic amacrine cells. This introduction presents a review of the myopia literature, an overview of retinal anatomy, describes the basic principles of confocal microscopy, and provides background information on the roles of dopamine and serotonin in the development of refractive errors.

1.1 Myopia, hyperopia, and emmetropia

Myopia and hyperopia are visual abnormalities, or ametropias, which arise from an imbalance between the optical components and size of the eye. Myopia occurs when incoming rays of light from a viewed object focus at a point in front of the retina, despite lens accommodation being at rest. This results in better vision for near objects rather than distant objects, and explains why myopic eyes are described as "near-sighted" eyes. On the other hand, hyperopia occurs when images focus at a theoretical point behind the retina, and compensatory lens accommodation is insufficient. Thus hyperopic or "far-sighted" eyes see distant objects more clearly than nearby ones. In both myopia and hyperopia, images are out-of-focus at the plane of the retina.

In emmetropic eyes with perfect vision, there is an ideal relationship between eye size and ocular refractive power. The precise focus of images at the retinal plane results from a delicate balance between the axial length of the eye and the focal powers of the lens and cornea. During

the course of normal ocular development, eye size and optical properties must be continuously matched on a rapidly changing basis. The slightest disturbance to this growth mechanism will result in ametropia. For example, as little as 0.3 mm discrepancy between focal length and eye size in humans will result in almost one dioptre (D) of ametropia (Hirsch and Weymouth 1991). Hence myopia may result from an eye that is abnormally large, or from excessive lens and/or corneal power. Conversely, hyperopia arises from an eye that is too short relative to the focal power of the lens and/or cornea. The particular signals which drive ocular growth have been the subject of intense study during the past few years, in the hope of eventually controlling abnormal eye growth that produces ametropia.

1.2 History of ametropias

The earliest recorded cases of myopia date back to the tenth century when Greek scientists incorrectly believed myopia originated from an eye whose "spiritual emanations" were too weak to perceive a distant object. This misconception was cleared up by the following century when Arabian scientists suggested that vision results from light entering the eye, rather than vice versa (Hirsch and Weymouth 1991). Scientific progress in the understanding of refractive errors came slowly over the next several centuries. Notable breakthroughs were Kepler's studies on refractive principles (1611), Helmholtz's invention of the ophthalmoscope (1851), and the subsequent development of retinoscopy (Cuignet 1873, as cited in Bennett and Rabbetts 1984). The ophthalmoscope permits examination of internal ocular morphology, while the retinoscope objectively measures ocular refractive state. Shortly thereafter, Arlt (1856) provided conclusive anatomical proof that myopia results from abnormal axial elongation of the eye.

1.3 Theories of ametropia

1.3.1 Use-abuse theory (Environmental factors)

In 1866, Herman Cohn proposed that excessive amounts of near-work, such as reading, induced myopia. Based on a study of 10,000 German schoolchildren, Cohn noted increasing amounts of myopia as the children progressed to higher grade levels. Cohn suggested that the observed myopia resulted from eyestrain due to inadequate illumination and the poor contrast of words printed in textbooks. Whether the causal link between reading and myopia was justified or not, Cohn's study initiated several positive reforms such as improved classroom lighting and better contrast of printed reading material with increased letter font sizes (Hirsch and Weymouth 1991).

Cohn's Use-Abuse hypothesis prompted a succession of other theories which attempted to correlate environmental effects and the genesis of refractive errors. For instance, when the head was inclined in the reading position, it was believed that gravity and the pull of the extraocular muscles during convergence might elongate the eye globe (Von Graefe 1857, Donders 1864). All theories based on Cohn's work followed a common theme: Environmental factors play the most important role in the development of refractive errors.

1.3.2 Biological or Statistical theory (Genetic factors)

Cohn's Use-Abuse theory did not encounter any serious opposition for nearly 50 years, until Steiger (1913) proposed that myopia may arise from variations of different ocular components such as lens thickness, corneal curvature, anterior chamber depth, and axial length. Steiger's theory suggested that refractive errors resulted from the combination of ocular elements, with the particular properties of each component being genetically determined. Steiger applied biometric

and statistical principles to analyze the population distributions of various ocular components, in order to correlate how much each element contributed to the final refractive state. However, practical application of Steiger's theory proved to be very difficult at the time, since technology was not available to accurately measure any deep internal components of the living eye. Nevertheless, Steiger was able to make detailed measurements of corneal curvature and found that these followed a normal distribution curve (Grosvenor and Flom 1991). From these results, Steiger speculated that other ocular components also exhibited normal distributions, which suggested they were under genetic control (Young and Leary 1991). Subsequent studies have indeed shown that many ocular components, with the exception of axial length, follow a normal distribution curve (Duke-Elder and Abrams 1970, Borish 1970). Overall, Steiger's approach was in keeping with the time, when statistical methodology was becoming widespread in all areas of scientific research.

1.4 Modern evidence regarding refractive error development

Results from recent studies support both environmental and genetic viewpoints. Thus it appears that a modern comprehensive theory regarding the etiology of refractive errors would best comprise both hereditary and environmental factors, although the relationship between the two elements remains unclear. Experimentally, it is difficult to isolate a single factor in order to categorize it as being purely environmental or purely genetic. It is possible that environmental factors may uncover a genetic predisposition in susceptible individuals.

1.5 Experimental studies of refractive error

1.5.1 Animal models

In 1975, Hubel and Wiesel made an unexpected discovery that myopia developed in monkeys as a result of lid-suture. Lid-suture myopia was subsequently confirmed in other species including tree shrews (Sherman, Norton, Casagrande 1977) and chickens (Wallman, Turkel, Trachtman 1978). Corneal opacification by latex particle injection also produced myopia in monkeys (Wiesel and Raviola 1979). This latter experiment addressed the concern that lid-suture might cause corneal flattening, and that this physical deformation produced myopia instead. Myopia can also be induced by applying plastic occluders over the eyes of experimental animals (Wallman et al. 1978, Irving 1991 and 1992). "Form deprivation myopia" was used to describe the myopia that occurs when an animal is prevented from seeing clear outlines of objects in its environment.

Myopia has also been induced in experimental animals by various other alterations to their visual and ocular environment. Studies include rearing cats in small cages to stimulate their near vision (Rose et al. 1974, Belkin et al. 1977), and varying the illumination levels to which chickens and monkeys are exposed (Lauber et al. 1961, Lauber and Kinnear 1979, Raviola and Wiesel 1978). In monkeys, lid-suture myopia does not occur in constant darkness, but progresses after exposure to light (Raviola and Wiesel 1978). In chickens, both constant dark and constant light causes severe corneal flattening which results in hyperopia despite overall eye enlargement (Dark: Yinon and Koslowe 1986, Gottlieb et al. 1987; Light: Li et al. 1995, Stone et al. 1995).

1.5.2 The chicken as an animal model

The domestic chicken (*Gallus domesticus*) is the most frequently chosen animal model in myopia research for several reasons. Chickens are diurnal, precocial birds which are readily available, grow rapidly, and inexpensive to maintain. These animals are self-sufficient with excellent vision almost immediately after hatching. Hence they can be exposed to experimental conditions during the earliest period of post-hatching development. In general, birds require good vision in order to properly forage for food and water. Chickens have large eyes with excellent resolving power and spatial acuity (Over and Moore 1981). In contrast, other animal species are less suitable for myopia research. For instance, nocturnal animals like cats and rabbits rely more on their senses of smell and hearing, rather than vision. The widespread use of primates is hindered by extremely high maintenance costs and long time periods required for growth. Related to primates, tree shrews (*Tupaia belangeri*) provide an alternative animal model, but high costs and import regulations also restrict their use in many laboratories.

1.5.3 Defocus-induced ametropias

Under normal light/dark conditions, concave and convex defocusing lenses will respectively induce myopia and hyperopia in chickens by changing the focal point within the eye (Schaeffel, Glasser, and Howland 1988, Irving et al. 1991). Eyes exposed to concave defocus will grow excessively such that they are myopic upon removal of the negative lens. Conversely, eyes treated with a positive convex lenses generally stop growing and become hyperopic. The treated eye accurately compensates for the imposed blur 80-90% of the time, which suggests there is a detector which can discern the sign and magnitude of the defocus (Bock and Widdows 1990).

Another possibility is that the eye responds to correctable versus non-correctable blur, with the former signaling myopia and the latter indicating hyperopia. It remains unclear exactly how the eye is able to accomplish this task, although it has been suggested that retinal amacrine cells are likely candidates (Bock and Widdows 1990). The properties of amacrine cells will be discussed in further detail later in this thesis.

1.5.4 Emmetropization

At birth or hatching, the eyes of many neonate animals display moderate to high refractive errors which eventually disappear after a period of normal ocular development (Walls 1942). This process of eye growth toward a zero refractive state is called emmetropization. Experiments in which recovery from induced ametropia, for instance by removing an occluder after a period of visual deprivation, have been cited as models for the study of emmetropization (Wallman and Adams 1987, Troilo and Wallman 1991). In fact, form deprivation myopia can be prevented by just a few minutes of daily exposure to normal vision (Gottlieb et al. 1992, Napper et al. 1995 and 1997). This evident bi-directionality in eye growth and refractive error development further highlights the plasticity of the ocular system.

1.5.5 Local control of eye growth

Much effort has been directed toward identifying the signal or signals which control eye development, since it may then be possible to control the abnormal growth which characterizes myopia and hyperopia. Several studies indicate that the growth mechanism originates from within the eye itself. Troilo et al. (1987), and later Wildsoet and Pettigrew (1988a), showed that myopia

still occurs in visually-deprived eyes of chickens despite optic nerve section, indicating that a connection with the brain is not necessary. However, when nerve-sectioned eyes are allowed to recover by exposure to normal vision, their refractive errors would reverse but overshoot emmetropia. This suggests that the brain may be involved in the fine-tuning of refractive development.

Localized eye growth is also evident in partial occlusion experiments, where enlargement is confined to the deprived region of the eye (Wallman et al. 1987). It is believed that accommodation plays a minimal role in refractive error development, according to lesioning experiments which purposely damage the Edinger-Westphal nucleus (Troilo et al. 1987, Schaeffel et al. 1990). Furthermore, when tetrodotoxin (TTX) is used to block ganglion cell activity in the optic nerve, the development of form-deprivation myopia is not significantly affected (tree shrews: Norton 1990, chicks: McBrien et al. 1995). Whatever the exact origin of the abnormal growth signals in myopia and hyperopia, there are far-reaching effects on many other aspects of ocular development including the sclera (Norton and Rada 1995), choroid (Wallman et al. 1995, Wildsoet and Wallman 1995), and even orbital bone (Wilson et al. 1997). The choroid itself appears to adjust the plane of retinal focus by thickening in response to myopic defocus, and thinning for hyperopic defocus. Upon recovery, the choroid rapidly compensates by reversing the direction of its original growth (Wallman et al. 1995). It remains unclear what signals are regulating these choroidal changes, although it may be possible that they originate from the retina.

A review of the myopia literature shows it is likely that various cell types in the retina may play a role in mediating eye growth. Most of the supporting evidence comes from neurochemical studies and observations on how the eye responds to various lighting conditions. Before

proceeding, a general overview of retinal organization will first be presented.

1.6 Retina

The retina is a thin neural and epithelial sheet which lines the inner back surface of the eye. Structurally, the retinal layer is separated from the outer protective sclera of the eye by the highly vascular choroid layer. Functionally, the retina serves as the first stage of the visual pathway to receive and process incoming visual information from the environment (for reviews: Stell 1972, Dowling 1987).

In many vertebrates, the retina develops embryologically as an outpouching of the forebrain. This hollow optic vesicle subsequently invaginates upon itself during formation of the double-walled optic cup. In the mature organism, the resulting "inverted" retina comprises three highly organized layers of nerve cell bodies separated from each other by plexiform (synaptic) layers (Figure 1). In brief summary, the retina consists of (from outer to innermost layer): a photoreceptor layer (rods and cones), an outer plexiform layer (OPL), an inner nuclear layer (INL) (horizontal, bipolar, amacrine, and interplexiform cells), an inner plexiform layer (IPL), and finally a ganglion cell layer. Ganglion cell axons leave the eye and connect with the brain as the optic nerve. Numerous glial cells are found throughout the thickness of the neural retina. Glial cells do not process neural information, but have diverse other functions such as providing structure, nutrients, and removing metabolic waste from surrounding neurons. The retinal pigment epithelium (RPE) is found at the outer margin of the photoreceptors.

The chicken retina is approximately 200 microns thick, tapering to 150 microns as it nears the ora serrata (Walls 1942). Unlike mammalian retinae, the avian retina itself is avascular and

Figure 1: Schematic representation of the vertebrate retina. The retina comprises three layers of nerve cell bodies (photoreceptors, inner nuclear layer, and ganglions) separated by synaptic regions (inner and outer plexiform layers). At the scleral side, the photoreceptor layer contains rods (R) and cones (C). Retinal pigment epithelium cells provide nourishment, metabolic functions, and prevent incoming light from scattering outside of the eye. The inner nuclear layer contains bipolar cells (B), amacrine cells (A), and horizontal cells (H). At the vitreous side, ganglion cell axons combine to form the optic nerve. Muller cells (M) are glial support neurons which provide structural and metabolic support throughout the retina. (Drawing adapted from Adler and Farber 1986).

SCLERA

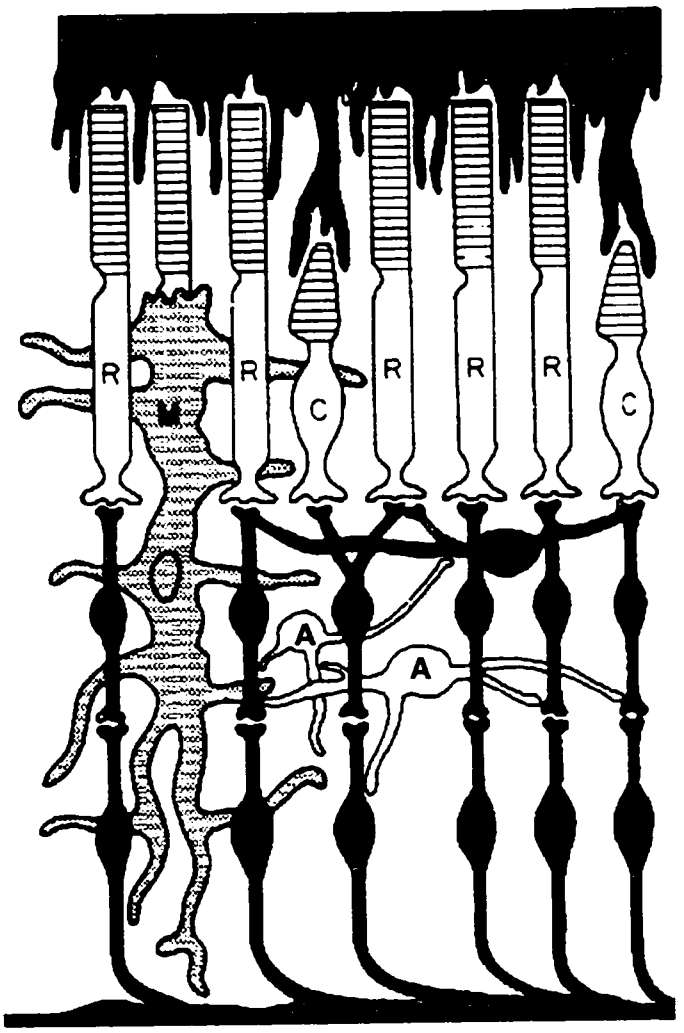

RETINAL PIGMENT EPITHELIUM

PHOTORECEPTORS

OUTER PLEXIFORM

INNER NUCLEAR LAYER

INNER PLEXIFORM

GANGLION CELLS

→ TO OPTIC NERVE

VITREOUS

derives most of its nourishment from the underlying choroid layer. The pecten is a large ridged structure, unique to the avian eye, that projects from the inferior quadrant of the eye into the vitreous cavity. Although its exact function remains unclear, it is believed that the pecten may provide oxygen and nutrients to the retina (Koch 1973) and act as an intraocular shade (King and McLelland 1975). The chicken eye is technically afoviate (Walls 1942), possibly bred out during domestication, although a shallow "round central area" does exist near the optic axis and appears to be the area of highest visual acuity (King and McLelland 1975). (For reviews of vision and optical development in the young chick, the reader is referred to May and Thanos 1992, and Irving et al. 1996).

1.7 Neurochemical studies in myopia research

Pharmacological and biochemical studies provide a different approach for understanding the neural connections, cell types, and receptors which may control myopia and hyperopia. Early studies examined how general neurotoxins affect retinal activity and form deprivation myopia.

Kainic acid is a toxic glutamate analog which destroys retinal cell populations in a dose-dependent manner (Ingham and Morgan 1983, Wildsoet and Pettigrew 1988b). Low doses (6 nM) of kainic acid selectively destroy amacrine cells, while higher doses (200 nM) also destroy bipolars and horizontal cells. The kainic acid treatments causes enlargement in both anterior and posterior segments of the eye, but in a manner seemingly independent from each other.

Formoguanamine damages the retinal pigment epithelium (RPE) and photoreceptors in chicken retina by decreasing the activity of ornithine amino-transferase, a key enzyme in the RPE (Oishi and Lauber 1988). Lid-sutured chicken eyes treated with formoguanamine did not develop

any characteristic myopic eye enlargement, suggesting that intact photoreceptors are necessary for eye growth to occur.

A subsequent study by Ehrlich and colleagues (1990) examined how tunicamycin affects occlusion-induced growth in chick retina. In amphibians (Fliesler et al. 1984) and squirrels (Anderson et al. 1988), tunicamycin selectively destroys photoreceptors, and presumably Ehrlich also wished to do the same in chicken. However, Ehrlich found that tunicamycin destroyed practically all cell populations in the chicken retina. While occlusion-induced myopia was indeed prevented, tunicamycin's neurotoxic actions were too generalized to permit identification of a particular retinal cell type responsible for mediating eye growth.

In 1989, Stone and associates showed that lid-suture and occluder-induced myopia provoked a decline in retinal dopamine levels, by approximately 30% (Stone et al. 1989). These results suggest that dopamine is involved in the regulation of eye growth. To further characterize the possible actions of dopamine, pharmacological studies were performed. A general dopamine receptor agonist such as apomorphine (Stone et al. 1989) or lesioning with 6-hydroxydopamine, 6-OHDA (Li et al. 1992) prevent occluder-induced axial elongation and myopia development. On the other hand, co-administration of apomorphine and haloperidol (a non-selective dopamine receptor antagonist) did not affect the development of lid-suture myopia or prevent ocular enlargement (Stone et al. 1989). This suggests that dopamine receptors participate in the eye growth process. Rohrer et al. (1993) examined specific dopaminergic receptor properties by co-administering apomorphine with antagonists specific for D_1 receptors (SCH 22390) or D_2 receptors (spiperone), and concluded that apomorphine prevents myopia by acting via D_2 receptors. These results confirm some of Stone and colleagues' earlier work (1990) where quinpirole and

bromocryptine (both selective D_2 receptor agonists) were found to prevent lid-suture myopia. Enhancement of myopia was seen during treatment with the dopamine antagonist, sulpiride (Schaeffel et al. 1995) and reserpine (Ohngemach et al. 1997), which depletes stores of dopamine. These experiments indicate that abnormal decreases in dopamine levels are linked with the development of myopia.

Weiss and Schaeffel (1993) reported striking day versus night differences in eye growth, where eyes grew during the day but actually shrank in size at night. Form deprivation myopia interfered with this cycle by abolishing the growth inhibition that occurs at night, resulting in excessive eye growth and axial elongation. A correlation with retinal dopamine was suspected, since retinal dopamine levels are normally elevated by day and reduced at night (Iuvone et al. 1978, Siuciak et al. 1992). 6-OHDA application to occluded eyes prevented the development of myopia and restored nocturnal growth inhibition (Weiss and Schaeffel 1993), indicating that normal dopaminergic rhythms are necessary for regulating ocular growth and refractive error.

However, it is unlikely that dopamine is the *only* factor which controls eye growth. Various studies suggest that other retinal cell populations and neurocircuitry may also be involved. For instance, muscarinic (cholinergic) receptors using acetylcholine (ACh) may participate in myopic axial elongation, as shown by studies using atropine (a non-selective agonist for all muscarinic receptors) and pirenzipine (specific for M1 muscarinic receptors). Pirenzipine inhibits the axial elongation which results from induced myopia (in chicks: Stone et al. 1991, in tree shrews: Cotriall and McBrien 1996), and atropine appears to do the same (McBrien et al. 1993).

Other studies have examined how excitotoxic amino acids such as N-methyl-D-aspartate (NMDA) and quisqualic acid (QA) affect eye growth in chicks. QA destroys amacrine and

horizontal cells, while NMDA selectively destroys amacrine cells. Barrington et al. (1989) noted that in non-occluded eyes, intravitreal injections of QA and NMDA would increase anterior chamber depth without affecting vitreous chamber size. A recent study by Fischer et al. (1997) found that NMDA by itself would induce myopia in chicks. Fischer and colleagues (1998b) have further characterized the effects of QA and NMDA in chicken retina, reporting damage to several amacrine cell populations. Among many others, these included amacrines containing serotonin, vasoactive intestinal polypeptide (VIP), GABA, Met-enkephalin, and choline acetyltransferase.

The possible roles of both VIP and Met-enkephalin in the development of myopia have been previously examined. Stone et al. (1988) noted that lid-suture myopia prompted increased levels of VIP in monkeys, a finding which was later confirmed by Raviola and colleagues (1991). Pickett-Seltner and Stell (1995) further characterized the pharmacological effects of VIP analogues and antagonists on FDM development. These latter investigators concluded that VIP applied exogenously does not directly affect ocular growth, although endogenous VIP within a subset of amacrine cells may play a role.

From this survey of the myopia literature, it is apparent that many factors are potentially involved in the control of ocular growth, and that these multiple elements inter-relate with each other in a complex and as yet undefined manner.

2.0 GENERAL INTRODUCTION

The majority of visual information passes through the retina along a vertical pathway, from photoreceptors to bipolar to ganglion cells, and then into the optic nerve and brain. However the lateral interactions between retinal cells also play an important role in visual processing. Such lateral connections include the horizontal cells which modulate information passing between the photoreceptors and bipolar cells. Amacrines are another cell type believed to be involved in lateral processing and possible modulation of the vertical information pathway. The large variety and strategic position of amacrines within the visual pathway make it plausible that these cells help mediate ocular growth during the progression of refractive errors (Bock and Widdows 1990).

In the field of myopia research, much attention has been focused on how dopamine is involved in the regulation of refractive errors. This thesis will consider how serotonin may also play a role, using confocal laser scanning microscopy to examine how both serotonergic and dopaminergic amacrine cell populations are affected by myopia and hyperopia. Hence a review of amacrine morphology and function will now be presented, followed by background information on dopamine, serotonin, and the basic principles of confocal microscopy.

2.1 Amacrine cells

"Amacrine" literally means a cell without an axon. Typically, axons convey information away from the cell body, while dendrites receive neuronal input. However, amacrine dendrites appear to have both input and output capabilities (Morgan 1992). Amacrine cells were first named by Cajal (1892) to replace the more confusing term "spongioblasts" which was originally assigned to this cell type (Dogiel 1883).

There is an extremely large variety of amacrine cells. Across animal species, it is estimated that 50-60 types of amacrine cells exist (Morgan 1992). Amacrine cell bodies are generally located in the inner nuclear layer (INL), immediately adjacent to the inner plexiform layer (IPL). Amacrine dendritic processes are distributed within the IPL where they make contact with ganglion, bipolars, and other amacrine cells.

Morphologically, amacrines have been classified according to their dendritic field spread (wide or narrow), their dendritic layering (uni-, bi-, multistratified or diffuse throughout the IPL) and dendritic appearance (thick branches, spiny, fine, etc). Further subclassifications can also be made based on the location, shape, and diameter of cell bodies.

The exact functions of most amacrine cells remain elusive, partly due to the technical difficulties in obtaining electrophysiological recordings from these cells. Hence some amacrine cell functions have been deduced based on their morphology, neurochemical content, and responses during pharmacological studies (for review, see Masland 1988).

2.2 Stratification of the inner plexiform layer (IPL)

Patterns of dendritic stratification within the retina can provide clues about cellular function, since synapses with other cell types are generally localized within specific layers. If there are known inputs and outputs to retinal cell populations, this can help us understand how certain neurons may participate in the control of myopia and hyperopia. This section describes stratification in the inner plexiform layer (IPL), since it is within this particular retinal region where amacrine dendrites are found.

The IPL is subdivided into five sublaminae. The first sublamina is located at the scleral

side of the IPL (closest to the inner nuclear layer, INL) while the fifth sublamina is found at the vitreous side (closest to the ganglion cell layer). Cajal (1892) credits the work of Dogiel (1883) for providing the first conclusive evidence of IPL stratification. Based on histological studies of lower vertebrate retinae (fish, reptiles, amphibians, and birds), Dogiel noted granular sublayers within the IPL using methylene blue staining (Ehrlich's method, 1886). The presence of five IPL sublaminae was later confirmed in birds by Cajal using Golgi staining, with the further observation that certain amacrine cells formed synaptic connections almost exclusively in one or a few of these sublayers. A similar arrangement was observed in mammalian retinae (Baquis 1890, Dogiel 1891).

Electrophysiological and ultrastructural studies later revealed that mammalian IPL could also be functionally divided into ON and OFF regions, based on the response of nerve cells to different light stimuli (Kuffler 1953, Enroth-Cugell and Robson 1966). In brief, ON-center cells show electrical activity (action potential spikes) when a spot of light is turned on, whereas OFF-center cells respond best when a spot of light is turned off. ON/OFF cells show transient activity at light onset or offset, but not during a period of sustained light or dark. Different populations of ganglion, bipolar, and amacrines cells comprise the ON and OFF neural circuitry. The ON and OFF pathways also appear to be physically confined to specific regions of the IPL. The outer sublayers of the IPL (sublayers 1 and 2, also designated "sublamina a") contain cells that participate in OFF pathways. In contrast, the inner region of the IPL (sublayers 3 to 5, or "sublamina "b") contain ON pathway circuits (Famiglietti and Kolb 1976). Hence it is possible to deduce amacrine cell functions by identifying synaptic connections with bipolars, ganglions, and other amacrine cells within particular ON and/or OFF sublayers.

2.3 Dopamine

2.3.1 Biosynthesis and metabolism of dopamine

Dopamine is a catecholamine that is found throughout the animal kingdom where it modulates a broad range of physiological activities in both the central and peripheral nervous systems. Dopamine is closely related to epinephrine and norepinephrine, and all three compounds arise from a common biosynthetic pathway:

$$\text{Tyrosine} \xrightarrow{1} \text{DOPA} \xrightarrow{2} \text{Dopamine} \xrightarrow{3} \text{Norepinephrine} \xrightarrow{4} \text{Epinephrine}$$

The enzymes in the biosynthetic pathway include: (1) tyrosine hydroxylase, (2) dopa decarboxylase, (3) dopamine β hydroxylase, and (4) phenylethanolamine-N-methyl transferase (Kandel et al. 1991). The major metabolites of dopamine are 3,4-dihydroxyphenylacetic acid (DOPAC) and homovanillic acid (HVA). Both DOPAC and HVA are end-products of a multi-step pathway in which the key degradative enzymes are monoamine oxidase (MAO) and catechol-O-methyltransferase (COMT) (Walker 1986).

Several decades ago, dopamine was merely considered an intermediate step toward the production of norepinephrine and epinephrine. However, the large amounts of dopamine found in the central nervous system (CNS) were not compatible with the idea that dopamine was playing a transitional role (Goodman Gilman et al. 1991). It was later discovered that various neurons in the brain exist which completely lack the enzyme dopamine β hydroxylase, and hence dopamine is the final end-product within these cells (Vogt 1973, Clark 1985). This discovery prompted many studies which have now firmly established that dopamine plays significant neurotransmitter

and neuromodulatory roles. Although dopamine exerts significant effects throughout the body (e.g. mediating cardiovascular function and nigrostriatal motor activity), this thesis will focus on retinal dopamine.

2.3.2 Retinal dopamine

Dopamine was first observed in amacrine cells within the rat retina (Malmfors 1963). The density and number of dopaminergic amacrine cells varies across species but is always quite low (no more than a few thousand cells per retina). Within the avian retina, dopamine is localized within a small population of amacrine cells that only comprises 1-5% of the total number of amacrine cells (Massey and Redburn 1987, Nguyen-Legros and Savy 1988). The amounts of epinephrine and norepinephrine within the chicken retina are negligible (Oyster et al. 1988, Siuciak et al. 1992).

The morphology of the individual dopamine amacrine cells in avian species has been examined previously using Falck-Hillarp autofluorescence (Corrodi and Jonsson 1967) and immunohistochemical labelling. In birds, the dopaminergic amacrines show a trilaminar arrangement of dendritic processes. These are located in sublaminae 1, 3, and 4 (Djamgoz and Wagner 1992, Su and Watt 1987, Kato et al. 1984, Brecha 1983) . The dendrites in the outermost layer are the most prominent and show the most branching (Nguyen-Legros and Savy 1988).

This thesis will concentrate on the role of dopamine as a retinal neurotransmitter and neuromodulator, although some of dopamine's other specific retinal activities will be briefly mentioned at this point (for review, see Bodis-Wollner and Piccolino 1988, Stone 1996). These include, in teleost fish, the control of retinomotor movements (cone retraction, rod elongation) and

the dispersion of RPE melanin pigments. Both of these mechanisms serve during light dark adaptation (Burnside and Dearry 1986). Dopamine also has a major impact on the electrical activity of horizontal cells. In studies on fish, reptiles, and amphibians, dopamine mimics the effects of light adaptation and uncouples the electrical junctions between horizontal cells (Djamgoz and Wagner 1992). This has been demonstrated using electrophysiological recordings and by fluorescent dye micro-injection. In the latter technique, single horizontal cells are filled with Lucifer Yellow (Parnas and Bowling 1981). In the absence of dopamine, the voltage-sensitive dye will pass through gap junctions into surrounding cells, but application of exogenous dopamine will prevent any inter-cellular dye transfer (Teranishi et al. 1984, Piccolino and Demontis 1988, Witkovsky and Dearry 1991). In mammals, dopamine decreases gap junction conductance between amacrines and cone bipolar cells. Hence dopamine enhances small-spot cone responses, thereby increasing visual acuity and improving photopic vision (Massey and Redburn 1987).

It is not yet certain whether dopamine amacrine cells have similar functions in birds. One way to answer this question is to first characterize the synapses between dopaminergic amacrines and other cell types in the avian retina. Glycinergic, cholinergic, and ENSLI (enkephalin, neurotensin, and somatostatin) inputs to dopaminergic amacrine cells have been documented in chicken retina (Boelen et al. 1991, 1993, 1994). One may also extrapolate, with caution, from various other vertebrate studies which have examined synaptic inputs onto dopaminergic cells. For example, inhibitory GABA and glycinergic inputs to dopamine cells have been reported in rat retina (Morgan and Kamp 1980 and 1983). In toad retina, dopaminergic amacrines mostly synapse with other amacrines although inputs from bipolars, and outputs to ganglion cells, are also seen (Gabriel, Zhu, Straznicky 1992). In fish retina, cholinergic (Laufer et al. 1981) and serotonergic

(Kato et al. 1983) inputs to dopamine cells have been observed.

2.3.3 The effects of light on retinal dopamine

In chicken and other species, it is well-documented that light stimulates retinal dopamine synthesis and release, while darkness inhibits this process (Nichols et al. 1967, Parkinson and Rando 1983). More specifically, light increases the activity of tyrosine hydroxylase, the rate-limiting enzyme for dopamine synthesis (Iuvone et al. 1978). In fact, retinal dopamine synthesis and release is maximal for flickering light rather than steady light stimuli, which further substantiates the correlation between neural activity and dopamine production (Kramer 1971, Kirsch and Wagner 1989, Dong and McReynolds 1992). These effects are reciprocal, as seen in studies where dopamine can also mimic the effects of light adaptation in the retina (Witkovsky et al. 1987, Iuvone 1988).

In chicks, both lens-induced and form deprivation myopia can be suppressed by stroboscopic light (Gottlieb et al. 1987, Rohrer et al. 1995). Different flicker parameters will suppress the development of hyperopia (Schwahn and Schaeffel 1997). These studies indicate that altering dopamine release by flickering light will counteract the progression of ametropias.

2.4 Serotonin

The term "serotonin" was first coined in the late 1940's, when an indoleamine compound isolated from blood serum was found to provoke vasoconstriction (Rapport et al. 1948). A few years later, Twarog and Page (1953) noted its presence in mammalian brain. At this point, neurobiologists began to examine serotonin with great interest, and many studies have shown that

serotonin plays important roles in sleep, level of awareness, perception, learning, memory, and emotional states such as anxiety and depression (Redburn 1985). Serotonin can also be found throughout diverse plant and animal kingdoms, where its functions are not necessarily related to endocrine or neural activity (Goodman Gilman et al. 1991).

2.4.1 Distribution of serotonin

In the adult human body, the great majority (90%) of serotonin is found in the gastrointestinal tract (where it was initially called "enterin"), with the remaining 10% distributed in the blood platelets and central nervous system (CNS) (Goodman Gilman et al. 1991). Within the CNS, approximately 90% of serotonin is localized in the pineal organ where it serves as a precursor for melatonin synthesis (Redburn 1985).

2.4.2 Biosynthesis and metabolism of serotonin

The chemical structure of serotonin is 5-hydroxytryptamine (5-HT) (Rapport et al. 1948). Two steps are involved in the biosynthesis of serotonin: Blood tryptophan is first converted to 5-hydroxytryptophan by the rate-limiting enzyme tryptophan hydroxylase. Next, 5-hydroxytryptophan is converted to 5-hydroxytryptamine (serotonin) by L-amino acid decarboxylase, a non-specific aromatic enzyme. (Redburn 1985, Goodman Gilman et al. 1991).

$$\text{Tryptophan} \xrightarrow[\text{hydroxylase}]{} \text{5-hydroxytryptophan} \xrightarrow[\text{decarboxylase}]{} \text{5-hydroxytryptamine (Serotonin)}$$

The major metabolite of serotonin, 5-hydroxy indole acetic acid (5-HIAA), results from various intermediate metabolites and the activity of two enzymes: monoamine oxidase (MAO) and aldehyde dehydrogenase (Goodman Gilman et al. 1991).

$$\text{Serotonin} \xrightarrow[\text{MAO, dehydrogenase}]{} \text{5-HIAA}$$

Another pathway exists that converts serotonin to melatonin via the activity of serotonin N-acetyltransferase (NAT) (Binkley 1973).

$$\text{Serotonin} \xrightarrow[\text{NAT}]{} \text{Melatonin}$$

2.4.3 Retinal serotonin

Although retinal serotonin is found in diverse animal species, there is great variation in the measurable amounts and cellular distribution. Virtually all teleosts, reptiles, amphibians, and birds display high levels of endogenous serotonin contained within certain amacrine and bipolar cell populations (Suzuki et al. 1976, Marc et al. 1988, Hurd and Eldred 1993, Wilhelm et al. 1993, Glasener et al. 1988, Parkinson and Rando 1981, review: Osborne 1984). Recent HPLC studies show that the serotonin content in normal chicken retina ranges from 70-114 pg/mg of tissue (Siuciak et al. 1992).

In contrast, serotonergic cells are not readily apparent in many mammalian retinae unless they are first pre-loaded by the application of exogenous serotonin, which is then taken up by serotonin-accumulating cells (Ehinger et al. 1981, Sandell and Masland 1986, Vaney 1986).

Interestingly, the serotonin re-uptake and receptor mechanisms within certain mammalian retinae appear to be identical to those found in bird and amphibian retinae, as well as established serotonergic regions of the brain (Massey and Redburn 1987).

2.4.4 Serotonin as a retinal neurotransmitter

Although there is little question that serotonin serves as a neurotransmitter in the brain, it was initially debated whether serotonin also functions as a neurotransmitter in the retina (For: Parkinson and Rando 1981, Osborne 1982a, Redburn 1985. Against: Floren and Hansson 1980). This controversy arose from the fact that measurable levels of serotonin in the retina are extremely low. However, serotonin satisfies all criteria for a neurotransmitter (Osborne 1982a and 1984), with the most important consideration being that it exists in the retina, no matter how small the amount. No one has demonstrated that a "lower limit" exists at which a neurotransmitter cannot function (Redburn 1985). To date, the overwhelming majority of physiological and pharmacological data support a neurotransmitter role for retinal serotonin (Brunken et al. 1993).

Another consideration is the possibility that serotonin may also be able to exert long-distance effects (similar to dopamine) within the eye and retina, thus circumventing the need for synaptic connections.

2.5 Confocal microscopy

Confocal microscopy allows visualization of thick biological samples, using thin optical sectioning which does not physically damage the original specimen. Proper spatial relationships are maintained within the specimen, and out-of-focus information is eliminated. The resulting

confocal images are hence much sharper and more detailed than what can be obtained using conventional light microscopy (White, Amos, Fordham 1987).

The original confocal microscope was invented in 1955 by Marvin Minsky at Harvard University (Minsky 1988). With a background in mathematics, physics, and neuroscience, Minsky had diverse research interests, one of which was studying how the brain works. Ultimately Minsky hoped to develop machines capable of "artificial intelligence" based on cell connectivity principles in the living nervous system. However, he was stymied by several factors, with the biggest issue being the poor microscope equipment at the time. When Minsky tried to examine three-dimensional cell connections in thick brain specimens, he encountered excessive light scattering within the tissue. Only meaningless blurry images could be seen due to the poor signal-to-noise ratio.

In response to this problem, Minsky found an ingenious solution: Excessive light scattering within the specimen could be eliminated by preventing unnecessary light from entering in the first place. To accomplish this, Minsky used pinholes and objective lenses at strategic locations along the light path. One pinhole selectively allowed incoming light rays to focus at a single point within the specimen. A second pinhole was positioned at the image plane on the exit side of the objective lens, to further reduce any out-of-focus light from reaching the eye of the observer. To scan across the specimen, Minsky decided that it was easier to move the specimen stage while keeping the optics fixed. This eliminated the need to maintain a precise alignment of two moving pinholes.

Modern versions of the confocal microscope incorporate several features which greatly improve performance for biological applications. The introduction of lasers to the confocal design

provide steady sources of high-intensity monochromatic light which can illuminate very small and select regions of the specimen (Egger and Petran 1967, Sheppard and Choudhury 1977, Wilson 1990, Inoue 1995). Multiple laser combinations can also be used, which optimizes the emission of various fluorochrome labels and facilitates double or triple labelling (Demandolx, Barois, Davoust 1997). Automated equipment now permits the pinhole and optics to be moved easily for scanning across a fixed specimen stage. This is preferable for biological specimens, since stage movement may cause excessive shifting within an aqueous mounting media. Computerized data acquisition, video, and imaging software also allows rapid capture, processing, and storage of extremely large amounts of image data. Many current confocal systems now only use one pinhole in the return light path, thus reducing the technical requirements for continuously aligning two pinholes (Pawley 1995).

3.0 THESIS OBJECTIVES

This study characterizes the effects of induced myopia and hyperopia on neuron distribution, dendritic morphology, and neurochemical content in the retina. More specifically, this research examines amacrine cell populations which contain either dopamine or serotonin, since a correlation between these biogenic amines and the development of refractive errors appears likely. If we can decipher the underlying mechanisms that cause myopia and hyperopia, we may eventually be able to prevent and correct these visual anomalies.

In order to facilitate the reading of this manuscript, the terminology "dopaminergic" and "serotonergic" cells will be used throughout this thesis with reference to "tyrosine hydroxylase-immunoreactive" and "serotonin-immunoreactive" cells respectively.

4.0 MATERIALS AND METHODS

This project comprised three stages. Part I used confocal microscopy to quantitatively assess any changes in the numbers of serotonergic and dopaminergic amacrine cells in response to induced myopia and hyperopia. Part II examined qualitative changes in the dendritic field spreads of the dopaminergic amacrine cells resulting from induced myopia and hyperopia. The dendrites of serotonergic amacrine cells were not examined because their dendritic fields were extremely dense, and it was impossible to distinguish individual cells from each other. Parts I and II both utilized immunohistochemistry and confocal laser microscopy to examine the amacrine cell populations. Part III involved using high-pressure liquid chromatography (HPLC) to quantitatively measure the levels of retinal dopamine, DOPAC, serotonin, and 5-HIAA from chicks in which myopia and hyperopia had been induced.

All animal experiments, immunohistochemical processing, image and data analysis were done at the School of Optometry, University of Waterloo. All confocal microscopy was accomplished at McMaster University in collaboration with Dr. Alexander Ball in the Department of Biomedical Sciences, Anatomy division. HPLC assays were performed in the laboratory facilities of Dr. Candace Gibson at the University of Western Ontario, Department of Pathology.

4.1 Animal care

Newly-hatched broiler chicks (White Rock cross) were obtained from a local hatchery (Big Four Chicks, New Hamburg, Ontario). A numbered aluminum wingtag was attached to each chick for identification purposes. Chicks were monitored for overall growth by weighing them on the first and last days of each experiment. The birds were housed in stainless steel brooder cages with

food (Shur-Gain Homestead Poultry Starter-Grower, B-W Feed & Seed Ltd., New Hamburg, Ontario) and water freely available for the duration of each experiment (6 to 10 days). Brooder temperature was maintained at 32°C during the first week, and lowered to 28°C during the second week. Fluorescent lighting was controlled to provide a 14 hour light versus 10 hour dark cycle (lights on at 06:00, lights off at 18:00). Ambient light within the brooder cage was 170 lux.

4.2 Experimental groups

The following abbreviations will be used throughout this thesis:

DIM = defocus-induced myopia

DIH = defocus-induced hyperopia

FDM = form deprivation myopia

For quantitative confocal analysis of the amacrine cell populations (Part I), six experimental conditions were assessed. The number of chicks (n) used for each experiment is indicated in brackets after each of the listings that follow (n of first trial, n of second trial). The six groups comprised: (1) DIM and dopaminergic amacrine cells (n=5, n=10), (2) DIM and serotonergic amacrine cells (n=10), (3) FDM and dopaminergic amacrine cells (n=7), (4) FDM and serotonergic amacrine cells (n=8), (5) DIH and dopaminergic amacrine cells (n=5, n=6), and (6) DIH and serotonergic amacrine cells (n=10). A total of 61 animals were used during this portion of the study. A time frame of 5-6 weeks was required for the completion of each experiment, which involved inducing the refractive errors in chicks, retinal dissection, immunohistochemistry, confocal imaging, cell counts, data processing, and statistical analysis.

Three experimental conditions were assessed during the qualitative confocal analysis of

the dendritic morphology (Part II) of dopaminergic amacrine cells: (1) DIM, (2) DIH, and (3) FDM. Analysis was performed on the same retinal samples as described above in Part I (n=34) in which dopaminergic cells were specifically labelled. However, a more detailed morphological examination was conducted on these specimens using special features of the confocal microscope. An additional group of DIH-treated animals (n=10) was also used for comparison by light microscopy during this portion of the study.

For the HPLC analysis, ten animals were examined after unilaterally inducing FDM with translucent goggles (n=5) and DIH with convex lenses (n=5).

4.3 Ocular measurements

The refractive state of each chick eye was measured using a streak retinoscope (Welch Allyn 18200/71000, 3.5V) and a set of concave or convex trial lenses. Refractive states were assessed daily, measured to the nearest ± 0.5 D, along the anterior-posterior axis of each eye. As in earlier studies (Irving et al. 1991 and 1992, Irving 1993), it was assumed that the chicks were fixating beyond the plane of the examiner and the retinoscope. On the first and last days, intraocular dimensions (axial length, vitreous chamber depth, and anterior compartment) were measured in triplicate by A-scan ultrasonography with a 3-mm diameter 10 MHz hard probe (Oculometer 4000, Radionics Medical Inc., Scarborough, Ontario). In this thesis, "anterior compartment" refers to the distance from the cornea to the posterior lens surface. All retinoscopy and ultrasonography measurements were performed on awake birds without anaesthesia.

4.4 Goggles

Ametropias were induced using a velcro-goggle combination as described in previous work (Irving 1993). Each goggle was created from a plastic laminate sheet (0.43 mm thick, Condors Laminations, Toronto, Ontario) that was pressed into a heated mold, resulting in a translucent dome with a 20 mm base diameter and 7 mm vertex distance. The outer surface of each goggle was lightly abraded with sandpaper to ensure that only diffuse light could enter through the material of the goggle itself. Chicks were unilaterally goggled, such that one eye served as the experimental eye, while the other untreated eye served the control.

For the defocusing experiments, a rigid contact lens (12 mm diameter, 8.1 mm base curve) of appropriate power was mounted into a circular aperture drilled in each goggle. A low-fogging glue was used to attach each contact lenses to the goggle (Loctite Prism 408 Instant Adhesive, Mississauga, Ontario). Goggles were designed such that the effective lens power at the corneal plane totalled -15.00 D to induce myopia, or +15.00 D to induce hyperopia. A goggle was attached to each chick using a set of velcro rings as follows: one velcro ring was glued to the flange around the base of the goggle, while a corresponding velcro ring was glued to the feathers around the chick eye (Figure 2A). A small notch was cut from the latter velcro ring to provide clearance for the chick's beak. A gap-filling glue (Loctite 416 Super Bonder, Newington, Connecticut) was used to attach the velcro rings to the goggle and the chick (Figure 2B). This velcro system allowed easy removal of the goggle for daily cleaning and refractive measurements. The velcro also permitted air circulation, thus reducing the amount of condensation that accumulated inside the goggle. After an initial adaptation period of 20-30 minutes, the chicks showed no behavioural signs of stress or abnormal activity in response to the goggles. Goggled chicks foraged normally and gained weight

Figure 2: Refractive errors were unilaterally induced in young chicks, starting within a few hours after hatching. A velcro ring was glued around the chick eye (A) upon which a lightweight plastic goggle was mounted (B). Goggles containing -15.00 D or +15.00 D hard contact lenses produced myopia or hyperopia respectively. Translucent goggles without contact lenses were used to produce form deprivation myopia. The ungoggled contralateral eyes served as controls.

A

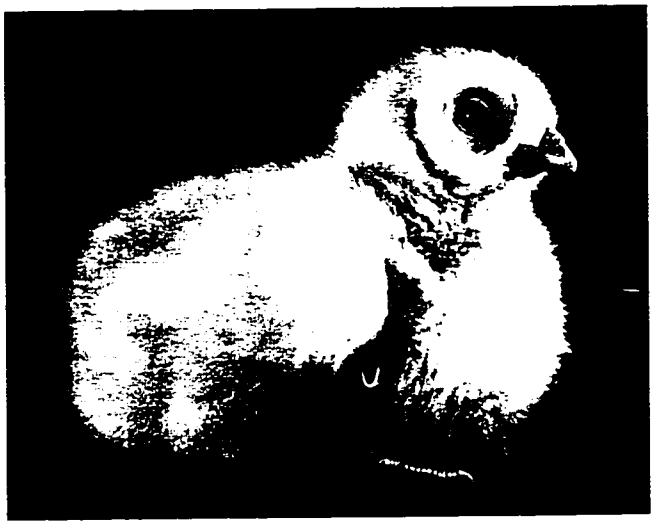

B

Photography: J. Wieczorek

as readily as non-goggled chicks.

Form-deprivation myopia was induced using translucent goggles without any contact lens inserts. These goggles were attached unilaterally around each chick eye, using the previously described velcro combination.

4.5 Final day measurements

Common to both confocal and HPLC studies, the following measurements were obtained from each chick on the final day of each goggle experiment: Overall body weights, final refractive states, and A-scan ultrasonographs of each eye (recorded in triplicate). Since the methodology for the confocal and HPLC studies differ greatly from each other after this stage, these will be described in separate sections.

4.6 Processing for confocal microscopy

For the confocal studies, chicks were sacrificed by $CO_{2(g)}$ asphyxiation, eyes were enucleated, and excess connective tissue and extraocular muscles were removed from the ocular surfaces. Wet eye weights were measured using an electronic balance (A&D Company, FX-300). Axial lengths and equatorial diameters were recorded in triplicate using digital calipers. After cutting along the ora serrata, the anterior portion of each eye (comprising the iris, cornea, and lens) was removed and discarded, and the diameter of the remaining circular opening (corneal diameter) in each posterior chamber was measured.

4.7 Fixation

As rapidly as possible after dissection, the posterior eye cups were placed in individually-labelled glass vials and fixed for one hour at room temperature. The tissue specimens were gently agitated throughout fixation using an automated tilt-table (Adams Nutator). The fixative was prepared fresh, immediately before each use, according to the following recipe: 4% paraformaldehyde (JBS, EM grade), 0.24% picric acid (VWR), 0.2 mM $CaCl_2$ (Sigma), 0.1 M monobasic sodium phosphate (NaH_2PO_4, JBS-Chem), 0.1 M dibasic sodium phosphate (Na_2HPO_4, Sigma), 1% sucrose (Sigma), pH adjusted to 7.4. The paraformaldehyde crystals were initially heated on a stir plate to 60-62°C in de-ionized distilled water, and undissolved particles were cleared by adding a few drops of 10 N NaOH (BDH Assured). The remaining ingredients were subsequently added to the cooled paraformaldehyde solution. After fixation, the eye cups were thoroughly rinsed in 2-3 changes of rinse buffer (5% sucrose, 0.002 M $CaCl_2$, 0.1 M NaH_2PO_4, 0.1 M dibasic Na_2HPO_4, pH 7.3). At this stage, the eyes could be stored for a few days in rinse buffer at 4°C until further processing.

4.8 Retinal dissection

Eye orientation was determined from the position of the optic nerve and the pecten (both are located in the inferior portion of the eye). In early experiments, a single-edge straight razor blade was used to cut the eye cup into four equal quadrants: temporal, superior, nasal, and inferior. These sections were labelled A, B, C, and D respectively (Figure 3A). In later experiments, a section was initially cut from the central portion of each retina using a circular stainless steel trephine blade with a 7 mm diameter. The remaining eye cup was subsequently divided into the

A

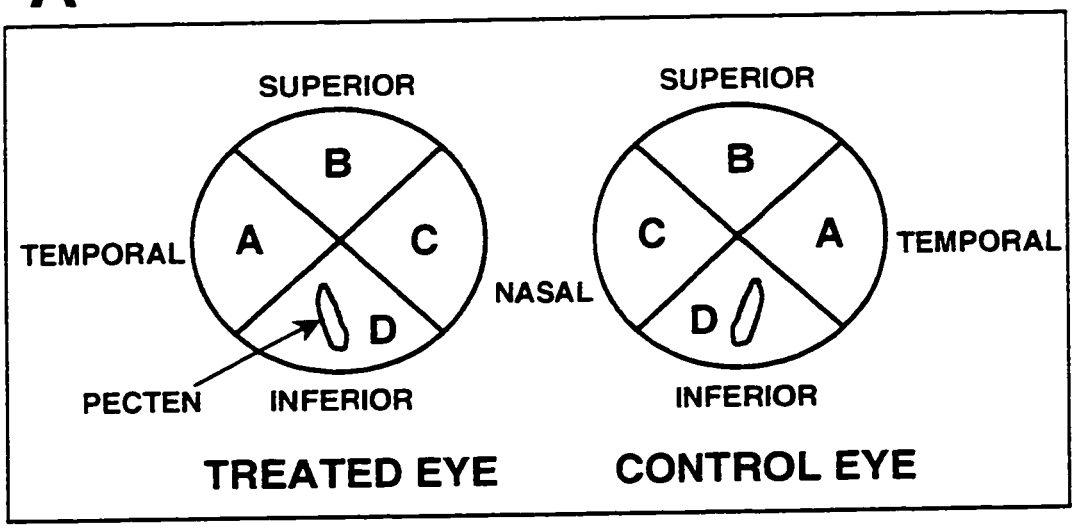

Figure 3A: Dissected wholemount retinae in early studies were cut into four equal quadrants: temporal, superior, nasal, and inferior which were respectively labeled as A, B, C, and D. Inferior retinal segments D containing the pecten were discarded.

B

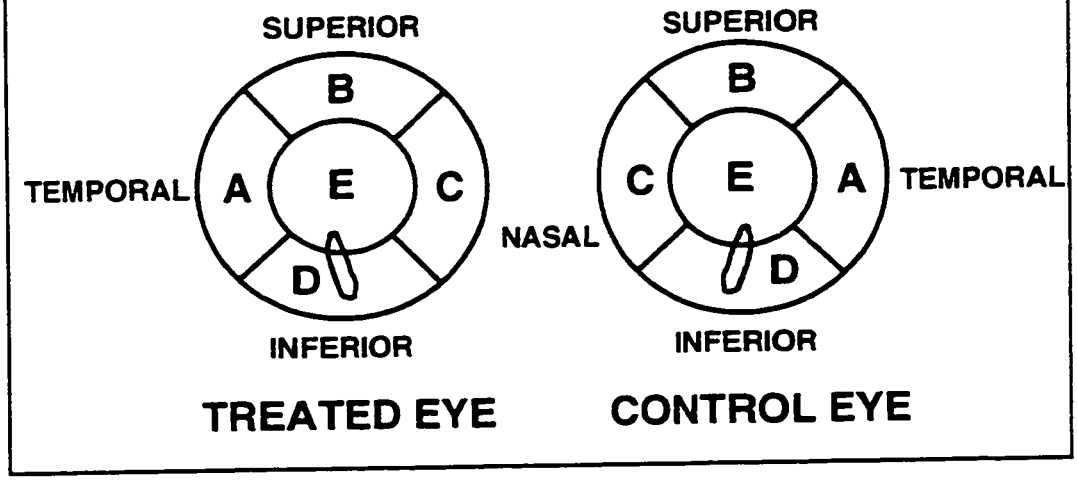

Figure 3B: Retinae in later studies were cut into five segments: temporal, superior, nasal, inferior, and central which were respectively labelled as A, B, C, D, and E. With the exception of one experiment, retinal segments D containing the pecten were discarded.

four previously-identified quadrants with a razor blade, resulting in sections A, B, C, D, and the newly-defined section E from the central portion of the retina (Figure 3B).

Wholemount retinae were carefully dissected from the eye sections using a dissecting microscope (Nikon) and needle-tip forceps (Dumont #5, Switzerland). Section D was discarded in all cases since the presence of the pecten and optic nerve head in this region made retinal dissection extremely difficult. If necessary, forceps were used to remove any adhering retinal pigment epithelium from the retina.

4.9 Pretreatment

Each isolated retinal piece was placed on a piece of clean dental wax, and gently blotted with a non-linting kimwipe tissue (Kimberly-Clark) to remove all traces of vitreous humour. A fine-gauge needle (30 gauge, Becton-Dickinson) was used to pierce each retinal section at approximately 1 mm intervals across its entire surface area. This served to improve antibody penetration across the thickness of the retina during later steps. Each retinal section was placed in 30% sucrose solution (15 g sucrose per 50 mL rinse buffer, recipe described previously) within individually-labelled and capped microcentrifuge tubes (VWRbrand, 0.5 mL). The retinal pieces were left to soak in this sucrose solution overnight at 4°C. The retinae were considered sufficiently cryoprotected when they were no longer floating at the top of the sucrose solution, but had sunk to the bottom of the tube.

4.10 Immunohistochemistry

The microcentrifuge tubes with the sucrose-infiltrated retinal sections were placed in a freezer at -20°C for 30-60 minutes until completely frozen, and allowed to thaw at room temperature. Using glass Pasteur pipettes to remove and add solutions from each tube, the 30% sucrose solution was withdrawn, and the retinal pieces were rinsed three times with rinse buffer. Retinae were gently agitated for 1 hour at room temperature in a pretreatment/blocking solution of 1% dimethyl sulfoxide (BDH Assured), 1% Triton X-100 (Biorad Laboratories), 1% normal goat serum (Jackson Immunoresearch), 0.2 mM $CaCl_2$ (Sigma), 0.1 M monobasic sodium phosphate (NaH_2PO_4, JBS-Chem), 0.1 M dibasic sodium phosphate (Na_2HPO_4, Sigma), and 5% sucrose (Sigma). The freeze-thaw procedure and Triton X-100 both served to enhance antibody penetration, while the normal serum reduced undesirable background staining in the retina by blocking non-specific binding sites.

The pretreatment solution was removed from each microcentrifuge tube, and without rinsing, a primary antibody solution was applied. Both primary and secondary antibodies were diluted in 1% normal goat serum (Jackson Immunoresearch), 1% dimethyl sulphoxide (BDH Assured), 1% Triton X-100 (Biorad Laboratories), 0.2 mM $CaCl_2$ (Sigma), 0.1 M monobasic sodium phosphate (NaH_2PO_4, JBS-Chem), 0.1 M dibasic sodium phosphate (Na_2HPO_4, Sigma), and 5% sucrose (Sigma), 1% bovine serum albumin (Sigma), and 0.5% sodium azide (NaN_3, Sigma).

To selectively label serotonergic cells, 1/800 dilution of polyclonal anti-serotonin (INCstar, Stillwater, Minnesota) was applied to the retinae within each microcentrifuge tube. The tubes were placed on a tilt-table (Adams Nutator) and gently rotated at room temperature for 20-24 hours. To

stain dopaminergic cells. 1 100 dilution of polyclonal antibody directed against tyrosine hydroxylase (Eugene Tech Institute. Ridgefield Park. New Jersey) was applied to each retinal piece. and rotated overnight in the same manner as previously described for the serotonin staining protocol. Tyrosine hydroxylase is widely used throughout the scientific community as a marker to identify dopaminergic cells (Roth 1979).

Specificities of the primary antibodies were tested during preliminary studies by comparison with primary antibodies obtained from different commercial sources: Monoclonal anti-tyrosine hydroxylase (Boehringer Mannheim) and polyclonal anti-serotonin (ICN).

After removing the primary antibody solution. retinal sections were rinsed 2-3 times with rinse buffer. A 1/200 dilution of goat anti-rabbit Texas Red fluorescent secondary antibody (Jackson Immunoresearch) was applied to the retinae, and the specimens were left to rotate on the tilt-table for 16-20 hours at room temperature. The microcentrifuge tubes were wrapped in aluminum foil and placed in a light-excluding black plastic bag while rotating. The latter step was a safety measure to minimize possible bleaching of the fluorescently-conjugated secondary antibody due to exposure to ambient room lighting.

Each retina specimen was rinsed in 3 changes of fresh rinse buffer, and mounted vitreous side up on a standard glass microscope slide. A "coverslip bridge" prevented the retina from being excessively flattened and damaged when coverslipped. This bridge comprised placing two small coverslips (22 x 22 mm^2, no.1 thickness) on the microscope slide, one on each side of the retina sample. Each of these coverslips was held in place by an underlying drop of glycerol (BDH Assured). These two coverslips provided clearance for the retina when a third coverslip was placed overtop. One drop of glycerol and one drop of Vectashield Anti-Fade Mounting Medium

(Vector Laboratories) were placed on each retinal sample before positioning the third and final coverslip. The slides with retinal specimens were stored flat in cardboard slide folders at -20°C, protected from light, until further analysis.

4.11 Confocal microscopy

A laser scanning confocal microscope (Zeiss LSM-10, Germany) at McMaster University in Hamilton, Ontario was used to capture digitized images of the cell bodies and dendritic fields of the fluorescently-labelled dopaminergic and serotonergic amacrine neuron populations. The confocal microscope was equipped with an internal helium-neon laser source (543 nm), and an Axioplan microscope with 10x and 20x fluor objectives. An omega filter block allowed selective emission for rhodamine at 590 nm. Optical section thickness was adjusted to 0.2 μm and zoom factor set at 20x. The minimum pinhole size was used on the confocal microscope which would provide the least depth of field for the objectives used. Emitted fluorescence from the retina specimens and the resulting digitized images were detected and displayed using a frame-by-frame cycle on an adjoining computer monitor screen. Preview images were captured in fast scan mode (scanning time/image = 2 seconds). Excess noise and background were subsequently cleared from each final image by adjusting the brightness and contrast levels, activating the 2- or 4-times line averaging function, and if necessary, increasing the scanning time (8 seconds/image). Images in PIC and TIFF file formats (263,168 bytes each) were transferred from the hard drive of the confocal microscope to Iomega zip disks (100 megabytes each, 378 image storage capacity) using Zeiss LSMnet custom software and a personal computer interface. At the end of all data acquisition, the complete set of image data (1.73 gigabytes total) was transferred for permanent storage onto recordable compact discs (CD-R).

5.0 PART I: Cell densities and cell counts

In order to assess cell population distribution and numbers, a total of 2000 confocal images were recorded at the plane of greatest cell body density within the retina specimens (Figure 4). Images were obtained in the following distribution across the six experimental groups: (1) DIM/dopamine = 434 images, (2) DIM/serotonin = 317 images, (3) FDM/dopamine = 245 images, (4) FDM/serotonin = 462 images, (5) DIH/dopamine = 244 images, (6) DIH/serotonin = 298 images. Three to six images were recorded from each of the previously-defined retinal sections labelled A, B, C, and (if applicable) E. Images were taken at regular intervals across the entire surface area of the retina, resulting in a range of 9 to 24 images per chick eye.

5.1 Cell densities

Cell density was individually determined from each of the TIFF format confocal images using image analysis computer software packages, either Imfad *Image-I* (Version 4.0, Pennsylvania) or Scion *ImagePC* (Beta 1 version, 1997 Release, Maryland).

Scion *ImagePC* is adapted for IBM-PC from the Macintosh-based *NIH Image*, and is available as public domain software from the internet (http://rsb.info.nih.gov/nih-image/). With Scion *ImagePC*, a custom macro program was designed, incorporating parameters for cell size and shape recognition. Processed images were manually inspected after each computerized analysis to ensure cell count accuracy. Certain images were not suitable for computer cell count analysis, due to high background noise. Cell numbers from such images were individually assessed by viewing these files on a computer screen, then using a mechanical hand counter in conjunction with a screen grid overlay.

Figure 4: Representative confocal images of (A) dopaminergic amacrine cells and (B) serotonergic amacrine cells in wholemount chick retina. Retinal specimens were immunohistochemically porcessed in order to selectively stain dopaminergic or serotonergic cell populations. The effects of induced ametropias on cell population distributions were assessed by recording 2000 digital images with a confocal laser scanning microscope (Zeiss). Cell densities and cell counts were determined from each of these images using analysis software.

A

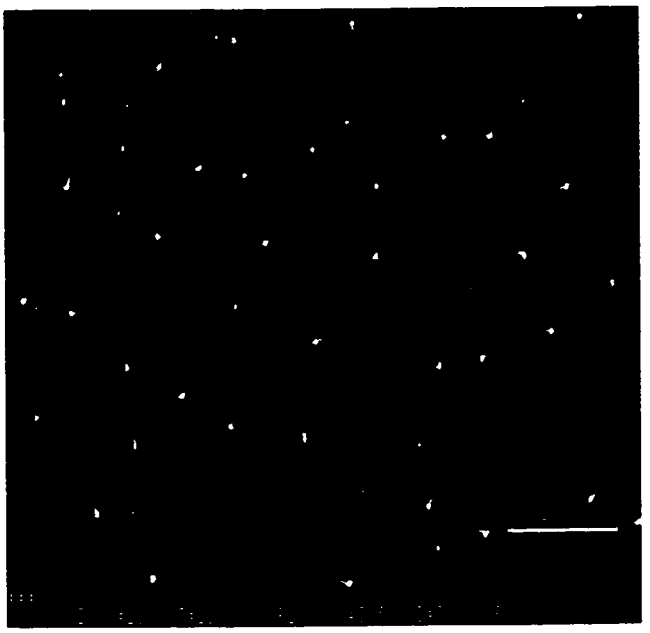

DOPAMINERGIC AMACRINE CELLS

B

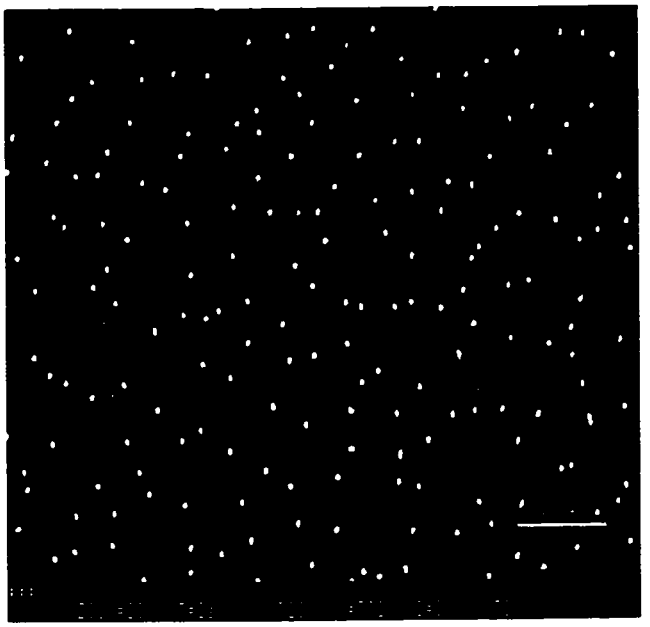

SEROTONERGIC AMACRINE CELLS

Image area was calculated from confocal images in PIC file formats. These PIC images contained measure bar information and required conversion (using LSM Zeiss confocal software) to another file format for importation into an image processing program such as Scion *ImagePC*. In Scion *ImagePC*, the pixel length of the measure bar was translated into μm values, and the image was corrected for aspect ratio balance. The entire image area was then determined along the x and y axes.

Cell density per image and per retinal section were expressed in terms of cells/μm^2. Cell count extrapolations per eye, described later, were assessed from cell densities and total retinal surface area calculations.

5.2 Retinal surface area calculations

Retinal surface areas were calculated from measured ocular parameters including equatorial diameter, vitreous chamber depth, and excised corneal diameter. "Cornea diameter" is a simplified term that will be used to describe the excised anterior portion of the eye, comprising the cornea and the immediate surrounding sclera to the anterior edge of the retina (ora serrata). In the chicken and pigeon eye, the ora serrata and posterior lens surface are aligned within the same plane (Walls 1942, and also corroborated by personal observations). Hence, vitreous chamber depth within the chicken eye (as measured by ultrasonography) can be used to define the anterior limiting edge of the retina.

The chicken eye can be mathematically represented as an ellipsoid which is flattened along its axial length (Figure 5A), and circular when viewed from anterior or posterior directions (Figure 5B). The lateral view of the schematic model eye drawing (Figure 5A) was obtained by tracing the frozen section outline of a chick eye which had been cut horizontally through the plane of

greatest equatorial diameter. An ellipsoid shape could then be fitted to the chick eye outline.

For each eye, retinal surface area was calculated using an equation which describes the surface area of an ellipsoid from which the cornea and part of the anterior sclera has been excised (Figure 6, *formula iv*).

A sample calculation: If the external equatorial diameter (2b) is 11.92 mm, excised cornea diameter (2d) is 9.37 mm, and vitreous chamber depth ($a + k$) is 5.73 mm, then the intermediate formulae shown by *formulae i, ii, iii* (Figure 6) can be used to calculate a = 3.60 mm and k = 2.13 mm, with an eccentricity e = 0.79. Eccentricity is an attribute which mathematically defines a particular ellipsoid shape.

The values for a, b, e, and k can then be substituted into *formula iv* (Figure 6) to obtain a total retinal surface area of 245.4 mm^2. Values for retinal surface area obtained using this mathematical extrapolation corresponded with what was physically measured from fresh retinae dissected in an initial test session.

All experimental measurements were taken with reference to the inner (retinal) surface of the eye, rather than the outside. Hence, vitreous chamber depths were determined from *in vivo* A-scan ultrasonography recordings, and external caliper measurements of equatorial diameters were corrected for scleral wall thickness. Average scleral wall thickness at the equatorial region of the eye was 0.15 mm ± 0.005, as measured by calipers from 12 randomly chosen scleral samples. The diameters of the excised anterior portions of the eye could be directly measured with calipers along the inner ocular surface.

Figure 5: Schematic representations of the chick eye from (A) lateral and (B) anterior perspectives. The chick eye can be mathematically fitted to an ellipsoid which is flattened along its axial length, and circular when viewed from anterior or posterior directions. The experimental parameters which are accessible by ultrasonography or caliper measurements include the vitreous chamber depth, excised cornea diameter, and equatorial diameter. These data can then be substituted into mathematical formulae to calculate the total retinal surface area for each chick eye. All measurements were taken with reference to the inner (retinal) surface of the eye. See text for details and a sample calculation.

SCHEMATIC EYE DIAGRAMS FOR RETINAL SURFACE AREA CALCULATIONS

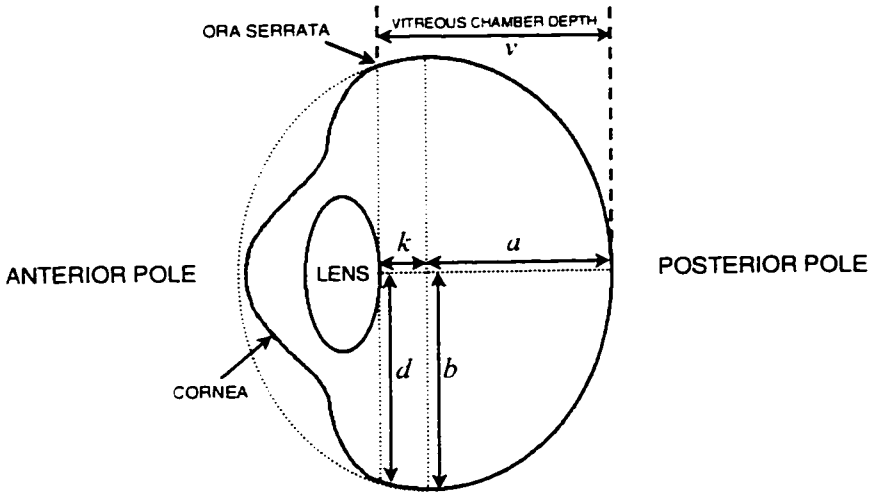

A LATERAL VIEW OF CHICK EYE

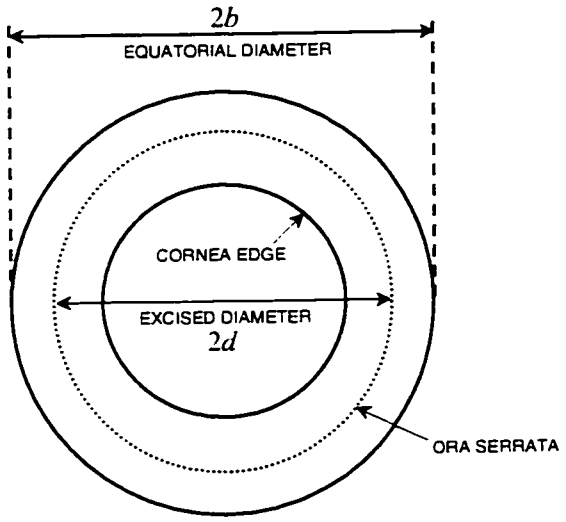

B ANTERIOR VIEW OF CHICK EYE

Where experimentally accessible measurements are v, $2d$, and $2b$:

$v = (a + k)$	is the vitreous chamber depth
$2d$	is the excised cornea diameter
$2b$	is the equatorial diameter

Figure 6: Retinal surface areas were calculated from ocular measurements which were experimentally accessible. These included vitreous chamber depth (a+k), excised cornea diameter (2d), and equatorial diameter (2b). These data were used in intermediate formulae (*i*, *ii*, *iii*) to obtain values for a, k, and e, which were then substituted into formula *iv* to calculate the total retinal surface area for each chick eye.

FORMULAE FOR CALCULATING RETINAL SURFACE AREA

Variables are defined in the schematic eye diagrams, shown previously (Figure 5).

The experimentally accessible ocular measurements are v, $2b$, $2d$:

Where,		
	$v = (a-k)$	is the vitreous chamber depth.
	$2d$	is the excised cornea diameter.
	$2b$	is the equatorial diameter.

For each eye, first calculate values for a, k, and e (eccentricity):

$$a = \frac{v}{1 - \sqrt{1 - \frac{d}{b}}} \qquad \text{..... } (i)$$

$$k = \frac{v\sqrt{1 - \frac{d^2}{b^2}}}{1 - \sqrt{1 - \frac{d^2}{b^2}}} \qquad \text{..... } (ii)$$

$$e = \sqrt{1 - \frac{a^2}{b^2}} \qquad \text{..... } (iii)$$

Then use the following ellipsoid formula to calculate the total retinal surface area:

$$s = \pi b^2 - 2\pi \frac{a^2}{e} \ln\left|\frac{1-e}{\sqrt{1-e^2}}\right| - \pi b^2 \frac{k}{a}\sqrt{1 - e^2\left(1 - \frac{k^2}{a^2}\right)} - \pi \frac{a^2}{e} \ln\left|\frac{a(1-e)}{ke - a\sqrt{1 - e^2\left(1 - \frac{k^2}{a^2}\right)}}\right| \qquad \text{..... } (iv)$$

5.3 Cell count extrapolations

Total cell counts per retinal section and per eye were calculated from image cell density measurements. In brief, the number of cells per image and image cell density were first determined from each of the 2000 confocal images using computerized image analysis software (described previously). Image densities which pertained to a particular retinal section (A,B,C, or E) were averaged. For each retinal section, a section-specific cell count was obtained by multiplying the average image density and the specific retinal surface area corresponding to the particular retinal segment. Specific retinal surface areas (calculated from total retinal surface areas) varied depending on the growth and size of the eye being considered.

Total cell counts were obtained by summing the section-specific cell counts for retinal segments A, B, C, D, and if applicable, E. With the exception of one experiment (form deprivation myopia/serotonergic cells), data for retinal section D needed to be extrapolated. This was accomplished by first statistically assessing (using one-way ANOVA analysis with a 0.05 confidence interval) the variability of cell density data within the peripheral regions (A,B,C) of each eye. No significant intraocular differences were found when comparing the peripheral density data within any eye. Hence a density value for each D region was taken to be the average of the A, B, and C densities within a particular eye. The appropriate specific retinal surface area was used to convert the cell density for section D into a cell count value.

5.4 Statistical analysis

The statistical significance between ocular measurements and their corresponding controls

was assessed using the Student t-test at a probability level of $p<0.05$ with a 95% confidence interval. Statistical comparisons between treated and control eyes were made for refractive errors, ocular wet weights, axial lengths, vitreous chamber depths, equatorial diameters, anterior compartments, retinal surface areas, retinal section cell densities, and retinal section cell counts.

6.0 PART II: Dendritic fields by confocal z sectioning

Qualitative changes in the dendritic fields of dopaminergic amacrine cells were first examined using an epi-fluorescent light microscope (Nikon Labophot-2A) with a Nikon G2-A filter module (main wavelength at 546 nm) suitable for visualizing Texas Red and other rhodamine fluorochromes. The confocal microscope was subsequently used to record z-sections across individual cells, which involved taking an automated series of optical sections at regularly spaced intervals across the thickness of the retina (i.e. along the z axis). Ten to twenty images were recorded at 1-5 micron intervals across each cell. Each series of images was stacked into composite overlays, resulting in final unified images topographically represented in two-dimensional format (Figure 7). Colour-coding was applied to the stacked images, to represent different depths of the cell and its dendrites within the composite image. This is comparable to the use of colour in geographical maps, which show mountains versus sea-level in different colours. All confocal parameters (magnification, line averaging, pinhole size, laser source, and filters) were identical to those previously described for the cell count data, with the only exception being that zoom factor was increased to 65-75x. Adobe Photoshop 4.0 was used to trace polygonal outlines around the dendritic tips of the imaged dopaminergic amacrine cells.

CONFOCAL IMAGE OVERLAYS

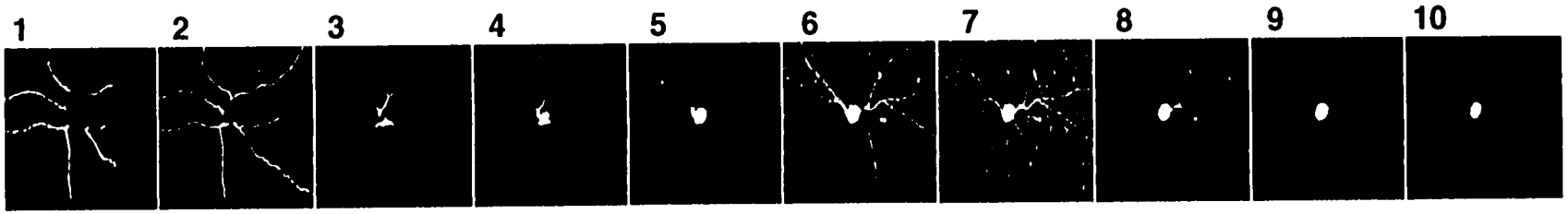

Figure 7A: The creation of an image overlay involves capturing a series of confocal images taken at regular intervals across the selected object. Upper and lower limits along the z axis are first selected, then features such as contrast, brightness, and picture resolution are optimized.

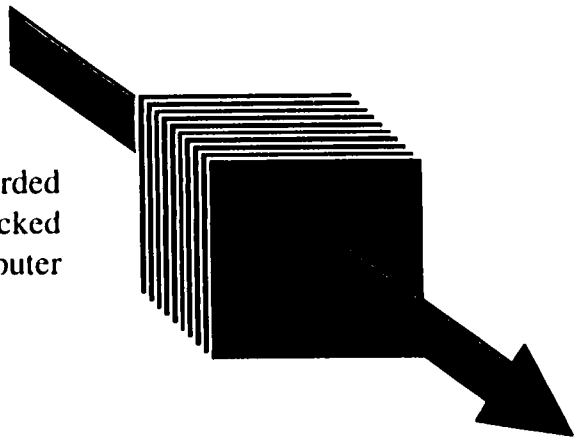

Figure 7B: The recorded confocal images are stacked together using computer imaging software.

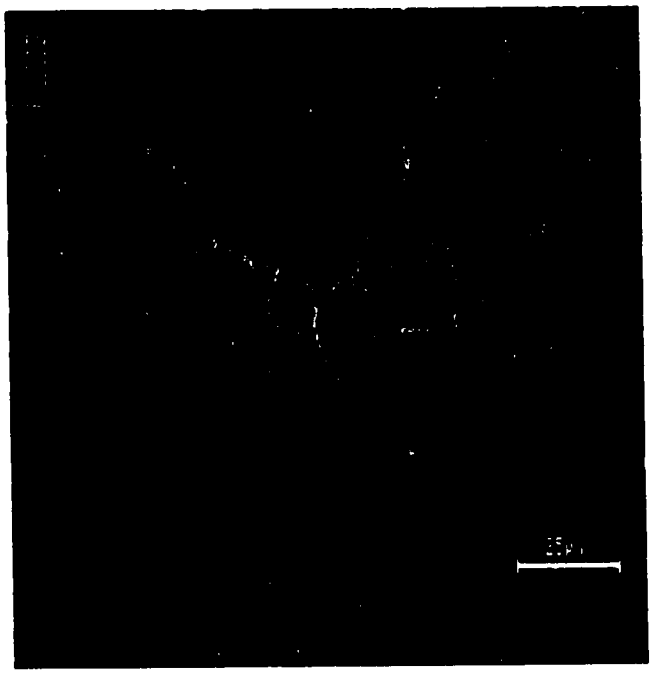

Figure 7C: The final confocal image overlay is a colour-coded composite which represents the three dimensional cell in a two dimensional format.

Any relative comparisons between a treated and a control eye were always made within a same animal. Paired comparisons were also adjusted to comprise the same image scale, brightness, and contrast levels. Confocal image overlays were stored as PIC files since this image format contains information about measure bars, colour, and general file parameters.

7.0 Part III: HPLC analysis

7.1 Retinal dissection

For the HPLC studies, form deprivation myopia and defocus-induced hyperopia were produced in chicks according to the same experimental and animal care protocols described earlier in this thesis. Chicks were sacrificed by decapitation during the middle of the light cycle, and the eyes were rapidly enucleated. In order to minimize the time between sacrifice and retinal tissue harvest, no wet weights or ocular dimensions of the enucleated eyes were measured. All dissections were performed as rapidly as possible, and tissue specimens were kept on ice-cooled glass petri dishes during all dissection procedures. Eyes were sectioned into 5 segments and coded A, B, C, D, and E, as described previously (Figure 3B). In brief, a central portion (E) was initially isolated with a circular trephine blade (7 mm diameter), and the remaining peripheral retina was divided into four quadrants: temporal (A), superior (B), nasal (C), and inferior (D). Section D was discarded since it is very difficult to dissect the retina from this region due to the presence of the optic nerve head and pecten. The retinae from the remaining sections A, B, C, and E were separated from the adhering retinal pigment epithelium (RPE) using fine forceps (Dumont #5, Switzerland) and a dissecting microscope (Nikon). It was extremely important to remove all traces

of RPE from the retina, since this would adversely affect HPLC measurements of serotonin and 5-HIAA. Dissected retinae samples were rinsed in ice-cold saline solution (0.9%), and transferred to microcentrifuge tubes (VWRbrand, 0.5 mL) that had been pre-cooled with $CO_{2(s)}$ (dry ice). Samples in microcentrifuge tubes were stored overnight in a styrofoam shipping box packed with dry ice, then hand-delivered the following day to The University of Western Ontario (UWO, London, Ontario) where HPLC-EC assays were performed in the laboratory of Dr. Candace J. Gibson (Department of Pathology). Retinal samples were stored at -80°C at UWO until further processing. A total of 10 animals were used to evaluate the effects of myopia (n=5) and hyperopia (n=5) on levels of dopamine (DA) and its major acid metabolite 3,4-dihydroxyphenylacetic acid (DOPAC), and serotonin (5HT) and its major acid metabolite 5-hydroxyindoleacetic acid (5-HIAA).

7.2 HPLC sample preparation and assay

Retinal tissue samples were sonicated in 300 µL homogenizing solution of 0.1 N perchloric acid with 0.1 mM EDTA. Dihydroxybenzylamine (DHBA) was added as an internal standard (100 pg/100µL). The samples were centrifuged (12000 ***g***, 15 min) in order to separate the supernatant from the protein pellet. HPLC analysis was done on the supernatant fraction, and a standard protein assay (Lowry et al. 1951) was performed on the pellet. All protein samples were resuspended in 100 µL of 0.1 N NaOH and measured during a single session, in duplicate, after completion of all HPLC assays. Supernatant and pellet samples were stored at 4°C until analysis.

For optimal measurements of catecholamines, the HPLC mobile phase solution consisted

of 0.05 M sodium phosphate, 0.1 mM EDTA, 0.17 mM of sodium octyl sulfate (pH adjusted to 3.2) and 9% methanol added. Mobile phase was initially run through the system overnight to equilibrate the column. A C-18 reverse phase column with 5-μm silica particles was used (Beckman Ultrasphere I.P. No. 235334). Prior to the sample run, 100 pg of dopamine, DOPAC, 5-HIAA, 5-HT, and DHBA were run through the column (flow rate=1.5 mL/min). Column temperature was maintained at ambient room temperature (25°C). Individual retinal samples (100 uL aliquots) were applied by manual injection to the column. Compounds were detected using a Coulochem II electrochemical detector (ESA, Inc.) with Detector 1 set at +350 mV and Detector 2 set at -280 mV. Sample peaks were identified based on retention times and oxidation potentials, and quantified by comparing the ratio between standard and sample peak heights. Retention times for monoamines using these parameters, optimized for catecholamines, were as follows: DHBA = 4.5 minutes, DOPAC = 6.5 minutes, DA = 7.5 minutes, 5-HIAA = 12.5 minutes, and 5HT = 23.5 minutes.

For the specific analysis of 5HT and 5-HIAA, a second sample aliquot (100 μL) was injected on an HPLC system optimized for measuring indoleamines. In this case, the mobile phase consisted of 0.05 M sodium acetate, 0.1 mM EDTA at pH 4.6 with 7% methanol added. The same type of reversed phase column was used as described for the catecholamine assay. Serotonin and 5-HIAA were detected using a Coulochem 5100A detector (ESA, Inc.) with Detector 1 set at 50 mV and Detector 2 set at +350 mV. Standards (100 pg) of each compound were taken through the entire process of sample preparation, and used to calculate final sample concentrations of 5HT and 5-HIAA in the retinal tissue. In addition, an external standard (100 pg of each compound) was run

to establish retention times and identity of the peaks (retention times: 5HT = 5 minutes, 5-HIAA = 8 minutes).

All HPLC measurements were performed without knowledge of what particular retinal sample was found in each of the numbered vials. These blind assay results were later correlated with sample identity.

7.3 Statistical analysis

HPLC results were statistically analysed using the Student t-test at a probability level of $p<0.05$ with a 95% confidence interval. Comparisons were made between retinal sections from eyes treated with FDM or DIH, and their corresponding controls. The DOPAC/DA and 5-HIAA/5HT ratios were similarly assessed. Overall comparisons were made by pooling all sections from one eye, and performing the Student t-test on these combined values.

8.0 RESULTS

The results of this study are presented in three parts. Part I involves cell densities, cell counts, and ocular data relating to how the three induced ametropias (form deprivation myopia FDM, defocus-induced myopia DIM, and defocus-induced hyperopia DIH) affect dopaminergic and serotonergic amacrine cell populations. Part II is based on serial confocal images acquired during the course of this study. Confocal images which illustrate changes in dendritic field size and density of dopaminergic amacrine cells in response to induced ametropias are presented. Part II also provides information about general retinal structure, amacrine cells, serotonergic bipolar cells, and photoreceptors. Part III reports HPLC data from retinae in which FDM and DIH were induced.

8.1 Part I: Refractive states, ocular dimensions, cell densities, and cell counts

8.1.1 Group #1: Dopaminergic amacrines and defocus-induced myopia.

In both the pilot and repeat groups of chicks, the treated eyes became significantly myopic (-10.7±1.2D and -11.0±2.1D respectively, $p<0.0005$) compared to control eyes (Figure 8) as measured on the final day of each experiment. Throughout the duration of the experiment, control eyes remained slightly hyperopic (pilot=2.3±0.1D, repeat=1.7±0.3D) in a manner comparable to what has been previously documented for the untreated eyes of young chicks (Irving et al. 1996). In all cases, myopic eyes were larger, heavier, and showed greater retinal surface areas relative to control eyes (Table 1). In the pilot study, there was a significant difference in vitreous chamber depth which was counterbalanced by flattening of the cornea. In the repeat study, the overall axial

length and anterior compartment were significantly different ($p<0.05$) in myopic versus control eyes. The other measured parameters did not show statistically significant differences, although the correct trend was generally observed (i.e. dimensions of the myopic eyes were larger than the corresponding dimensions in control eyes). Although the two batches of chicks responded differently to the treatment with respect to their ocular dimensions, the net result was myopia in both groups.

There were no significant differences ($p>0.05$) in dopaminergic cell densities between myopic and control eyes, with the exception of one region of the retina. In the pilot study, no significant differences were found (Tables 2A and 2B). In the repeat group of chicks, there was a slight but significant decrease ($p<0.05$) in cell density in the superior retinal segment in the treated eyes of the repeat group of chicks (Table 2C). Cell densities were then converted into ocular cell counts which accounted for any changes in ocular size between treated and control eyes (Table 2D). These normalized cell counts showed there were no statistically significant differences in dopaminergic cell numbers between treated (myopic) and control eyes, either on a section-by-section or whole eye basis.

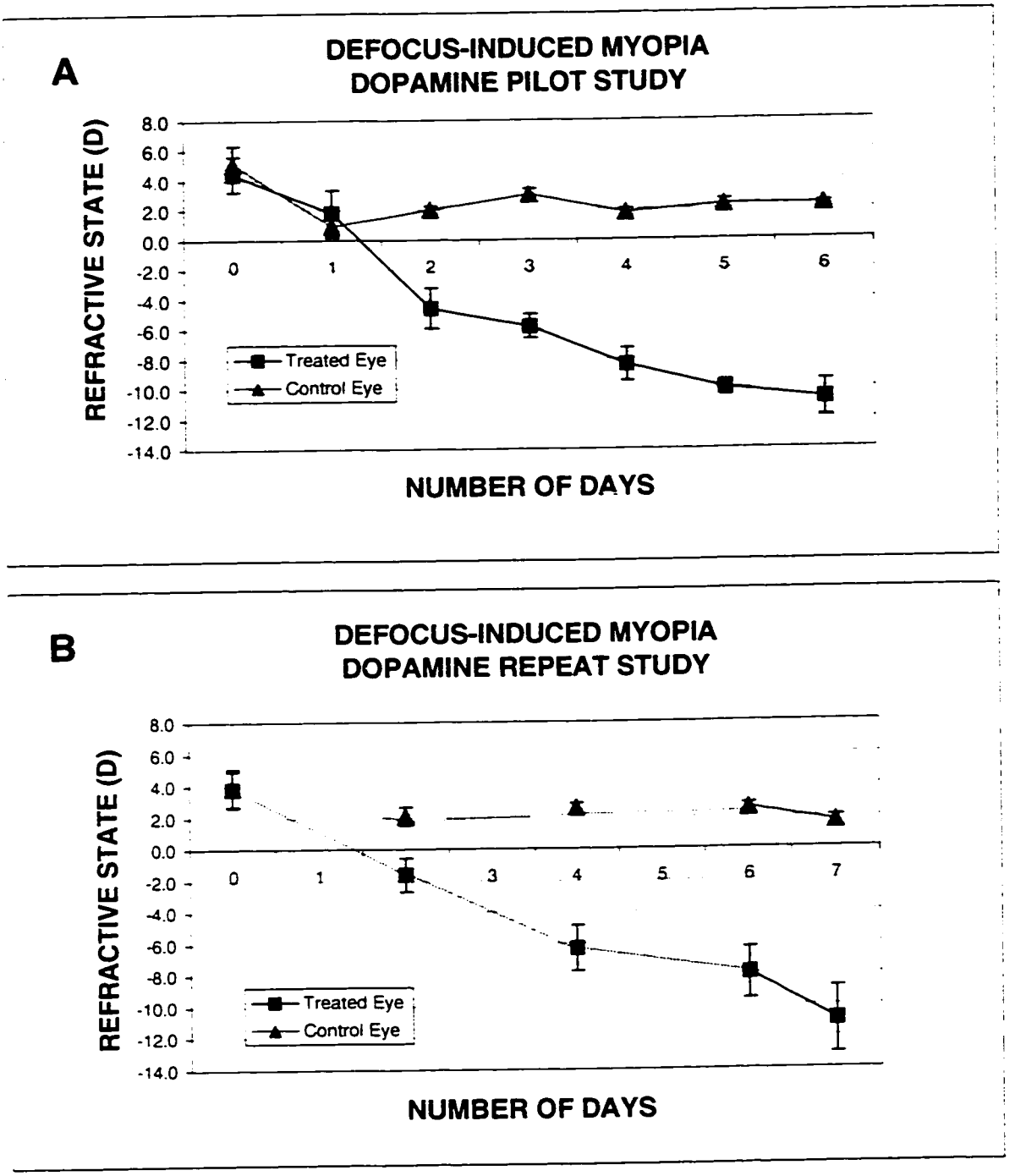

Figure 8: Refractive error development in (A) pilot (n=5) and (B) repeat (n=10) groups of chicks in which dopaminergic amacrine cells were studied by confocal microscopy. Concave lenses unilaterally produced myopia in treated eyes, while the ungoggled contralateral eyes served as controls. Error bars represent standard errors of the mean. In both pilot and repeat groups, final day refractive errors in treated eyes were significantly different compared to control eyes ($p<0.005$).

DEFOCUS-INDUCED MYOPIA
DOPAMINE STUDIES

	n	TREATED EYE	CONTROL EYE
OCULAR WET WEIGHT (g)			
Pilot	5	0.688 ± 0.011	0.655 ± 0.011
Repeat	10	0.642 ± 0.019	0.613 ± 0.012
AXIAL LENGTH (mm)			
Pilot	5	9.45 ± 0.17	9.23 ± 0.11
Repeat	10	* 9.28 ± 0.11	8.89 ± 0.09
VITREOUS CHAMBER DEPTH (mm)			
Pilot	5	** 6.19 ± 0.13	5.64 ± 0.06
Repeat	10	5.66 ± 0.09	5.44 ± 0.06
ANTERIOR COMPARTMENT (mm)			
Pilot	5	3.25 ± 0.16	3.59 ± 0.15
Repeat	10	*** 3.19 ± 0.11	2.75 ± 0.05
EQUATORIAL DIAMETER (mm)			
Pilot	5	11.93 ± 0.10	11.71 ± 0.11
Repeat	10	11.77 ± 0.12	11.68 ± 0.07
RETINAL SURFACE AREA (mm^2)			
Pilot	5	* 249.7 ± 2.3	240.4 ± 3.2
Repeat	10	235.8 ± 4.5	230.4 ± 3.4

* $p < 0.05$
** $p < 0.01$
*** $p < 0.005$

Table 1: Final day changes in ocular size and dimensions resulting from defocus-induced myopia. Data are followed by ± standard errors of the mean. Significant differences between treated and control eyes are indicated by one or more asterisks. In both pilot and repeat groups of chicks, the retinal surface areas of treated eyes were always larger compared to control eyes, although this was only statistically significant for the pilot study. Dopaminergic amacrine cell populations within the retinae of these chicks were examined by confocal microscopy.

DEFOCUS-INDUCED MYOPIA
DOPAMINE PILOT STUDY

SECTION DENSITIES (cells·mm^{-2})

RETINAL SECTION	TREATED EYE	CONTROL EYE
A (Temporal)	23.0 ± 2.6	25.2 ± 1.3
B (Superior)	25.0 ± 1.3	28.6 ± 2.2
C (Nasal)	25.6 ± 2.2	27.9 ± 2.1
D (Inferior)[$]	24.5 ± 1.2	27.2 ± 1.1

[$] extrapolated from surrounding retinal regions

Table 2A: Comparison of treated versus control cell densities in specific retinal sections of pilot group animals (n=5). Data are expressed as cells/mm^2 ± standard errors of the mean. Treatment with concave lenses did not cause any significant differences in cell density between any localized portion of the retinae in this pilot study.

NORMALIZED CELL COUNTS PER SECTION

RETINAL SECTION	TREATED EYE	CONTROL EYE
A (Temporal)	1438.1 ± 166.6	1535.0 ± 50.6
B (Superior)	1563.4 ± 90.7	1740.3 ± 103.0
C (Nasal)	1600.5 ± 146.2	1701.6 ± 118.0
D (Inferior)[$]	1532.4 ± 114.0	1659.7 ± 78.6
TOTAL CELL COUNT PER EYE	6134.4 ± 455.6	6636.6 ± 314.4

[$] extrapolated from surrounding retinal regions

Table 2B: Normalized cell counts in each section. When dopaminergic cell densities in each section (from Table 2A above) were converted to cell counts that accounted for changes in eye size, there were no overall significant differences between treated and control eyes. Data are followed by ± standard errors of the mean.

DEFOCUS-INDUCED MYOPIA
DOPAMINE REPEAT STUDY

SECTION DENSITIES (cells mm^2)

RETINAL SECTION	TREATED EYE	CONTROL EYE
A (Temporal)	24.2 ± 2.4	24.1 ± 1.6
B (Superior)	* 25.0 ± 0.9	27.9 ± 1.3
C (Nasal)	30.4 ± 2.2	27.8 ± 1.4
D (Inferior)[$]	26.6 ± 1.2	26.6 ± 0.9
E (Central)	31.4 ± 1.8	31.5 ± 2.0

[$] extrapolated from surrounding retinal regions
*p <0.05

Table 2C: Comparison of myopic versus control dopaminergic amacrine densities in specific retinal sections. Data was obtained from a repeat group of chicks (n=10) in which DIM had been produced and dopaminergic amacrine cells studied. Data values are expressed as cells/mm^2 ± standard errors of the mean. A slight but significant decrease in cell density was found within the superior region of the treated retinae (indicated by an asterisk *).

NORMALIZED CELL COUNTS PER SECTION

RETINAL SECTION	TREATED EYE	CONTROL EYE
A (Temporal)	1193.0 ± 124.8	1151.6 ± 68.8
B (Superior)	1232.1 ± 53.6	1332.9 ± 51.0
C (Nasal)	1497.8 ± 114.8	1332.3 ± 67.5
D (Inferior)[$]	1307.7 ± 86.5	1272.4 ± 51.5
E (Central)	1209.8 ± 67.7	1255.0 ± 82.2
TOTAL CELL COUNT PER EYE	6440.4 ± 410.0	6344.1 ± 278.8

[$] extrapolated from surrounding retinal regions

Table 2D: Normalized cell counts in each section. Dopaminergic cell counts which were calculated from cell densities showed there were no localized or overall significant differences between treated and control eyes. Data are followed by ± standard errors of the mean.

8.1.2 Group #2: Serotonergic amacrines and defocus-induced myopia.

Treated eyes became significantly myopic (-9.9±1.5D, $p<0.000025$) in response to concave lenses, while control eyes remained slightly hyperopic (2.4±0.2D, Figure 9). Treated eyes also became larger, in all physical dimensions, compared to control eyes (Table 3). Axial lengths and anterior compartments in treated eyes were significantly larger than controls. Wet weights, equatorial diameters, vitreous chamber depths, and retinal surface areas were not significantly different, but the correct trend was still observed in these parameters when comparing treated measurements relative to controls (i.e. treated eyes were larger).

There were no significant differences in serotonergic cell densities (Table 4A) or overall cell counts (Table 4B) when comparing treated (myopic) versus control eyes on a section-by-section or whole eye basis.

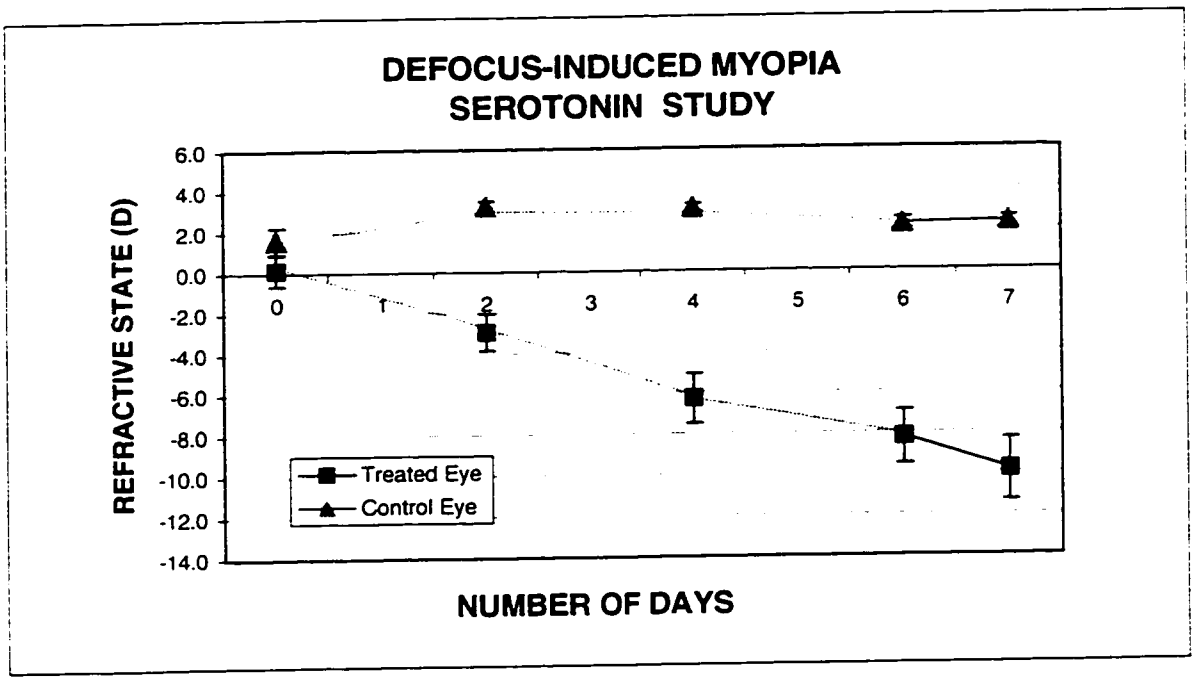

Figure 9: Refractive error development in chicks (n=10) unilaterally treated with concave lenses to induce defocus-induced myopia. The contralateral eyes were left ungoggled and served as controls. Error bars represent standard errors of the mean. Initial day refractive states were not significantly different between either eye. Final day refractive measurements were significantly different from one another when comparing treated versus control eyes ($p<0.000025$). Retinae from these chicks were specifically stained in order to examine the serotonergic amacrine cells.

DEFOCUS-INDUCED MYOPIA
SEROTONIN STUDY

	n	TREATED EYE	CONTROL EYE
OCULAR WET WEIGHT (g)	10	0.612 ± 0.015	0.582 ± 0.009
AXIAL LENGTH (mm)	10	*** 9.11 ± 0.11	8.63 ± 0.05
VITREOUS CHAMBER DEPTH (mm)	10	5.55 ± 0.07	5.42 ± 0.05
ANTERIOR COMPARTMENT (mm)	10	*** 3.25 ± 0.08	2.94 ± 0.06
EQUATORIAL DIAMETER (mm)	10	11.63 ± 0.11	11.59 ± 0.07
RETINAL SURFACE AREA (mm^2)	10	229.0 ± 4.9	224.7 ± 3.2

*** $p < 0.005$

Table 3: Final day ocular size and dimensions of chick eyes in which defocus-induced myopia was produced using concave lenses, compared to untreated control eyes. Values are presented as the mean and standard error of the mean. In all aspects, treated eyes were larger than control eyes. Highly significant differences between treated and control eyes are marked with asterisks. Serotonergic cell populations were subsequently examined in these retinae.

SECTION DENSITIES (cells/mm²)

RETINAL SECTION	TREATED EYE	CONTROL EYE
A (Temporal)	518.4 ± 24.9	472.6 ± 23.3
B (Superior)	548.2 ± 26.8	545.8 ± 24.5
C (Nasal)	493.0 ± 24.7	477.6 ± 26.3
D (Inferior)[$]	519.9 ± 14.8	498.7 ± 15.1
E (Central)	725.2 ± 23.6	779.4 ± 31.8

[$] extrapolated from surrounding retinal regions

Table 4A: Comparison of myopic versus control serotonergic amacrine densities in specific retinal sections (n=10). Values are expressed as number of cells/mm² ± standard errors of the mean. No significant differences in serotonergic amacrine cell densities were observed between eyes treated with concave lenses and their respective control eyes.

NORMALIZED CELL COUNTS PER SECTION

RETINAL SECTION	TREATED EYE	CONTROL EYE
A (Temporal)	24987.5 ± 1469.8	21852.2 ± 1027.3
B (Superior)	25975.7 ± 1697.8	25817.2 ± 1171.0
C (Nasal)	22973.5 ± 1188.0	22180.1 ± 1110.6
D (Inferior)[$]	24644.7 ± 1192.9	23283.1 ± 725.0
E (Central)	28177.4 ± 967.3	29992.4 ± 1224.9
TOTAL CELL COUNT PER EYE	126758.8 ± 4984.4	123125.1 ± 3272.9

[$] extrapolated from surrounding retinal regions

Table 4B: Normalized serotonergic cell counts in each section, converted from values in Table 4A. There were no significant differences in regionalized or overall cell counts, as determined from serotonergic amacrine cell densities within the retinae. Values are expressed as number of cells/mm² ± standard errors of the mean.

8.1.3 Group #3: Dopaminergic amacrines and form deprivation myopia.

Figure 10 shows that translucent goggles produced significant amounts ($p<0.000001$) of myopia in treated eyes (-27.4±1.5D) versus controls (2.1±0.3D). The form deprivation method generally provokes approximately three times more myopia than is possible with concave lenses.

Tables 5A and 7A show typical initial day *in vivo* measurements of the eyes of newly-hatched chicks. On the initial day of these experiments, there were no significant differences between either eye for any measured optical or physical parameter. After treatment with translucent goggles, all measured dimensions of treated eyes were significantly different from control eyes. This included significant increases in axial lengths, vitreous chamber depths, anterior compartments, and retinal surface areas of the treated eyes relative to the control eyes (Table 5B).

When comparing localized regions of the retina or when averaging the data across whole eyes, there were no significant differences in dopaminergic cell densities (Table 6A) or cell counts (Table 6B) between control and treated eyes in which form deprivation myopia had been induced.

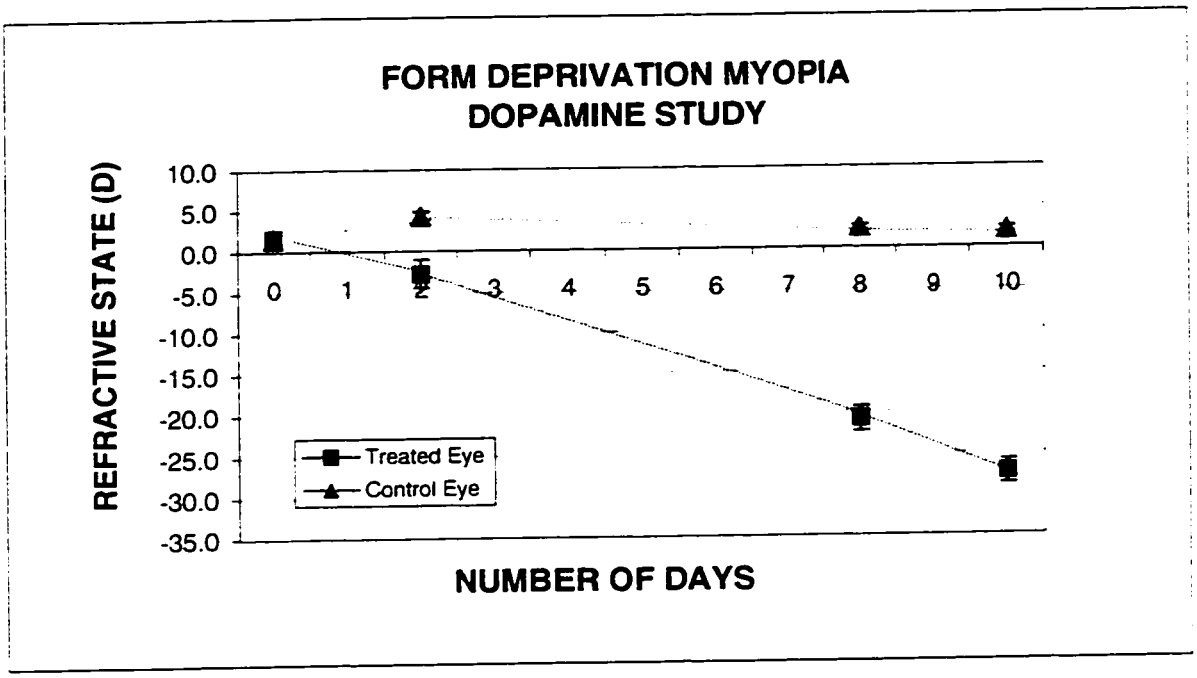

Figure 10: Refractive error development in chicks (n=7) in which form deprivation was unilaterally induced using translucent goggles. Error bars represent standard errors of the mean. Final day refractive states between treated and control eyes were significantly different from each other ($p<0.000001$). Dopaminergic amacrine cells within the retinae of these chicks were subsequently assessed by confocal microscopy.

FORM DEPRIVATION MYOPIA
DOPAMINE STUDY

A

INITIAL DAY MEASUREMENTS	n	TREATED EYE	CONTROL EYE
AXIAL LENGTH (mm)	7	7.79 ± 0.11	7.67 ± 0.05
VITREOUS CHAMBER DEPTH (mm)	7	5.27 ± 0.11	5.28 ± 0.03
ANTERIOR COMPARTMENT (mm)	7	2.52 ± 0.06	2.39 ± 0.03

B

FINAL DAY MEASUREMENTS	n	TREATED EYE	CONTROL EYE
AXIAL LENGTH (mm)	7	*** 10.19 ± 0.15	8.49 ± 0.08
VITREOUS CHAMBER DEPTH (mm)	7	*** 6.82 ± 0.10	5.72 ± 0.07
ANTERIOR COMPARTMENT (mm)	7	*** 3.38 ± 0.13	2.77 ± 0.06
RETINAL SURFACE AREA (mm^2)	7	*** 304.4 ± 2.7	257.2 ± 1.9

*** $p < 0.005$

Table 5: Initial and final day ocular measurements. Initial day measurements showed no significant differences between any physical ocular parameters (A). On the final day of the experiment, highly significant differences in ocular dimensions existed between control and treated eyes in which form deprivation myopia had been induced (B). Data are followed by ± standard errors of the mean. Dopaminergic amacrine cells from these retinae were subsequently examined by confocal microscopy.

FORM DEPRIVATION MYOPIA
DOPAMINE STUDY

SECTION DENSITIES (cells/mm²)

RETINAL SECTION	TREATED EYE	CONTROL EYE
A (Temporal)	25.5 ± 2.5	26.5 ± 2.2
B (Superior)	29.1 ± 2.3	28.6 ± 1.2
C (Nasal)	27.8 ± 1.4	30.6 ± 3.7
D (Inferior)[$]	27.5 ± 1.2	28.6 ± 1.2

[$] extrapolated from surrounding retinal regions

Table 6A: Comparison of form-deprived versus control dopaminergic amacrine densities in specific retinal sections (n=7). There were no significant differences were found between corresponding regions of form-deprived versus control retinae. Data are expressed as cells/mm² ± standard errors of the mean.

NORMALIZED CELL COUNTS PER SECTION

RETINAL SECTION	TREATED EYE	CONTROL EYE
A (Temporal)	1943.5 ± 194.4	1702.0 ± 145.6
B (Superior)	2215.5 ± 180.9	1839.7 ± 81.2
C (Nasal)	2115.3 ± 106.5	1973.2 ± 243.3
D (Inferior)[$]	2093.1 ± 146.7	1838.0 ± 141.9
TOTAL CELL COUNT PER EYE	8367.4 ± 588.1	7352.8 ± 568.7

[$] extrapolated from surrounding retinal regions

Table 6B: Normalized dopaminergic cell counts in each section. Conversion of dopaminergic cell densities to cell counts did not reveal any localized or overall significant differences between treated and control eyes. Data are followed by ± standard errors of the mean.

8.1.4 Group #4: Serotonergic amacrines and form deprivation myopia.

Form deprivation myopia produced similar effects on ocular dimensions and refractive state as group #3. All final day physical and optical measurements from eyes treated with translucent goggles were significantly different than control eyes. These included significant differences in refractive states (Figure 11, $p=1.2x10^{-7}$), wet weights, axial lengths, vitreous chamber depths, anterior compartments, equatorial diameters, and retinal surface areas (Table 7B). This contrasts with initial day measurements, where there were no significant differences between either eye (Table 7A).

Interocular comparisons between form-deprived and control eyes showed highly significant differences in cell densities and cell counts within localized areas of the retina. There was a significant decrease ($p<0.01$) in the serotonergic cell densities in the superior, nasal, and central regions of the retina (Table 8A). Conversion of these density values to cell counts (Table 8B) showed that two out of three significant density differences were simply due to increased retinal surface area as a result of treatment with the goggles. The only region that remained significantly different ($p<0.05$) was the central portion of the retina, with the myopic eye showing significantly fewer cells compared to control eyes. Comparison on a whole eye basis (i.e. pooling intraocular regional data) showed there were no overall significant cell count differences between treated and control eyes (Table 8B), although a trend for lower cell counts was evident in treated eyes. All serotonergic cell counts in retina segments of myopic eyes were lower than the corresponding regions in control eyes.

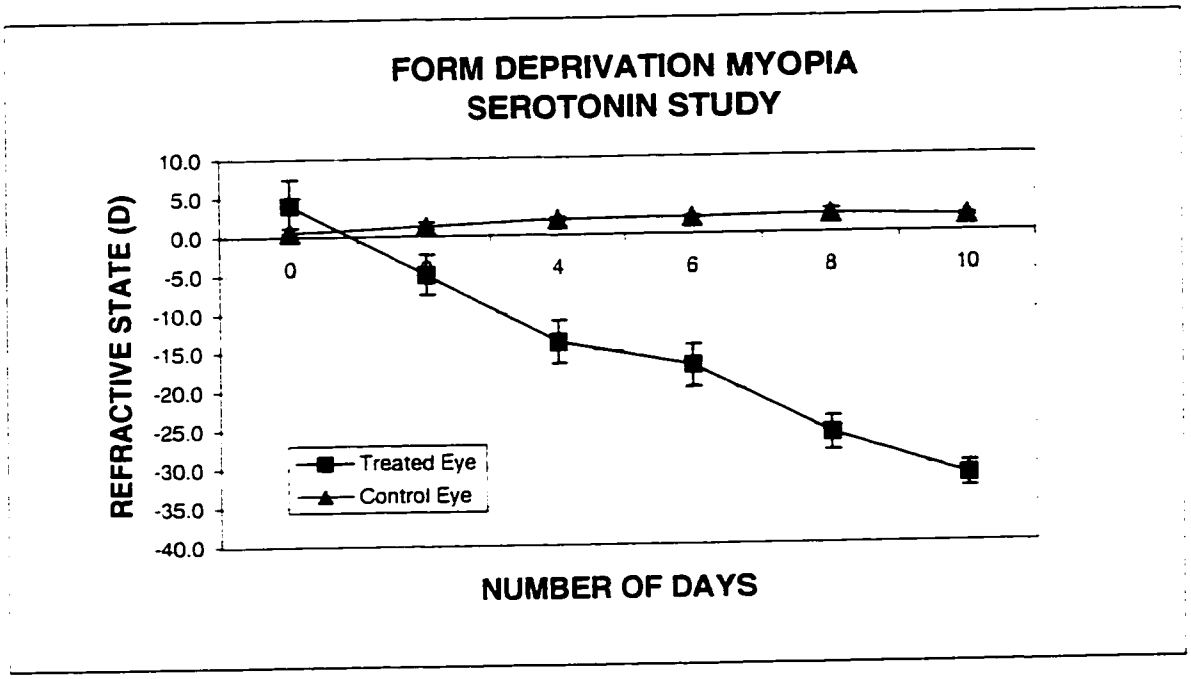

Figure 11: Progression of refractive error in the eyes of chicks (n=8) treated with translucent goggles to produce form deprivation myopia. Untreated contralateral eyes served as controls. Error bars represent standard errors of the mean. The difference in final day refractive errors between treated and control eyes was highly significant ($p<0.000001$). Retinae from these chicks were immunohistochemically processed to examine the serotonergic amacrine cells.

FORM DEPRIVATION MYOPIA
SEROTONIN STUDY

A

INITIAL DAY MEASUREMENTS	n	TREATED EYE	CONTROL EYE
AXIAL LENGTH (mm)	8	7.83 ± 0.04	7.82 ± 0.05
VITREOUS CHAMBER DEPTH (mm)	8	5.35 ± 0.02	5.41 ± 0.04
ANTERIOR COMPARTMENT (mm)	8	2.49 ± 0.03	2.41 ± 0.04

B

FINAL DAY MEASUREMENTS	n	TREATED EYE	CONTROL EYE
OCULAR WET WEIGHT (g)	8	*** 0.868 ± 0.018	0.714 ± 0.011
AXIAL LENGTH (mm)	8	*** 10.90 ± 0.15	9.40 ± 0.05
VITREOUS CHAMBER DEPTH (mm)	8	*** 6.60 ± 0.09	5.65 ± 0.06
ANTERIOR COMPARTMENT (mm)	8	*** 3.65 ± 0.11	2.91 ± 0.08
EQUATORIAL DIAMETER (mm)	8	* 12.76 ± 0.13	12.29 ± 0.08
RETINAL SURFACE AREA (mm^2)	8	*** 299.1 ± 4.8	258.5 ± 3.5

* $p < 0.05$
*** $p < 0.005$

Table 7: Initial and final day ocular parameters for form-deprived retinae in which serotonin amacrines were examined. On the initial day, there were no significant physical differences between either eye prior to unilateral application of translucent goggles in this group of chicks (A). At the end of the experiment, all ocular dimensions were significantly larger in the form-deprived eyes compared to the untreated control eyes (B). Values represent the mean and SEM measurements. These retinae were processed immunohistochemically to examine serotonergic cell populations.

FORM DEPRIVATION MYOPIA
SEROTONIN STUDY

SECTION DENSITIES (cells/mm²)

RETINAL SECTION	TREATED EYE	CONTROL EYE
A (Temporal)	335.9 ± 31.7	400.2 ± 18.9
B (Superior)	** 381.2 ± 23.3	484.9 ± 28.0
C (Nasal)	*** 343.0 ± 22.6	448.7 ± 22.9
D (Inferior)	436.9 ± 63.9	428.6 ± 22.1
E (Central)	*** 524.9 ± 46.5	692.6 ± 28.3

** $p < 0.01$
*** $p < 0.005$

Table 8A: Comparison of cell densities in form-deprived eyes and their corresponding controls (n=8). Highly significant decreases in serotonergic amacrine cell densities were found in the superior, nasal, and central regions of the treated retinae (indicated by asterisks). Data are expressed as cells/mm² ± standard errors of the mean.

NORMALIZED CELL COUNTS PER SECTION

RETINAL SECTION	TREATED EYE	CONTROL EYE
A (Temporal)	18788.7 ± 2058.5	20689.4 ± 1187.9
B (Superior)	22084.9 ± 1437.6	25806.9 ± 1932.0
C (Nasal)	19669.7 ± 1480.9	23000.1 ± 1555.3
D (Inferior)	22705.5 ± 1619.4	22970.7 ± 1545.5
E (Central)	*19560.7 ± 1710.7	26590.6 ± 525.3
TOTAL CELL COUNT PER EYE	102809.4 ± 6271.0	119057.8 ± 5104.4

* $p < 0.05$

Table 8B: Normalized serotonergic amacrine counts per section. When cell densities were converted to cell counts, a significant decrease in the number of serotonergic amacrine cells was observed within the central region of the form-deprived retinae compared to control eyes (see asterisk). After normalization to account for changes in eye size, the significant differences in nasal and superior retinal densities did not translate into significant differences in cell count. There were no statistically significant differences between overall cell counts per eye, although the general trend appeared to be decreased cell numbers in treated versus control eyes. Data represents the mean cell count per area ± SEM.

8.1.5 Group #5: Dopaminergic amacrines and defocus-induced hyperopia.

In both pilot and repeat groups, convex lenses provoked the development of significant ($p<0.0005$) hyperopia in treated eyes compared to control eyes. In the pilot group of chicks, treated eyes showed 8.8±2.3D of hyperopia relative to 1.8±0.3D in control eyes (Figure 12A.). In the repeat group, 7.3±1.0D of hyperopia was measured in treated eyes relative to 1.7±0.6D in control eyes (Figure 12B).

Eye growth responses to convex lenses were more variable (Table 9) than when inducing myopia with concave lenses or translucent goggles. In the pilot group, certain final day parameters in treated eyes were larger than controls, but this was counterbalanced by other measurements being smaller. Measurements for ocular wet weights, axial lengths, and anterior compartments were larger in the treated eyes of the pilot group relative to control eyes. In contrast, vitreous chamber depths, equatorial diameters, and retinal surface areas were smaller in treated versus control eyes. For the repeat group of chicks, the overall axial lengths of treated eyes were significantly shorter ($p<0.05$) than control eyes. Comparisons between vitreous chamber depths, wet weights, and retinal surface areas also followed the same trend. Treated eyes of the repeat group appeared to compensate for the reduction in ocular size by developing slightly larger anterior compartments and equatorial diameters compared to control eyes.

In both pilot and repeat studies, there were no significant differences in dopaminergic cell densities (Tables 10A and 10C) or cell counts (Tables 10B and 10D) when comparing treated (hyperopic) versus control eyes, either on a retinal section-by-section or whole eye basis.

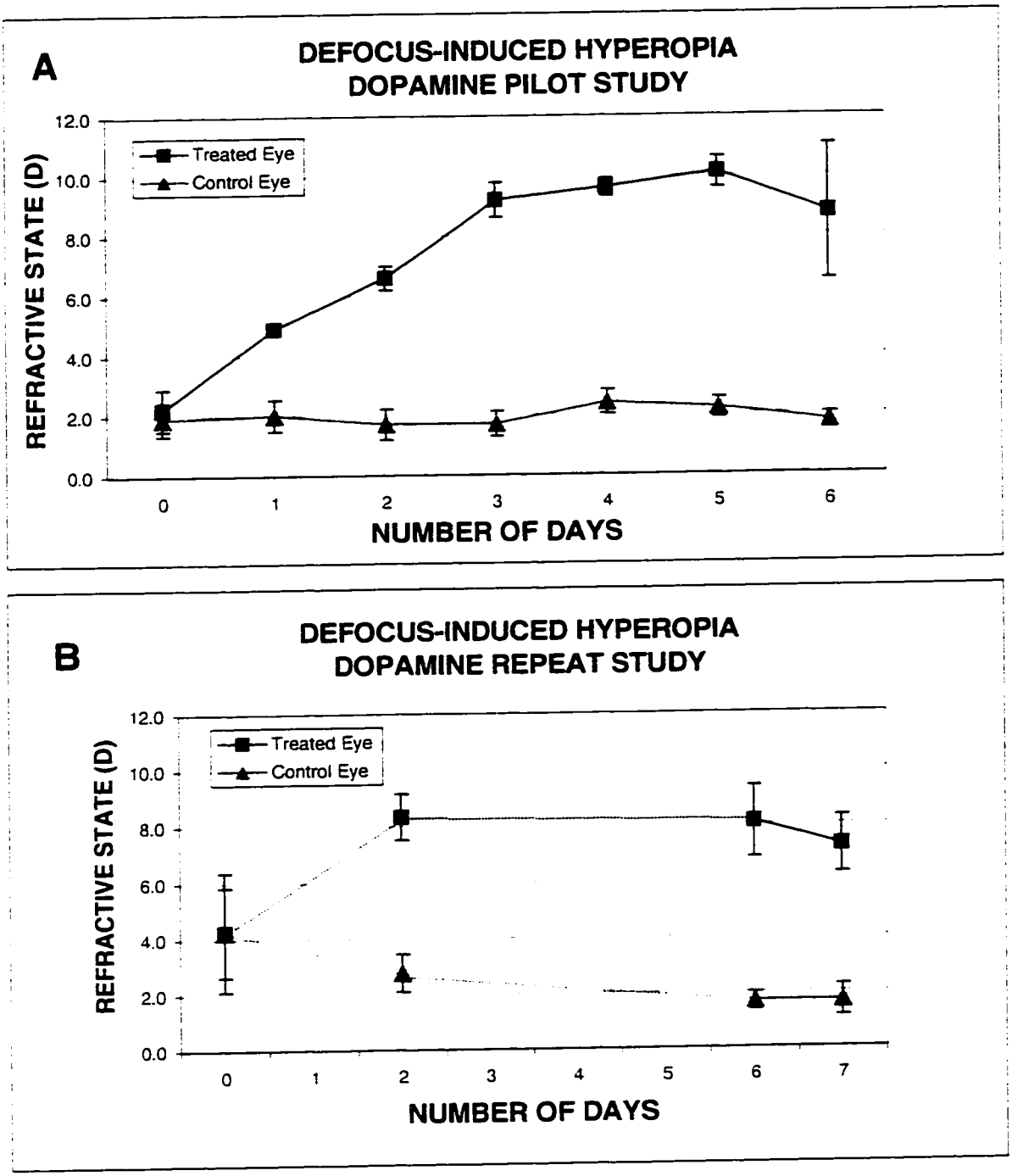

Figure 12: Refractive error development in (A) pilot (n=5) and (B) repeat (n=6) groups of chicks in which convex lenses unilaterally produced defocus-induced hyperopia. Contralateral ungoggled eyes served as controls. Error bars represent standard errors of the mean. Final day refractive errors within treated eyes of both groups were significantly different compared to their respective controls ($p \leq 0.000$. Dopaminergic amacrine cell populations were examined within these retinae.

DEFOCUS-INDUCED HYPEROPIA
DOPAMINE STUDIES

	n	TREATED EYE	CONTROL EYE
OCULAR WET WEIGHT (g)			
Pilot	5	0.539 ± 0.021	0.522 ± 0.032
Repeat	6	0.630 ± 0.013	0.634 ± 0.015
AXIAL LENGTH (mm)			
Pilot	5	8.15 ± 0.15	8.09 ± 0.22
Repeat	6	* 8.64 ± 0.05	8.91 ± 0.08
VITREOUS CHAMBER DEPTH (mm)			
Pilot	5	5.32 ± 0.19	5.33 ± 0.19
Repeat	6	4.92 ± 0.25	5.48 ± 0.06
ANTERIOR COMPARTMENT (mm)			
Pilot	5	* 2.99 ± 0.07	2.71 ± 0.07
Repeat	6	3.28 ± 0.19	2.90 ± 0.09
EQUATORIAL DIAMETER (mm)			
Pilot	5	11.03 ± 0.16	11.33 ± 0.12
Repeat	6	11.86 ± 0.12	11.81 ± 0.13
RETINAL SURFACE AREA (mm^2)			
Pilot	5	203.5 ± 4.4	210.2 ± 5.8
Repeat	6	222.3 ± 8.8	234.4 ± 6.5

* $p < 0.05$

Table 9: Final day ocular measurements for eyes in which dopaminergic amacrine cells were examined. Unilateral treatment with convex lenses produced variable changes in physical ocular dimensions in both pilot (A) and repeat (B) groups of chicks (see text for details). Data values are followed by ± standard errors of the mean. Significant differences between final day measurements of treated and control eyes are indicated with an asterisk.

DEFOCUS-INDUCED HYPEROPIA
DOPAMINE PILOT STUDY

SECTION DENSITIES (cells mm^{-2})

RETINAL SECTION	TREATED EYE	CONTROL EYE
A (Temporal)	24.3 ± 1.8	22.2 ± 2.4
B (Superior)	24.1 ± 3.5	23.5 ± 3.0
C (Nasal)	23.8 ± 2.6	20.8 ± 2.2
D (Inferior)[$]	24.1 ± 1.5	22.2 ± 1.4

[$] extrapolated from surrounding retinal regions

Table 10A: Comparison of treated versus control cell densities in specific retinal sections of pilot group animals (n=5). Data values are expressed as cells/mm^2 ± standard errors of the mean. Treatment with convex lenses did not produce any significant differences in cell density between any localized portions of the retinae within this pilot study.

NORMALIZED CELL COUNTS PER SECTION

RETINAL SECTION	TREATED EYE	CONTROL EYE
A (Temporal)	1234.3 ± 94.7	1139.7 ± 93.8
B (Superior)	1223.3 ± 171.5	1221.1 ± 125.5
C (Nasal)	1206.8 ± 123.8	1082.7 ± 105.3
D (Inferior)[$]	1221.0 ± 72.0	1143.4 ± 113.0
TOTAL CELL COUNT PER EYE	4885.4 ± 288.9	4586.9 ± 449.8

[$] extrapolated from surrounding retinal regions

Table 10B: Normalized dopaminergic cell counts per section, derived from cell density values. No overall significant differences were found between hyperopic and control eyes. Data represents the mean and SEM.

DEFOCUS-INDUCED HYPEROPIA
DOPAMINE REPEAT STUDY

SECTION DENSITIES (cells mm^{-2})

RETINAL SECTION	TREATED EYE	CONTROL EYE
A (Temporal)	26.8 ± 3.0	24.6 ± 2.4
B (Superior)	28.4 ± 2.8	28.9 ± 2.8
C (Nasal)	30.8 ± 1.4	30.3 ± 3.8
D (Inferior)[$]	28.7 ± 1.4	28.0 ± 1.5
E (Central)	33.2 ± 2.3	33.3 ± 2.6

[$] extrapolated from surrounding retinal regions

Table 10C: Comparison of hyperopic versus control cell densities in specific retinal sections of repeat group animals (n=6). Convex lenses did not produce any statistically significant changes in dopaminergic cell densities between treated and control eyes. Data are shown as cells/mm^2 ± standard errors of the mean.

NORMALIZED CELL COUNTS PER SECTION

RETINAL SECTION	TREATED EYE	CONTROL EYE
A (Temporal)	1220.3 ± 125.2	1086.7 ± 146.4
B (Superior)	1295.0 ± 117.5	1443.5 ± 136.0
C (Nasal)	1415.6 ± 89.6	1501.4 ± 153.5
D (Inferior)[$]	1310.2 ± 98.3	1421.5 ± 70.0
E (Central)	1276.2 ± 89.2	1469.7 ± 143.5
TOTAL CELL COUNT PER EYE	6517.3 ± 452.1	6922.8 ± 298.3

[$] extrapolated from surrounding retinal regions

Table 10D: Normalized dopaminergic amacrine counts per section, calculated from cell densities in Table 10C. Cell counts did not indicate any localized or overall significant differences between treated and control eyes. Data are followed by ± standard errors of the mean.

8.1.6 Group #6: Serotonergic amacrines and defocus-induced hyperopia.

Treated eyes became significantly ($p=0.00006$) more hyperopic (7.3 ± 1.0D) in response to convex lenses relative to control eyes (1.9 ± 0.3D) (Figure 13). There were no significant differences in other measured ocular parameters, although certain trends were observed (Table 11). Convex lenses produced slightly greater ocular wet weights and retinal surface areas in treated versus control eyes, mostly resulting from an increase in equatorial diameter. Conversely, axial lengths, vitreous chamber depths, and anterior compartments were all reduced in treated eyes compared to controls.

Significant differences in serotonergic cell densities were observed when treated versus control eye data was statistically analyzed. The nasal and central regions of treated chick eyes showed significantly higher cell densities relative to control eyes (Table 12A). Since the treated eyes were actually larger than the control eyes, this increase in cell density translated into a significant increase ($p<0.05$) in overall cell numbers within the nasal and central portions of the retina (Table 12B).

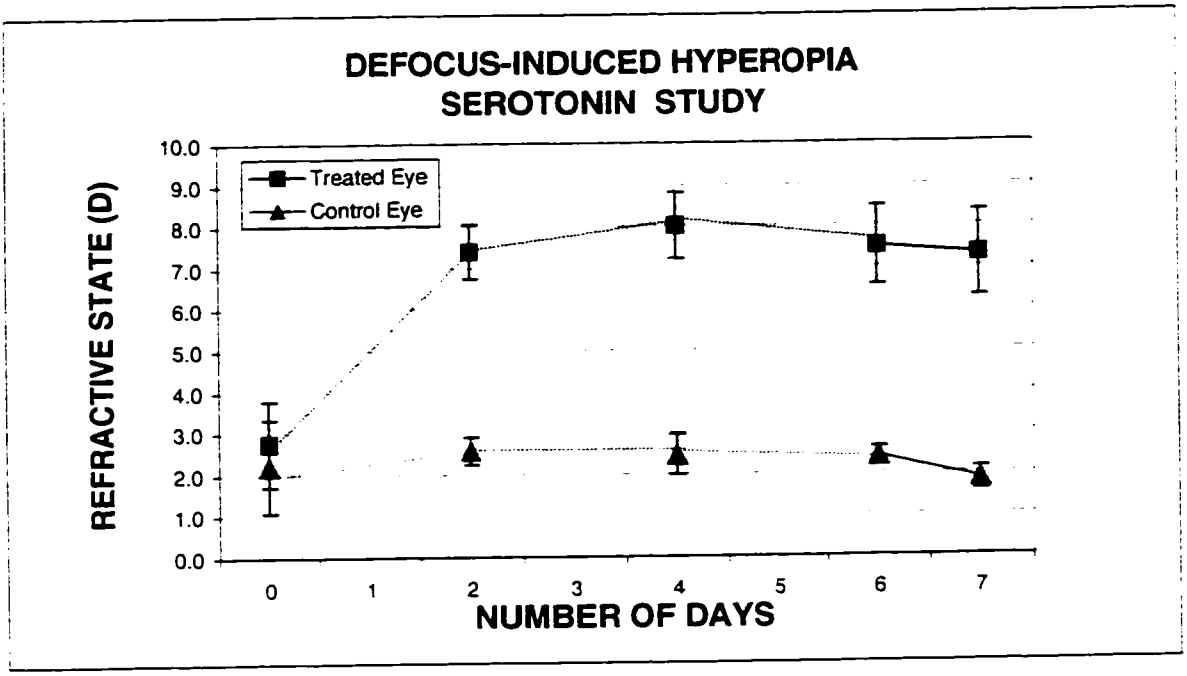

Figure 13: Progression of refractive state in treated and control chick eyes (n=10). Convex lenses unilaterally produced hyperopia in treated eyes, while the contralateral ungoggled eyes served as controls. Error bars represent standard errors of the mean. The final day refractive errors in the treated eyes were significantly different than the corresponding controls ($p<0.0001$). Retinae were processed immunohistochemically and the serotonergic cell populations were examined by confocal microscopy.

DEFOCUS-INDUCED HYPEROPIA
SEROTONIN STUDY

	n	TREATED EYE	CONTROL EYE
OCULAR WET WEIGHT (g)	10	0.620 ± 0.013	0.598 ± 0.013
AXIAL LENGTH (mm)	10	8.71 ± 0.09	8.75 ± 0.09
VITREOUS CHAMBER DEPTH (mm)	10	5.30 ± 0.09	5.39 ± 0.05
ANTERIOR COMPARTMENT (mm)	10	3.05 ± 0.09	3.08 ± 0.05
EQUATORIAL DIAMETER (mm)	10	11.74 ± 0.10	11.65 ± 0.08
RETINAL SURFACE AREA (mm^2)	10	231.3 ± 4.9	228.7 ± 4.2

Table 11: Final day ocular measurements for eyes in which serotonergic amacrine cells were examined. Convex lenses did not produce any overall significant differences in physical ocular dimensions between treated and control eyes. With the exceptions of wet weights and equatorial diameters, it appeared that treated eye parameters were generally smaller than control eyes. Values are followed by ± standard errors of the mean.

DEFOCUS-INDUCED HYPEROPIA
SEROTONIN STUDY

SECTION DENSITIES (cells/mm²)

RETINAL SECTION	TREATED EYE	CONTROL EYE
A (Temporal)	534.5 ± 18.7	474.5 ± 35.6
B (Superior)	543.0 ± 27.8	490.7 ± 25.3
C (Nasal)	* 506.4 ± 21.5	447.2 ± 14.1
D (Inferior)[3]	527.4 ± 12.9	470.8 ± 15.1
E (Central)	* 701.3 ± 21.5	620.8 ± 25.2

[3] extrapolated from surrounding retinal regions
* $p < 0.05$

Table 12A: Serotonergic amacrine densities in retinae in which hyperopia was induced (n=10). Treatment caused significant increases in serotonergic cell densities within the nasal and central portions of the retinae (indicated by asterisks). Data are shown as cells/mm² ± standard errors of the mean.

NORMALIZED CELL COUNTS PER SECTION

RETINAL SECTION	TREATED EYE	CONTROL EYE
A (Temporal)	25858.2 ± 1354.6	22926.2 ± 1983.6
B (Superior)	26098.0 ± 1420.0	23703.7 ± 1344.3
C (Nasal)	* 24461.9 ± 1306.7	21103.9 ± 754.2
D (Inferior)[3]	25419.5 ± 967.2	22545.5 ± 1100.4
E (Central)	* 26985.0 ± 825.5	24369.0 ± 873.4
TOTAL CELL COUNT PER EYE	128822.6 ± 5353.6	114648.3 ± 4410.2

[3] extrapolated from surrounding retinal regions
* $p < 0.05$

Table 12B: Size-adjusted counts of serotonergic amacrine cells, derived from cell densities in Table 12A. Treatment caused a significant increase in the number of cells within the nasal and central regions of the retinae (indicated by an asterisk). No significant differences in cell counts were observed within the peripheral retinal sections. Data are followed by ± standard errors of the mean.

8.2 Part II: Confocal image overlays

8.2.1 General morphology of the dopaminergic amacrine cell in chick retina

Dopaminergic amacrine cells observed in the wholemount chick retina had ovoid to round cell bodies (12-20 μm diameter) located in the innermost layer of the inner nuclear layer (INL). Two sublayers of dendritic arborization arose from the dopaminergic cell bodies and stratified toward the vitreous within the first and fourth sublayers of the inner plexiform layer (IPL). The first IPL sublayer was immediately adjacent to the cell bodies in the INL, while the fourth IPL sublayer was located closer to the retinal ganglion cell layer. The fine dendritic processes in the first sublayer did not have definable field spreads when viewed in confocal image overlays. Instead, these processes appeared as a multitude of small speckles which could not be traced to their cell body of origin. Processes in the first sublayer processes became stratified at a level approximately 10 μm from the scleral border of the IPL where the cell bodies reside. On the other hand, the fourth IPL sublayer contained thick and discrete dendritic branches which could be readily traced back to particular soma. Dendritic processes in this more distal sublayer of the IPL were generally situated 35-45 μm from the INL/IPL border. Within the normal chick retina, there appears to be a very slight but non-significant increase in dopaminergic amacrine cells within the central retina compared to the peripheral regions of the retina.

8.2.2 General morphology of serotonergic amacrines and bipolars in chick retina

8.2.2.1 Amacrines

Serial confocal imaging through chick retina revealed the morphology of serotonergic amacrine cells. Brightly fluorescent serotonergic amacrines in the chick retina consisted of cell bodies (10-11 μm in diameter) at the INL/IPL border, with two layers of dendritic processes stratifying within the IPL (Figure 14). The most prominent dendritic layer (7 μm thick) was located approximately 30 μm from the cell bodies, whereas a much fainter band (5 μm thick) of sparse dendrites was located immediately adjacent to the cell body layer. Fine vertically-oriented neurites formed connections between the two dendritic layers in the IPL. The thickest dendritic sublayer comprised an extremely dense arrangement of fine and highly fluorescent processes which could not be traced back to their cell body of origin. Thus it was impossible to discern the dendritic morphology of individual serotonergic amacrine cells using standard immunohistochemical staining techniques. The distribution of serotonergic amacrine cells varied greatly across the retina: from 335.9±31.7 cells/mm^2 in peripheral regions, up to 725.2±23.6 cells/mm^2 in the central retina. These figures are highly dependent on changes in eye size, a factor which will be considered in more detail in the discussion which follows.

SEROTONERGIC AMACRINE CELL MORPHOLOGY

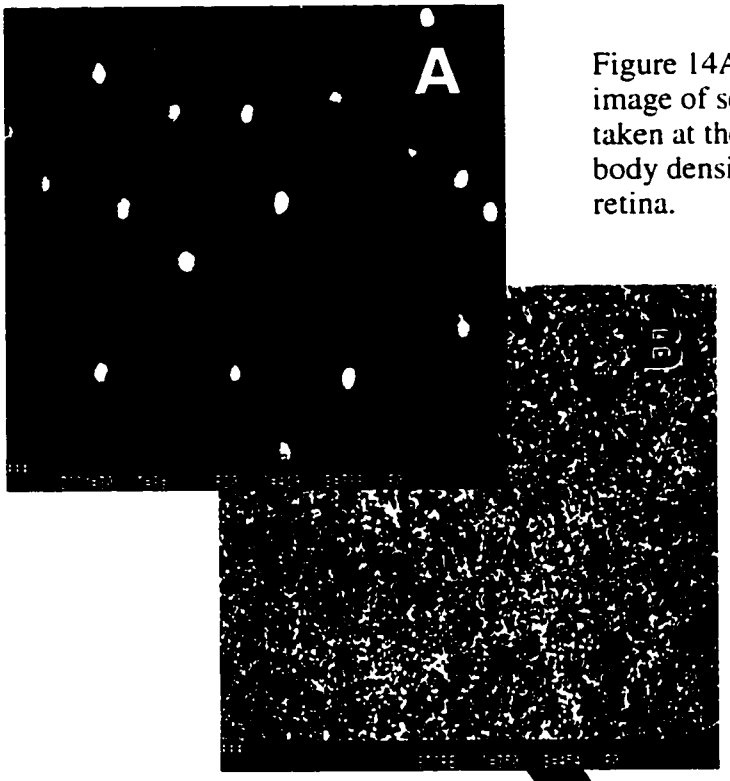

Figure 14A: Digitized confocal image of serotonergic amacrines taken at the plane of greatest cell body density in wholemount chick retina.

Figure 14B:
A stacked overlay representing a series of 20 confocal images taken at 1.7 µm intervals across dendrites corresponding to the serotonergic amacrine cell bodies in Figure A.

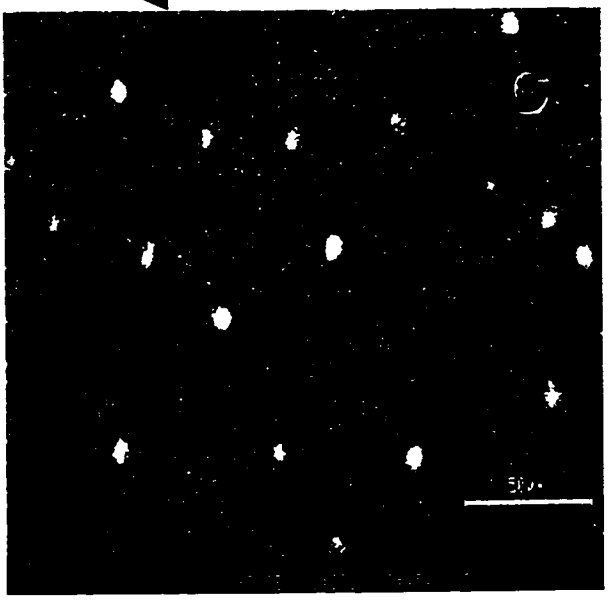

Figure 14C: Composite overlay of figures A and B (above). It was not possible to discern individual serotonergic amacrine cell morphology due to the extremely dense arrangement of the serotonergic dendritic processes.

8.2.2.2 Bipolars

Within the INL, the serotonergic bipolar cells were located in a different plane from the serotonergic amacrine cells. The bipolar cell bodies measured 5-6 μm in diameter, and were separated from the serotonergic amacrine cell body layer by approximately 12-15 μm. Serotonergic bipolars fluoresced at a much lower intensity compared to the serotonergic amacrine cells. On average, there were approximately 14 times more serotonergic bipolar cells compared to serotonergic amacrine cells (Figure 15).

8.2.3 Photoreceptors

Photoreceptors were occasionally seen when obtaining confocal images from chick retina specimens. The photoreceptors were not specifically labelled using the antibodies directed against serotonin or tyrosine hydroxylase. Instead, oil droplets within the avian photoreceptor cells (Bowmaker and Knowles 1977) reflected the excitation light from the confocal laser source, allowing visualization of the photoreceptors under certain circumstances. Figure 16 shows a triple overlay of amacrines, bipolars, and photoreceptors. In this specimen, the bipolars and tightly-packed photoreceptors were respectively located 14.8 μm and 56.7 μm from the amacrine cell layer, as determined by measurement along the z axis during serial confocal imaging.

Figure 15: Overlay of two digitized confocal images representing serotonergic amacrine and bipolar cells within a normal chick retinal wholemount. Each image was taken at the plane of greatest cell body diameter along the same vertical axis, then colour-coded such that amacrine cells are shown in red while bipolar cells are shown in blue. The brightly fluorescent serotonergic amacrine cell bodies were typically 10 μm in diameter. The less intensely stained bipolar cells (5-6 μm diameter) were 14-fold more numerous than amacrine cells. The horizontal amacrine and bipolar cell body layers were located 15 μm apart within the retina. Image area = 79460.5 μm^2.

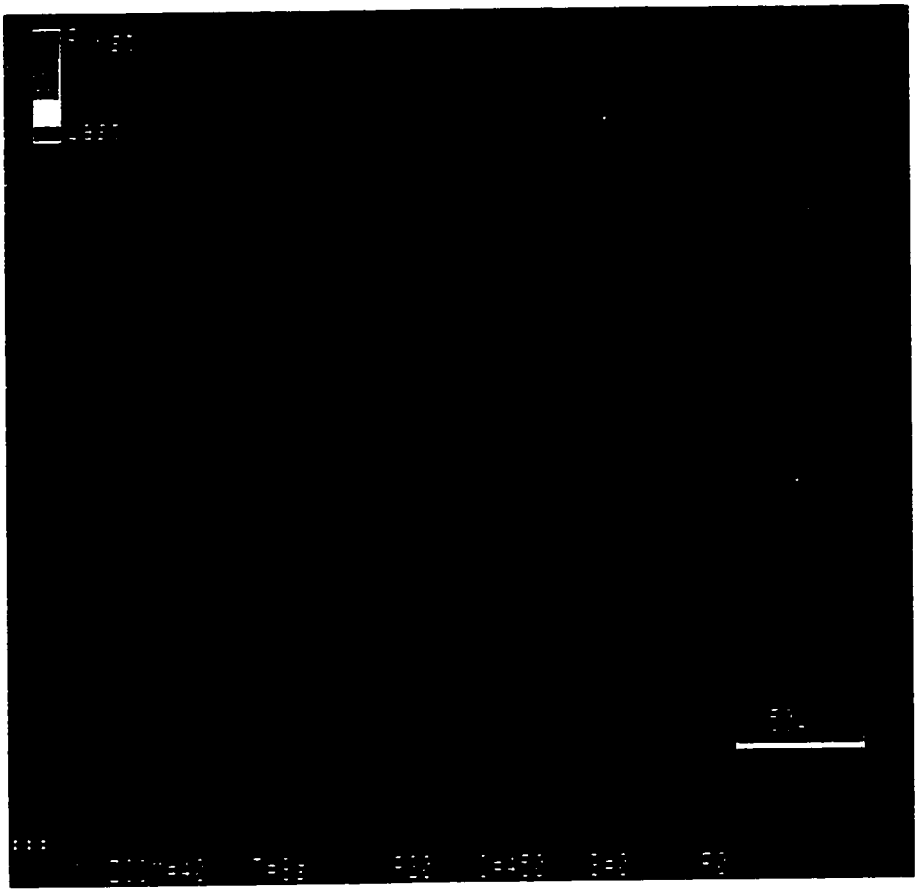

Figure 16: Triple confocal image overlay representing serotonergic amacrine cells, bipolars, and photoreceptors in wholemount chick retina. Each image was recorded at the plane of greatest cell body density along the same vertical axis within the retinal specimen. Superimposed images show amacrine cells in red, bipolars in green, and tightly-packed photoreceptors in blue. The bipolar and photoreceptor cell bodies were respectively located 14.8 μm and 56.7 μm from the plane of amacrine cell bodies. Image area = 79460.5 μm^2.

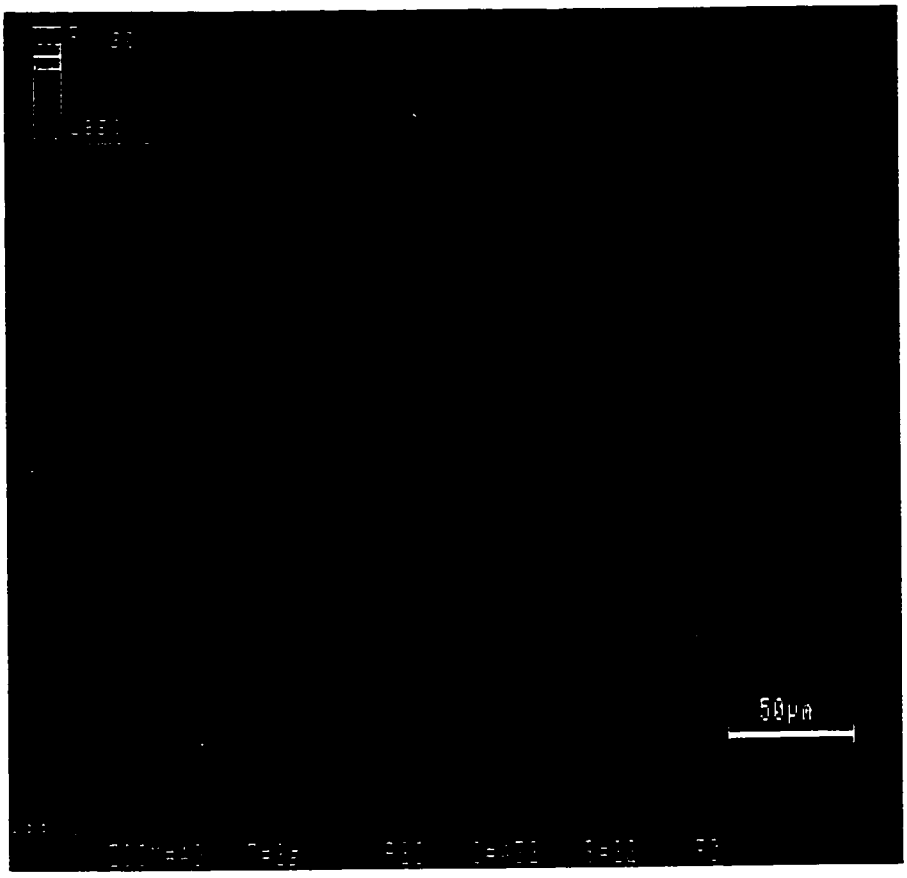
50µm

8.2.4 Doublet and triplet serotonergic amacrine cells

During the acquisition of confocal image data from wholemount retinal specimens, pairing between two or three serotonergic amacrine cell bodies was sometimes observed (Figure 17). Cell bodies would be either touching or found extremely close to one other. This phenomenon appeared in various retinae across a very broad range of experimental conditions, including those treated for form deprivation myopia, defocus-induced myopia, defocus-induced hyperopia, and their respective controls. When present, these linked amacrine cell bodies would be found in both central to peripheral regions of the retina (58 specimens from 27 different chicks).

Figure 17: Double confocal image overlay showing serotonergic amacrine and bipolar cell bodies within chick retina. The confocal microscope was used to acquire images at the planes of greatest cell body diameter, by focusing at the appropriate depths along the same vertical axis. When superimposed, the final composite image shows amacrine cells colour-coded in red, and bipolars in blue. Certain amacrines in this specimen displayed intercellular pairing where cell bodies appear to physically touch each other (white arrows). This contrasts with a more common serotonergic amacrine distribution where soma are normally spaced at least 20-100 μm apart. Image area = 79460.5 μm^2.

8.2.5 Effects of myopia and hyperopia on the dendritic field spread and field density of dopaminergic amacrine cells.

8.2.5.1 Form deprivation myopia

The morphological appearance of dopaminergic amacrine cells in response to FDM treatment varied among individual animals. In order to properly assess any changes as a result of treatment, comparisons between cells in treated versus control eyes were always made within the same animal. Approximately 80% of retinal samples showed that FDM treatment provoked increased dendritic field spreads and densities of dopaminergic amacrines (Figure 18A) relative to cells in control eyes (Figure 18B).

More detailed examination of individual dopaminergic cells showed that many cells in myopic retinae displayed more dendrites within the first sublayer of the IPL, while there appeared to be little difference in the amount of dendrites within IPL sublayers 3 and 4 (Figure 19). The images shown in Figure 19 are representative examples of what was typically seen in FDM-treated retinae. Since there was variable response across different animals, paired comparisons between treated and control eyes were always made within a same animal.

Figure 18: Confocal image overlays which compare dendritic field spreads of form-deprived versus control dopaminergic amacrine cells in chick retina. Each of these representative overlays was created from a series of 10 images taken at 3.5 μm intervals across sets of dopaminergic amacrine cells. Using imaging software, polygon outlines were traced around the dendritic tips of each dopaminergic amacrine cell to illustrate its dendritic field spread. Although there was morphological variability between different animals, dopaminergic cells in treated eyes generally showed larger dendritic field spreads (A) compared to control eyes (B). Paired comparisons between treated and control eyes were always made within a same animal, while maintaining the same image scale and brightness/contrast adjustments.

DOPAMINERGIC AMACRINE CELL FIELD SPREADS FORM DEPRIVATION MYOPIA

A

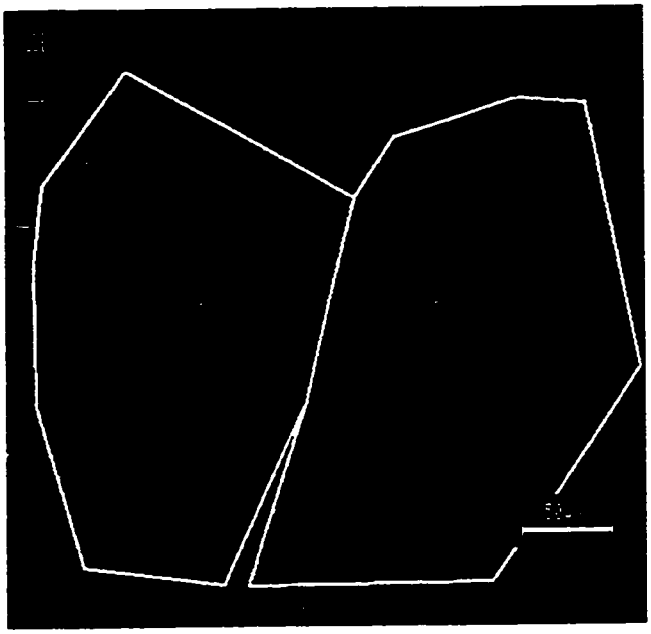

TREATED EYE

B

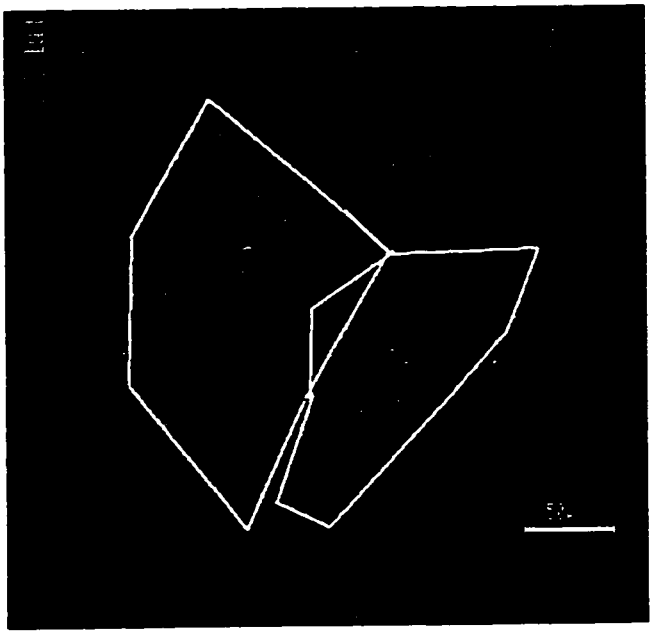

CONTROL EYE

Figure 19: Confocal image overlays showing changes in dopaminergic amacrine cell morphology within chick retina in response to form deprivation myopia. Each overlay was created from a series of 10 images taken at 3.4 μm intervals across individual dopaminergic amacrine cells. Form deprivation myopia produced variable changes in dendritic morphology. The general trend comprised cells in treated eyes showing greater dendritic field density and staining intensity (A) compared to control eyes (B). In this specimen, changes in field density were most evident within the first sublayer of the inner plexiform layer, as seen by increased amounts of dendrites (speckles) within this particular layer of the retina. Any paired comparisons between treated and control eyes were always made within a same animal, while maintaining the same image scale and brightness/contrast adjustments.

DOPAMINERGIC AMACRINE CELLS FORM DEPRIVATION MYOPIA

A

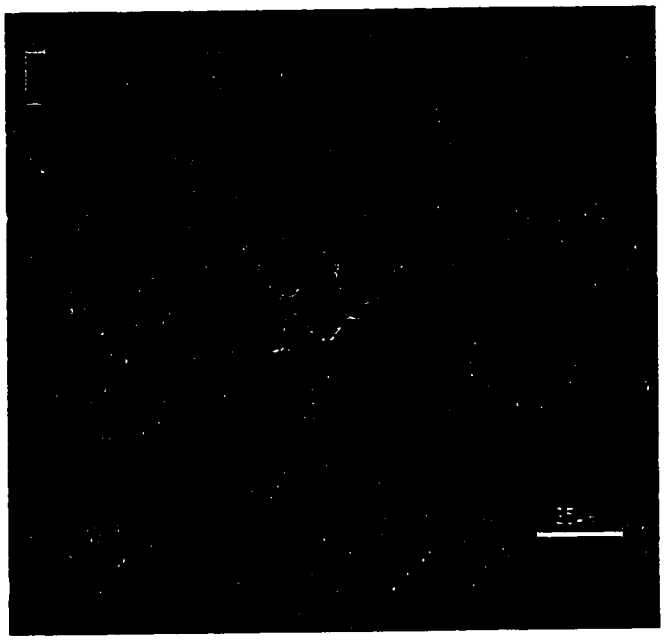

TREATED EYE

B

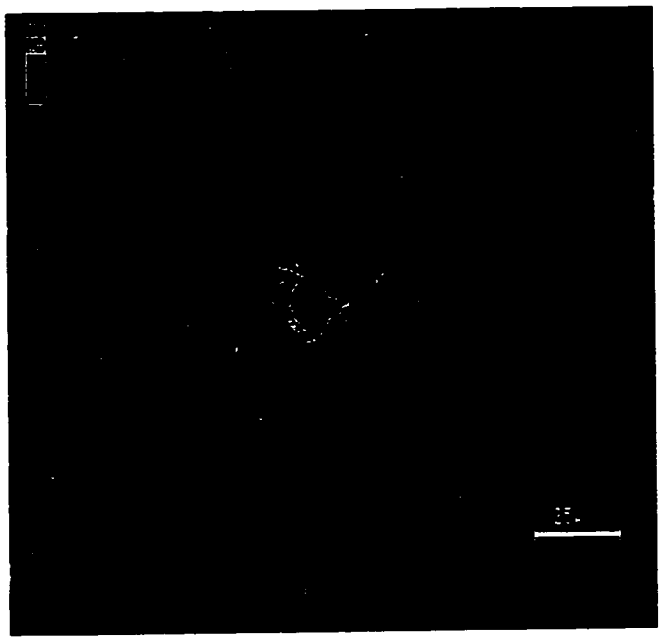

CONTROL EYE

8.2.5.2 Defocus-induced myopia

There was great variation in the morphology of dopaminergic amacrine cells in response to defocus from concave lenses. Dendritic field spreads increased in approximately 40% of treated retinal samples, decreased in 40%, with the remaining 20% showing no noticeable change between treated and control eyes. This was not correlated to magnitude of refractive error, or any other experimental parameter. No image data is shown since there was no consistent trend regarding the morphological response of the dopaminergic amacrine cells to defocus-induced myopia.

8.2.5.3 Defocus-induced hyperopia

Hyperopia arising from convex lenses consistently produced striking decreases in dendritic field size, branching, and staining intensity of dopaminergic amacrine cells in treated versus (Figure 20A) control eyes (Figure 20B). This phenomenon was consistent in all specimens examined by confocal microscopy (n=11), and also within an additional batch of chicks (n=10) in which observations were made using fluorescent light microscopy alone. High magnification confocal images showed that hyperopia caused substantially reduced dendritic branching of dopaminergic cells within the IPL, evident from the sparseness of the first, third, and fourth sublayers in which extensive processes are normally found (Figure 21).

Figure 20: Representative confocal image overlays that compare dendritic field spreads of dopaminergic amacrine cells from retina exposed to defocus-induced hyperopia versus control retina. Each of these confocal image overlays was created from a series of 10 images taken at 1.8 μm intervals across the dopaminergic amacrine cells. Computer imaging software was used to trace polygonal outlines around the dendritic tips of particular amacrine cells to reveal their dendritic field spreads. Dopaminergic amacrine cells in hyperopic eyes typically showed smaller dendritic field spreads (A) compared to control eyes (B). Even at this magnification scale, the much greater amount of IPL sublayer 1 dendrites is apparent within the control retina, in contrast to the treated retina. Paired comparisons between treated and control eyes were always made within a same animal, while maintaining constant image scales and brightness/contrast levels.

DOPAMINERGIC AMACRINE CELL FIELD SPREADS DEFOCUS-INDUCED HYPEROPIA

A

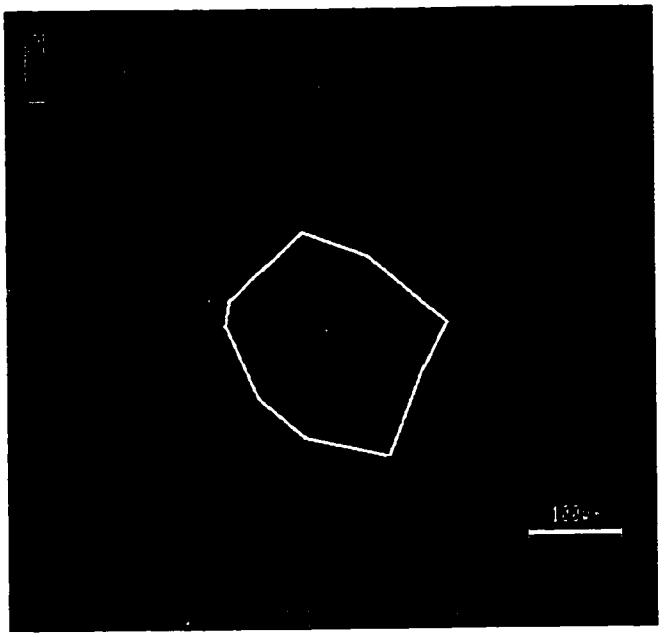

TREATED EYE

B

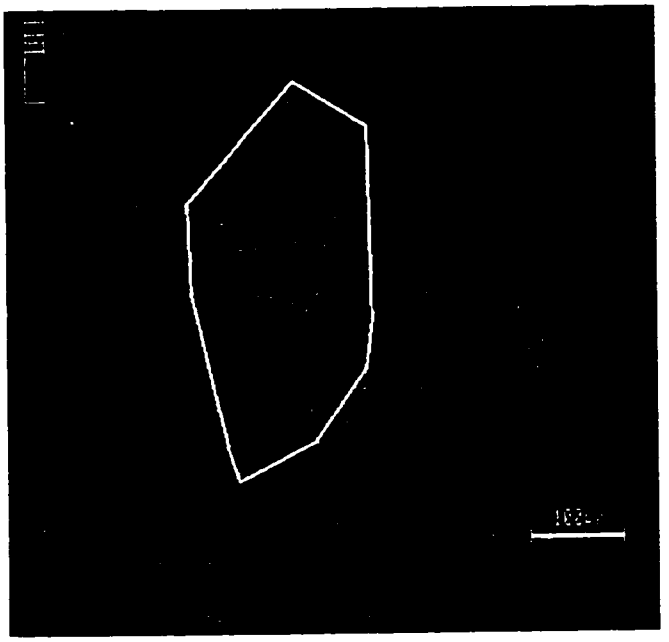

CONTROL EYE

Figure 21: Representative confocal image overlays showing how defocus-induced hyperopia affects dopaminergic amacrine cell morphology in treated versus control retinae. Each overlay was created from a series of 10 images taken at 4.5 μm intervals across individual dopaminergic amacrine cells. Defocus-induced hyperopia consistently produced a dramatic reduction in dendritic quantity and staining intensity relative to controls. Dendrites in sublayers 1, 3, and 4 of the inner plexiform layer were substantially reduced in (A) treated eyes versus (B) control eyes. Without exception, this phenomenon was observed in all retinal specimens examined. Any paired comparisons between treated and control eyes were always made within a same animal, while maintaining identical image scales, brightness, and contrast adjustments.

DOPAMINERGIC AMACRINE CELLS DEFOCUS-INDUCED HYPEROPIA

A

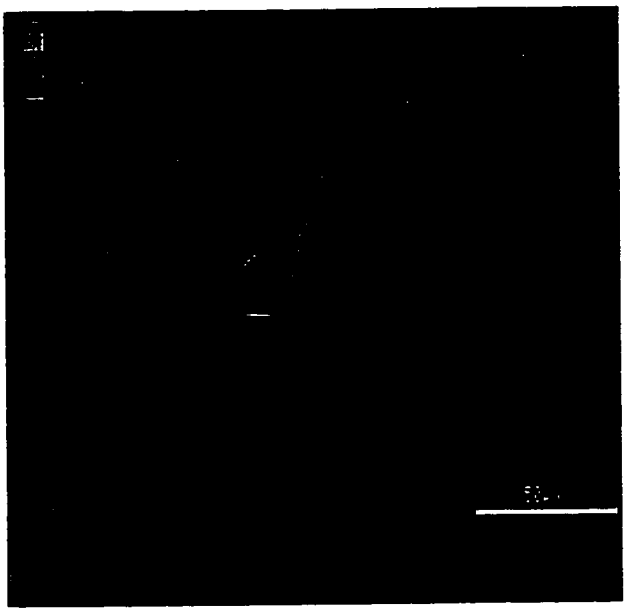

TREATED EYE

B

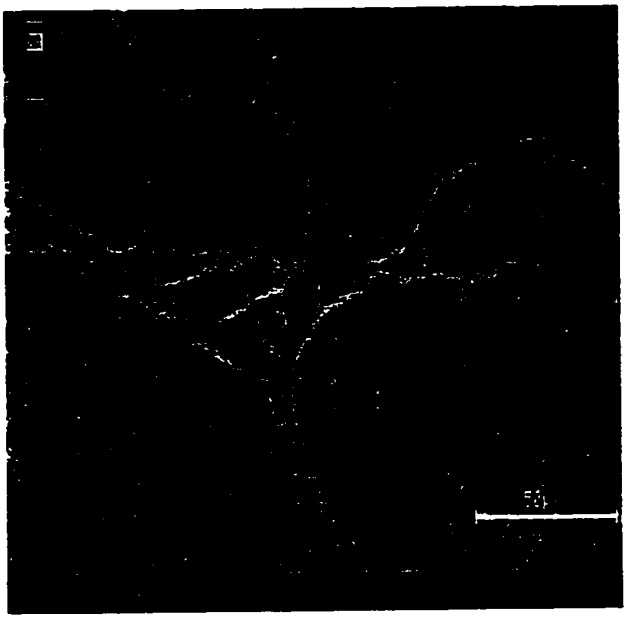

CONTROL EYE

8.3 Part III: HPLC analysis of dopamine, DOPAC, serotonin, and 5-HIAA levels

There were significant differences ($p<0.005$) in the refractive errors between treated and control eyes for both induced myopia (FDM) and hyperopia (DIH) (Tables 13A and 13B). FDM produced significant increases ($p<0.005$) in axial length and vitreous chamber depth (Table 13A). On the other hand, DIH produced mixed results, with an increase in overall axial length counterbalanced by a decrease in vitreous chamber depth (Table 13B).

HPLC results are presented in two formats: (1) Actual tissue levels of DA, DOPAC, 5HT, and 5-HIAA (shown as pg/mg protein), and (2) ratios of DOPAC/DA and 5-HIAA/5HT. Ratios were obtained by converting each quantity of monoamine from pg/mg protein to pmol/mg protein, then dividing product over reactant using these picomolar values. Ratios are better for describing synthetic activity and transmitter release, since retinal mechanisms may maintain steady-state levels of dopamine and serotonin, despite large changes in the actual production or metabolism of these compounds.

8.3.1 Effects of ametropias on dopamine and DOPAC levels

FDM treatment caused significant decreases ($p<0.05$) in dopamine levels within the temporal retinae, with other retinal sections also showing the same trend (Table 14A). On a whole eye basis, FDM caused a very significant decrease (-24.3%) in overall dopamine in treated eyes compared to controls (Table 14A). In the case of DOPAC, FDM caused a very significant decrease ($p<0.005$) in the central retina, which translated into an overall 47.1% decrease between treated and control eyes (Table 14B). Similar to the dopamine results, each retinal section always showed reduced DOPAC levels from FDM treatment compared to controls. Comparisons of the

DOPAC/DA ratios showed significant decreases ($p<0.05$) in the superior and nasal portions of the retina, which corresponded to highly significant ($p<0.005$) overall decreases (-30.0%) when considering the overall states of the whole retina compared to control (Table 14C).

Defocus-induced hyperopia produced significant decreases in dopamine and DOPAC levels within specific regions of the retina. Dopamine levels decreased in the temporal retina (Table 15A), while DOPAC decreased significantly within the temporal and central areas of the retina (Table 15B). In fact, all portions of the treated retinae showed decrease levels of DOPAC relative to control, and this translated into a highly significant decrease (-34.2%) when all retinal regions were pooled together to compare treated versus control eyes (Table 15B). Hyperopia also significantly affected DOPAC/DA ratios on a regionalized (superior and central retina) and whole eye basis. Overall, hyperopia caused a decrease in the DOPAC/DA ratio by 29.2% (Table 15C), parallelling what was seen for myopia.

8.3.2 Effects of ametropias on serotonin and 5-HIAA levels

The HPLC assay for serotonin and 5-HIAA showed much higher variability relative to the catecholamine assay. Reasons for this variability will be provided in the discussion. FDM did not provoke any significant changes in the levels or ratios of serotonin and 5-HIAA although certain trends were observed. Serotonin and 5-HIAA levels were slightly less (2.1 to 7.0%) in treated eyes relative to control eyes (Tables 16A and 16B), with an 8.7% decrease noted when comparing the 5-HIAA/5HT ratios (Table 16C).

DIH produced a significant increase in 5-HIAA levels for the nasal retinal region, but no significant changes were observed in the other retinal sections (Table 17B). Once again, there was a trend for serotonin and 5-HIAA to be slightly higher (3.7 to 5.4%) in treated versus control eyes (Tables 17A and 17B), but there was no difference in the overall 5-HIAA/5HT ratios (Table 17C).

HPLC STUDIES

TABLE 13A: FORM DEPRIVATION MYOPIA, OCULAR PARAMETERS

OCULAR PARAMETER	n	TREATED EYE	CONTROL EYE
INITIAL DAY REFRACTIVE STATE (D)	5	2.8 ± 0.8	3.8 ± 1.4
FINAL DAY REFRACTIVE STATE (D)	5	*** -19.6 ± 4.5	1.5 ± 0.4
FINAL DAY AXIAL LENGTH (mm)	5	*** 10.06 ± 0.18	8.77 ± 0.21
FINAL DAY VITREOUS CHAMBER DEPTH (mm)	5	*** 6.60 ± 0.13	5.79 ± 0.08

*** $p < 0.005$

Table 13A: Measurements for eyes in which FDM was induced using translucent goggles. There were very significant differences in final day refractive states and physical ocular dimensions between treated eyes and controls. Treated eyes were significantly larger ($p<0.005$) as measured by A-scan ultrasonography. There were no significant differences between any initial day parameters. Data are followed by ± standard errors of the mean. These retinae were assayed by HPLC to measure levels of dopamine, DOPAC, serotonin, and 5-HIAA.

TABLE 13B: DEFOCUS-INDUCED HYPEROPIA, OCULAR PARAMETERS

OCULAR PARAMETER	n	TREATED EYE	CONTROL EYE
INITIAL DAY REFRACTIVE STATE (D)	5	1.8 ± 1.4	1.8 ± 0.9
FINAL DAY REFRACTIVE STATE (D)	5	*** 5.3 ± 1.3	1.0 ± 0.4
FINAL DAY AXIAL LENGTH (mm)	5	9.21 ± 0.12	9.13 ± 0.07
FINAL DAY VITREOUS CHAMBER DEPTH (mm)	5	5.61 ± 0.23	5.75 ± 0.13

*** $p < 0.005$

Table 13B: Measurements for eyes in which hyperopia was induced using convex lenses. By the final day, treated eyes were significantly hyperopic compared to controls. There were no overall significant differences in final day physical ocular dimensions, although an increase in axial length was counterbalanced by a decrease in vitreous chamber depth. Data are followed by ± standard errors of the mean. The retinae from this group of chicks were analysed by HPLC to measure dopamine, DOPAC, serotonin, and 5-HIAA levels.

FORM DEPRIVATION MYOPIA
DOPAMINE AND DOPAC STUDY

DOPAMINE HPLC RESULTS (pg mg protein)

RETINAL SECTION	TREATED EYE	CONTROL EYE
A (Temporal)	* 741.0 ± 41.6	1074.0 ± 90.8
B (Superior)	749.0 ± 81.8	1062.0 ± 152.4
C (Nasal)	692.3 ± 111.9	774.0 ± 103.1
E (Central)	625.2 ± 108.3	874.2 ± 92.7
MEAN DOPAMINE PER EYE	*** 699.8 ± 42.2	924.9 ± 57.4

* p < 0.05
*** p < 0.005

Table 14A: Pooled HPLC measurements of dopamine, comparing form-deprived eyes versus control eyes (n=5 chicks). In treated eyes, there was a significant decrease ($p<0.05$) in the temporal retinal region compared to control eyes. When compared on a section-by-section basis, treated eyes tended to have lower values than controls, and this is reflected by an overall significant decrease ($p<0.005$) when considering pooled values across whole eyes. Data are expressed as pg/mg protein ± standard errors of the mean.

DOPAC HPLC RESULTS (pg/mg protein)

RETINAL SECTION	TREATED EYE	CONTROL EYE
A (Temporal)	131.8 ± 21.6	232.0 ± 45.0
B (Superior)	120.0 ± 23.1	271.3 ± 44.9
C (Nasal)	121.5 ± 16.8	207.8 ± 35.4
E (Central)	*** 118.4 ± 23.4	235.2 ± 13.3
MEAN DOPAC PER EYE	*** 123.2 ± 10.0	232.8 ± 16.3

*** p ≤ 0.005

Table 14B: Pooled HPLC measurements of DOPAC, comparing form-deprived eyes with control eyes (n=5 chicks, same retinal samples as Table 13A). A highly significant decrease ($p\leq0.005$) in the amount of DOPAC was observed in the central region of the retina. Overall, there was significantly less DOPAC in treated versus control eyes ($p<0.001$). Data (pg/mg protein) are followed by ± standard errors of the mean.

DOPAC/DOPAMINE RATIOS

RETINAL SECTION	TREATED EYE	CONTROL EYE
A (Temporal)	0.16 ± 0.02	0.20 ± 0.03
B (Superior)	* 0.14 ± 0.01	0.23 ± 0.02
C (Nasal)	0.17 ± 0.03	0.24 ± 0.02
E (Central)	* 0.17 ± 0.02	0.25 ± 0.03
MEAN DOPAC/DA PER EYE	*** 0.16 ± 0.01	0.23 ± 0.01

* p < 0.05
*** p < 0.005

Table 14C: Calculated DOPAC/dopamine ratios in form-deprived versus control eyes (converted from pg/mg to pmol mg. See text for details). Significant decreases ($p<0.05$) in the ratio were observed in the superior and central regions of the retina. Overall, there was a highly significant decrease ($p<0.005$) in the DOPAC/DA ratios in treated eyes. Data are followed by ± standard errors of the mean.

DEFOCUS-INDUCED HYPEROPIA
DOPAMINE AND DOPAC STUDY

DOPAMINE HPLC RESULTS (pg mg protein)

RETINAL SECTION	TREATED EYE	CONTROL EYE
A (Temporal)	* 783.6 ± 76.5	998.8 ± 46.4
B (Superior)	1020.3 ± 141.4	950.0 ± 78.3
C (Nasal)	847.2 ± 52.7	834.8 ± 71.8
E (Central)	745.8 ± 69.3	824.2 ± 120.3
MEAN DOPAMINE PER EYE	840.2 ± 45.2	896.8 ± 43.3

* $p \leq 0.05$

Table 15A: Pooled HPLC measurements of dopamine, comparing eyes treated with convex lenses versus control eyes (n=5 chicks). Treatment produced a significant decrease in dopamine levels for temporal retinal regions ($p \leq 0.05$). Data are expressed as pg/mg protein ± standard errors of the mean.

DOPAC HPLC RESULTS (pg/mg protein)

RETINAL SECTION	TREATED EYE	CONTROL EYE
A (Temporal)	* 145.4 ± 16.2	248.0 ± 34.3
B (Superior)	154.8 ± 26.2	227.4 ± 27.0
C (Nasal)	176.6 ± 14.6	249.8 ± 61.7
E (Central)	** 138.4 ± 15.4	212.0 ± 16.6
MEAN DOPAC PER EYE	*** 153.7 ± 8.8	233.6 ± 18.3

* $p \leq 0.05$
** $p \leq 0.01$
*** $p < 0.005$

Table 15B: Pooled HPLC measurements of DOPAC, comparing hyperopic eyes with control eyes (n=5 chicks, same retinal samples as above). Significant decreases in the amounts of DOPAC were observed in the temporal ($p \leq 0.05$) and central regions ($p \leq 0.01$) of the retina. Overall, treatment produced highly significant decreases in DOPAC levels compared to control eyes ($p < 0.005$). Values, expressed as pg/mg protein, are followed by ± standard errors of the mean.

DOPAC/DOPAMINE RATIOS

RETINAL SECTION	TREATED EYE	CONTROL EYE
A (Temporal)	0.18 ± 0.02	0.22 ± 0.02
B (Superior)	* 0.14 ± 0.01	0.22 ± 0.03
C (Nasal)	0.19 ± 0.01	0.27 ± 0.06
E (Central)	* 0.17 ± 0.01	0.25 ± 0.03
MEAN DOPAC/DA PER EYE	*** 0.17 ± 0.01	0.24 ± 0.02

* $p < 0.05$
*** $p < 0.005$

Table 15C: Calculated DOPAC/dopamine ratios in hyperopic versus control eyes (converted from pg/mg to pmol/mg). Significant decreases ($p < 0.05$) in the ratios were observed in the superior and central regions of the retina. The overall trend was decreased DOPAC/DA ratios in treated eyes. Data are followed by ± standard errors of the mean.

FORM DEPRIVATION MYOPIA
SEROTONIN AND 5-HIAA STUDY

SEROTONIN HPLC RESULTS (pg/mg protein)

RETINAL SECTION	TREATED EYE	CONTROL EYE
A (Temporal)	830.0 ± 76.8	1053.3 ± 164.9
B (Superior)	1014.0 ± 94.1	1294.7 ± 125.1
C (Nasal)	971.8 ± 50.3	841.0 ± 198.9
E (Central)	748.3 ± 113.8	796.8 ± 72.4
MEAN SEROTONIN PER EYE	891.0 ± 63.3	958.0 ± 83.4

Table 16A: Pooled HPLC measurements of serotonin, comparing form-deprived eyes versus control eyes (n=5 chicks). There were no significant differences between measurements when comparing results on a section-by-section or whole eye basis, although the general trend was decreased serotonin levels in form-deprived eyes. Data are expressed as pg/mg protein ± standard errors of the mean.

5-HIAA HPLC RESULTS (pg/mg protein)

RETINAL SECTION	TREATED EYE	CONTROL EYE
A (Temporal)	206.0 ± 45.1	162.3 ± 37.9
B (Superior)	246.3 ± 53.2	196.7 ± 7.2
C (Nasal)	150.3 ± 48.9	186.6 ± 37.4
E (Central)	159.3 ± 14.2	226.6 ± 43.4
MEAN 5-HIAA PER EYE	190.4 ± 21.0	194.4 ± 18.5

Table 16B: Pooled HPLC measurements of 5-HIAA, comparing form-deprived eyes with control eyes (n=5 chicks, same retinal samples as above). No significant differences were found between treated or control eyes. Values (pg/mg protein) are followed by ± standard errors of the mean.

5-HIAA/SEROTONIN RATIOS

RETINAL SECTION	TREATED EYE	CONTROL EYE
A (Temporal)	0.22 ± 0.06	0.17 ± 0.07
B (Superior)	0.23 ± 0.08	0.14 ± 0.02
C (Nasal)	0.16 ± 0.06	0.30 ± 0.13
E (Central)	0.22 ± 0.06	0.26 ± 0.05
MEAN 5-HIAA/5-HT PER EYE	0.21 ± 0.03	0.23 ± 0.04

Table 16C: Calculated 5-HIAA/serotonin ratios of form-deprived versus control eyes (converted from pg/mg to pmol/mg). No significant differences were found between treated and control eyes. Values are followed by ± standard errors of the mean.

DEFOCUS-INDUCED HYPEROPIA
SEROTONIN AND 5-HIAA STUDY

SEROTONIN HPLC RESULTS (pg/mg protein)

RETINAL SECTION	TREATED EYE	CONTROL EYE
A (Temporal)	882.6 ± 140.7	973.7 ± 194.3
B (Superior)	929.7 ± 21.6	751.8 ± 144.3
C (Nasal)	1058.4 ± 103.4	964.7 ± 116.9
E (Central)	719.0 ± 43.2	843.4 ± 60.6
MEAN SEROTONIN PER EYE	893.8 ± 55.5	861.9 ± 62.2

Table 17A: Pooled HPLC measurements of serotonin, comparing eyes treated with convex lenses versus control eyes (n=5 chicks). There were no significant differences between measurements when comparing results on a section-by-section or whole eye basis, although serotonin levels in hyperopic eyes tended to be higher relative to controls. Data are expressed as pg/mg protein ± standard errors of the mean.

5-HIAA HPLC RESULTS (pg/mg protein)

RETINAL SECTION	TREATED EYE	CONTROL EYE
A (Temporal)	227.8 ± 40.1	256.0 ± 73.0
B (Superior)	214.3 ± 26.6	203.8 ± 24.9
C (Nasal)	*** 253.3 ± 11.9	174.7 ± 7.3
E (Central)	214.4 ± 24.4	236.6 ± 18.7
MEAN 5-HIAA PER EYE	227.5 ± 14.1	215.9 ± 14.1

*** $p < 0.005$

Table 17B: Pooled HPLC measurements of 5-HIAA, comparing hyperopic eyes versus control eyes (n=5 chicks, same retinal samples as above). Treatment provoked a highly significant increase ($p<0.005$) in the nasal portion of the retina. Values (expressed as pg/mg protein) are followed by ± standard errors of the mean.

5-HIAA/SEROTONIN RATIOS

RETINAL SECTION	TREATED EYE	CONTROL EYE
A (Temporal)	0.28 ± 0.08	0.20 ± 0.06
B (Superior)	0.21 ± 0.03	0.29 ± 0.08
C (Nasal)	0.22 ± 0.03	0.17 ± 0.02
E (Central)	0.28 ± 0.04	0.26 ± 0.03
MEAN 5-HIAA/5-HT PER EYE	0.25 ± 0.03	0.25 ± 0.03

Table 17C: Calculated 5-HIAA/serotonin ratios in hyperopic versus control eyes (converted from pg/mg to pmol/mg). No significant differences were found between treated and control eyes. Data are followed by ± standard errors of the mean.

9.0 DISCUSSION

9.1 New research approaches and significance

This thesis examined how the retina may contribute to abnormal eye growth mechanisms and the resulting visual problems such as myopia or hyperopia. Previous researchers have used many different approaches to examine how the retina, choroid, and other ocular components may participate in the development of refractive errors. However, this study is unique in many aspects. First, a new method was developed using the confocal laser scanning microscope to assess specific retinal cell population numbers and distribution. Confocal microscopy is particularly well suited for retinal studies, since optical confocal sectioning maintains proper spatial relationships within the tissue, unlike physical sectioning which may distort the specimen (For review, see Cavanaugh et al. 1995, Masters 1990). As detailed earlier in the introduction and methods sections, the principles of confocal microscopy allow much better visualization of fluorescently-labelled cell structures such as dendritic morphology, in comparison to traditional methods (e.g. light microscopy). The goggle technique, as described previously in landmark studies (Schaeffel, Glasser, and Howland 1988, Irving et al. 1991 and 1992), also permits the induction of significant refractive errors in newly post-hatch birds. This allows the use of extremely young animals, which is an essential experimental consideration since retinal plasticity is optimal at this stage (Cronly-Dillon 1991). Other novel features in this study include a comparative assessment of how refractive errors affect specific retinal regions, the putative involvement of serotonin in refractive error development, and also an analysis of how hyperopia influences retinal morphology and catecholamine levels. Relative to myopia, very little attention has been focused on elucidating the possible mechanisms which produce hyperopia.

The confocal microscope approach allows the quantitative examination of a dramatically

higher number of retinae compared to any previous studies of a similar nature. For instance, Teakle and colleagues (1993) used standard immunohistochemical staining methods and regular light microscopy to examine how FDM affected dopaminergic amacrine cells in chick retina. Their study was limited to only two retinae, in part due the labour-intensive analysis required to manually count retinal cells on a one-by-one basis. In another representative study, five normal chicks were used to study the morphology of retinal cell populations, and another thirty animals (3 animals for each of 10 cell types) were used to survey various retinal cell distributions (Kiyama et al. 1985). The work presented in this thesis examined the effects of three visual conditions (FDM, DIM, DIH) on two different amacrine cell populations (dopaminergic and serotonergic), with up to fifteen animals being considered in each category (61 animals total). Hence a major advantage when using the confocal microscope is a two to thirty-fold increase in the number of animals ("n" value) which can be considered within the same amount of time as other studies.

9.2 Refractive error, ocular size, and dimensions

In all experimental groups studied during the course of this work, goggles produced highly significant final day refractive error differences between the treated and control eyes. The amount and progression of myopia resulting from concave defocus (Figures 8, 9) and form deprivation (Figures 10, 11) was comparable to that seen in numerous previous studies using the chick as an animal model (Irving et al. 1991 and 1992, Irving 1993).

The magnitude of hyperopia induced by convex lenses in this study was less than what has been observed by other researchers using similar techniques (Wilson et al. 1997, Irving et al. 1991 and 1992). However, the observed final day refractive differences between eyes treated with convex lenses and ungoggled control eyes were still highly significant (Figures 12, 13).

For the induction of myopia, different types of goggles produce different amounts of refractive error. When using concave lenses, the amount of myopia produced is limited by the power of the lens, and reaches an absolute maximum of about -17 dioptres despite the application of higher power lenses (Irving 1993). In contrast, translucent goggles routinely produce two or three times the amount of myopia compared to defocusing lenses.

It remains unclear whether defocus-induced and form deprivation myopia arise from a common source (merely shifted along the same continuum) or whether the two are separate entities (each with unique origins). There has been much debate over this issue, with proponents both for (Diether et al. 1997) and against (Irving 1993, Bartmann et al. 1994, Schaeffel et al. 1994, Schwahn et al. 1997, Kee et al. 1998) a common mechanism. It is also unclear whether myopia and hyperopia arise from opposite ends of the same spectrum, or whether the causes for their onset are completely unrelated to each other.

This study cannot definitively answer these questions. However, trends in the data suggest that all ametropic mechanisms share a common pathway. As will be detailed later, the serotonergic cell count results and changes in dopaminergic morphology both support this viewpoint.

Ocular growth responses to goggle treatment were similar to what has been previously documented in the literature (Irving et al. 1991 and 1992, Wilson 1997). In all experimental groups, myopic eyes were larger compared to controls while hyperopic eyes, with some exceptions, tended to be smaller. It should be noted that the methodology and mathematical extrapolations used in this study are applicable to the posterior retinal portion of the eye. Hence no conclusions can be made about possible changes in the cornea and anterior chamber. Previous studies suggest that growth of the anterior and posterior compartments of the eye are independently controlled

(Wildsoet and Pettigrew 1988b, Barrington et al. 1989). Hence this study directed more attention at characterizing the effects of ametropia on vitreous chamber and retinal development.

Form deprivation myopia, resulting from translucent goggles, consistently produced eyes that were significantly larger in all measured dimensions (Tables 5, 7). For defocus-induced myopia, increased eye growth responses were not as pronounced as those observed in form deprivation myopia. Nonetheless, treatment with concave lenses produced enlargement of virtually all measured ocular parameters (Tables 1, 2). The only exception occurred in the pilot group from which dopaminergic amacrine cells were studied, where corneal flattening was observed. In this instance, the anterior compartment of treated eyes had reduced growth relative to control eyes, possibly to compensate for excessive vitreous chamber growth. Once again, this highlights the separate developmental responses of anterior versus posterior ocular compartments.

There was even more variability in ocular size resulting from the application of convex lenses to produce hyperopia. There was no consistent trend in measured ocular parameters that accounted for the hyperopic refractive state. Surprisingly, the hyperopic eyes were sometimes larger and often heavier than controls, which may reflect fluid retention within ocular tissues in an effort to reduce intraocular dimensions (Wildsoet and Wallman 1995). However, even the enlarged hyperopic eyes showed decreases in their vitreous chamber depths relative to control.

The literature reflects the great diversity in ocular responses to induced ametropias. In particular, this applies to the anterior portion of the eye where enlargement (Schaeffel and Howland 1988), reduction (Lauber and Oishi 1987), or no consistent change (Schaeffel et al. 1986, Wallman and Adams 1987) have all been reported. Some of these differences may reflect the use of different breeds of chickens used by various groups of researchers (Troilo et al. 1995). However, the considerable differences in ocular responses within the current study also suggest

there is inherent variability *within* a breed. While individual ocular components may respond differentially to visual manipulation, the major determining factor for final refractive state appears to be the net axial length (Sivak et al. 1990), and more specifically, changes in vitreous chamber depth. Results from this study generally reflect the correct trend (longer measurements for myopia, and shorter for hyperopia), although the differences were not always statistically significant.

9.3 Cell densities

The use of cell densities to characterize neural populations in the retina is widely accepted throughout the scientific community. However, in cases where eye size may change dramatically as a result of inducing myopia or hyperopia, a comparison of cell densities between treated and control eyes is not necessarily meaningful. For instance, if eye size increases significantly and cell density decreases, what is really happening to this cell population? Are the cell numbers remaining static and merely spreading out over a greater retinal surface area? Or are net increases or decreases in cell number being masked by the changes in eye size when cell density is the only parameter considered? Hence, unless the compared eyes are of very similar size, it is generally not sufficient to consider cell density alone, but also to evaluate other parameters such as overall cell counts. Certain exceptions do exist, such as when both eye size and density increase, or vice versa, when eye size and density both decrease. In these cases it is intuitively apparent that overall cell number must be increasing or decreasing respectively, despite any change in eye size.

9.3.1 Dopaminergic amacrine cell densities

A survey of the literature and comparison with results from this study will help illustrate the aforementioned issues. Teakle and colleagues (1993) examined how lid-suture myopia affected dopaminergic amacrine cells in older (4 to 7 months) chick retinae with retinal surface areas of control eyes ranging from 439 to 473 mm^2. On the other hand, Kiyama et al. (1985) considered dopaminergic cells in the normal retinae of much younger animals, likely one day after hatch, based on their reported chicks' body weights of approximately 50 g each. The latter study (Kiyama et al. 1985) noted an even retinal distribution of dopaminergic amacrine cells at about 40 cells/mm^2, while the former group (Teakle et al. 1993) recorded approximately 10 cells/mm^2 in control eyes of their chicks. Results from 7 day old control retinae in this dissertation showed mean dopaminergic cell densities ranging from 20.8 to 33.3 cells/mm^2, with corresponding retinal surface areas of 210.2 to 234.4 mm^2. If all of these results were plotted together, it would be apparent that as retinal size increases during the course of normal ocular development, there is a corresponding decrease in cell density.

According to results presented by Teakle et al. (1993), dopaminergic amacrine cell distributions in the myopic chick retina indicate there is an increase in cell density within the temporal regions of the retina. During embryogenesis of normal chick retina, Gardino and co-workers (1993) have also noted higher temporal densities of dopaminergic amacrines until the 14^{th} embryonic day, after which the cells appear evenly distributed across the retina. Does this suggest that myopia causes regression toward a more primitive phenotype and function? Results from the current study actually find the opposite distribution from what was reported by the Teakle group of researchers: higher dopaminergic cell densities in the nasal (and occasionally superior) retinal regions. Perhaps these conflicting results merely highlight the extremely plastic and variable

nature of dopaminergic amacrine cell distribution within the retina. It is also possible that changes in retinal cell distribution may reflect localized changes in ocular growth, with little correlation between specific cell location and cell function. The effects of ametropias on overall dopaminergic cell numbers will be considered shortly.

9.3.2 Serotonergic amacrine cell densities

Earlier studies have examined the general properties of serotonergic cells in chick retina. These include cross sectional examinations of cell morphology (Hauschild and Laties 1973, Floren 1979) and also quantitative assay measurements of indoleamine levels (Parkinson and Rando 1983, reviews by Osborne 1982a, Brunken et al. 1993). However, there are relatively few reports about serotonergic cell distribution and numbers within chick retina, and even fewer that consider, in detail, the effects of induced ametropias on this particular cell population. In young normal chicks, Kiyama et al. (1985) noted 219.7 to 285.3 serotonergic amacrine cells per mm^2 in peripheral retina, compared to 592.3 cells/mm^2 in the central region. In the current study, a few animals showed retinal cell densities in a similar range to the work by Kiyama et al. (1985). However, when pooled together into groups, the mean serotonergic amacrine density was much higher than what was found by the Kiyama group. Data from the control eyes will be considered for the purposes of comparison: peripheral regions contained approximately 400-500 cells/mm^2 while central retina contained a range of 620-780 cells/mm^2. In both cases, there was always a definite cell density increase noted in the central portions of the retina. However, differences between the data cannot be accounted for by differential eye size resulting from normal ocular growth, since the chicks in the Kiyama study are apparently much younger (newly-hatched or one day post-hatch) compared to the ones used in this study (7-10 days old when assessed). Possible explanations for the

difference include the smaller sample size used by Kiyama's group, differences in staining methodology, and the use of different chicken breed (the Japanese group possibly using an Asian breed, unidentified in their article, which is not available in North America).

The induction of ametropias caused significant changes in serotonergic amacrine cell densities in various retinal regions, although in the case of form deprivation myopia, some of these differences were due to significant changes in eye growth (more details in the next section). With form deprivation myopia, significant decreases in serotonergic amacrine densities were observed in the superior, nasal, and central retinal regions (Table 8A). When defocus-induced hyperopia was produced, significant increases in serotonergic amacrine densities were found in the nasal and central retinal regions (Table 12A). Since the size of the eyes did not change significantly in the case of hyperopia, it was already apparent that these density changes would translate into real differences between cell population numbers and distribution. Conversely, defocus-induced myopia did not produce any significant density changes in any retinal region compared to the control eyes.

9.4 Cell counts

As outlined previously, the exclusive use of cell densities is not the optimal method for comparing between eyes of changing size. A more comprehensive approach would also include other parameters that normalize for the differences in ocular size. The protocol developed in this thesis calculated specific retinal surface areas by mathematically fitting an ellipsoid to each chick eye according to experimentally-accessible ocular measurements (vitreous chamber depth, equatorial diameter, and the excised anterior diameter along the ora serrata) (Refer to *Formula iv*, Figure 6). Thus cell densities could be translated into normalized cell count data that accounts for

changes in eye size, and from which total cell counts per retinal region and per eye could be extrapolated and compared.

One should note that using these mathematical formulae does not account for possible changes in anterior corneal curvature or depth, since the ellipsoid is fit to the posterior eye cup where the retina lies. Therefore no comments can be made about the effects of myopia or hyperopia on the cornea, or how certain retinal cell populations may differentially affect anterior versus posterior compartments of the eye.

9.4.1 Dopaminergic amacrine cell counts

Dopaminergic amacrine cells comprise 2-5% of the total amacrine cell population (Massey and Redburn 1987, Nguyen-Legros 1996). The cell count data for dopaminergic amacrine cells obtained in this study ranged from approximately 4500 to 7350 in control eyes, and 4890 to 8370 in eyes in which various ametropias had been induced. There were no significant regionalized differences in normalized cell counts, although treatment did appear to cause slightly increased cell numbers in nasal or superior retinal regions. Teakle et al. (1993) appear to be the only other researchers who have examined how myopia affects dopaminergic amacrine cell distribution. They also found no significant difference between treated and control eyes, with total cell numbers ranging from 4800 to 5500 dopaminergic amacrines per eye.

The large amount of individual variation existing between animals would account for the differences in the reported values. The study by Teakle and associates (1993) used a very small number of animals and they also admit that certain areas of the retinae were poorly stained, thus requiring extrapolations about cell numbers in those regions. Considering that the current investigation and the work by Teakle and her collaborators (1993) both utilize extrapolation in

their methodology, the differences between the data sets are reasonable and to be expected. In both cases, it is more useful to compare the relative differences between treated and control eyes, rather than focus on the absolute numbers.

9.4.2 Serotonergic amacrine cell counts

Form deprivation myopia provoked a significant decrease in serotonergic amacrine cell counts within the central retina (Table 8B), while defocus-induced hyperopia caused significant increases in the nasal and central regions of the retina (Table 12B). Defocus-induced myopia did not show any significant differences in serotonergic cell counts as a result of the treatment (Table 4B). These data, which are adjusted for ocular growth, provide evidence that serotonin may participate in the development of refractive error. Since overall cell counts per eye do not appear to change when comparing the treatment to control situation, it appears that *redistribution* of serotonergic amacrine cells has occurred (either into or out of the central retina). It is interesting to note that changes are found predominantly within the central retina. During the course of normal ocular embryogenesis, development always begins at the most posterior pole of the eye and proceeds anteriorly (Duke-Elder 1963, Mann 1969, Remington 1998). Hence at later stages of chick ocular development (not examined in this study), it is possible that changes in serotonergic cell distribution may extend to the more peripheral regions of the retina.

Other studies in teleost retina have also documented changes in cell numbers, depending on retinal size and overall growth of the fish. For example, Negishi et al. (1985) have noted an increase in the number of serotonin-accumulating cells in carp retina, due to circumferential addition of serotonin-accumulating cells in the retina.

Furthermore, if one were to correlate the changes in serotonergic cell numbers with the

amount of refractive error, there appears to be a near linear relationship as illustrated in Figure 22 which follows. This suggests that all ametropias lie along the same continuum, arising from a common source and producing effects which are related to each other.

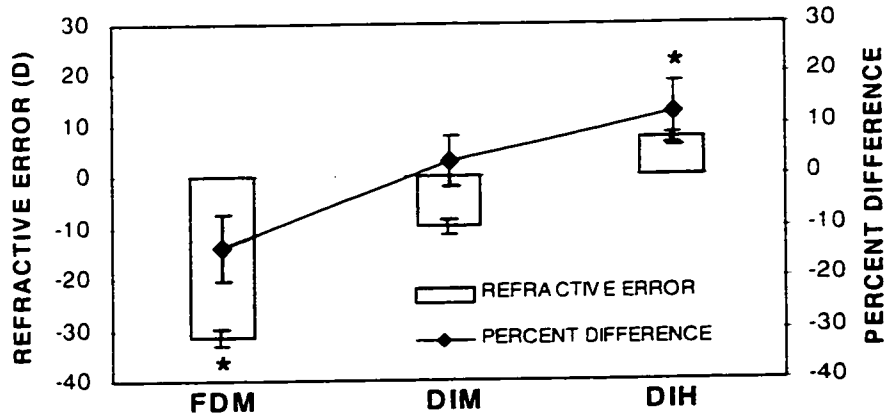

FIGURE 22: Change in serotonergic amacrine cell number is linearly correlated with the magnitude of the induced refractive error in the treated eye. The changes in cell number are represented as relative percent differences which indicate how much each treatment condition affected the cell populations relative to controls. Significant differences, in both refractive states and cell numbers, are shown by asterisks. Error bars indicate ± standard errors of the mean.

9.4.3 Possible mechanisms for serotonergic cell number changes

Various factors may account for the abnormal localized changes seen with respect to the number of serotonergic amacrine cells in the central retina. First, myopia and hyperopia may alter the normal baseline levels of endogenous serotonin production, accumulation, and release from these cells. If there were larger amounts of intracellular production and accumulation of serotonin, then immunohistochemical staining may reveal cells that had not previously been visible. Conversely, fewer cells would be immunohistochemically labelled if there were decreased intracellular production, increased release, or permeability changes that prevented the storage of serotonin.

Neurons within the chicken retina will readily take up exogenous serotonin via a high-affinity sodium dependent channel (Osborne 1984). It is believed that this re-uptake mechanism serves as the main route by which retinal serotonin's neurotransmitter and neuromodulatory functions are inactivated (Shaskan and Snyder 1970). If myopia and hyperopia affected the serotonergic re-uptake process, this may account for the observed changes in serotonergic cell numbers. Myopia and hyperopia may also influence intercellular communication between serotonergic amacrines and other cell types. Hence serotonin may pass into a cell which did not originally contain any indoleamine, in a similar manner to dopamine changing horizontal cell gap junction permeability, as seen by the passage of tracer dyes from one cell to another (Teranishi et al. 1984). Dopamine is also reported to modulate gap junction permeability between amacrine cells in mammalian retina (Edith et al. 1992). As mentioned previously, changes in cell numbers may also arise from neuronal redistribution resulting from active or passive migratory processes within the retina.

A final possibility is that myopia and hyperopia may respectively decrease or increase mitotic cell division. It has been generally accepted that within the adult retina or central nervous system, mitotic cell division no longer occurs after the final differentiation of progenitor neuroblasts. However, it is possible that alterations can be made during the window of development in which neural differentiation occurs. For instance, studies that examine retinal development of 1-day old normal postnatal mice have shown 23% of central cells and 37% of peripheral cells remain mitotically active, and that DNA synthesis continues for 6 days in the central retina, and up to 11 days in the periphery (Young 1985). In humans, the macula is immature at birth and post-natal development of the fovea region proceeds for at least four months (Duke-Elder 1963, Mann 1969). In other parts of the human visual pathway, refinement of

synaptic connections continues throughout the striate cortex until 2 years of age (Horton 1992). Hence the use of young chicks in this study provides an ideal opportunity to study any shifts in neural plasticity within the posthatch avian retina.

9.5 General retinal structure

Confocal microscopy was also used to examine other spatial relationships within the retina. Figures 15 and 16 show overlays of amacrines, bipolars, and photoreceptors. These images illustrate the relationship between different planes of retinal cells in a manner which would be difficult to achieve using traditional fluorescent microscopy. The digitized format of confocal images and availability of imaging software also facilitates quantitative measurements along the horizontal x-y plane and vertical z plane.

Twinning of serotonergic amacrine cell bodies was noted in various retinal specimens (Figure 17). The significance of this finding is not known. It may reflect intercellular passage of serotonin between adjacent cell bodies, perhaps via gap junctions (Vaney 1994). Another possibility is that cell division is occurring, reflecting a high degree of neural plasticity in the young chick retina. Twin amacrines were found on a regular basis in many retinal specimens, including control retinae and those in which all types of ametropias had been induced. Thus it appears these doublet amacrine somas naturally occur on a widespread basis within the normal avian retina, and do not affect the interpretation of cell count results.

9.6 Dendritic morphology

Within thick biological preparations, laser scanning confocal microscopy facilitates the acquisition and storage of an image series across a structure of interest that may be embedded deep

within a tissue specimen. During the course of this study, the confocal microscope was used to examine both dendritic field spreads (at low magnification) and individual dendritic morphology (at high magnification) of amacrine cells. To accomplish this, the confocal microscope was used to digitally acquire series of images across individual cells, along the vertical z axis of the retina. These image series were then stacked into colour-coded overlays to reveal the dendritic morphology of the dopaminergic, and to a lesser extent, serotonergic amacrine cells.

9.6.1 Dopaminergic amacrine cell morphology

9.6.1.1 Effects of induced myopia on dopaminergic amacrine cell morphology

The general trend for myopia to produce increased dendritic field spreads in dopaminergic amacrine cells appears to be correlated with the magnitude of the refractive error. Hence FDM produced the largest amount of dendritic field growth (Figure 18), while defocus-induced myopia invoked field changes to a lesser degree. This phenomenon likely occurred to maintain consistent coverage by the same number of cells across the enlarged retinal surface area. The observations from this study substantiate data previously reported by Teakle et al. (1993), where an increase in the dendritic field spreads of dopaminergic amacrines was noted in chick retina as a result of lid-suture myopia.

Higher magnification views of individual dopaminergic cells showed that FDM caused greater amounts of dendrites to appear within the first sublayer of the IPL, but there appeared to be minimal changes in the dendrites of sublayers 3 and 4 (Figure 19). This indicates that myopia provokes development of a greater amount of synapses within the "OFF" functional sublayer of the IPL. Although the synaptic connectivity of dopaminergic amacrine cells has been very well characterized in fish and mammals (Djamgoz and Wagner 1992), the neural connections in bird

and reptilian retinae are still poorly understood. A relevant summary of what is known about avian neurochemical connections to dopaminergic amacrine cells includes glycinergic, cholinergic, and ENSLI (enkephalin, neurotensin, and somatostatin) inputs in chick retina (Boelen et al.1994, Morgan and Boelen 1996). However, these studies derive most of their information from biochemical assays of retinal homogenates. Hence the particular regions of synaptic input onto avian dopaminergic cells within the IPL remain unclear, and ultrastructural analysis is required to elucidate particular synapses. It is thus difficult to extrapolate a functional significance for the observed increase of dopaminergic amacrine dendrites as a result of myopia.

One must also consider the possibility that synapses between cell types are not always necessary for the transmission of neurochemical effects. Dearry and Burnside (1988) have noted that dopamine can readily diffuse in culture medium, which suggests it may also act over long distances within the eye. Hence dopamine from retinal interplexiform or amacrine cells may affect distant tissues such as the RPE, without requiring any direct physical connection between the two regions. It may thus be more appropriate to examine host and target receptors for dopamine, rather than specific neural circuitry.

9.6.1.2 Effects of induced hyperopia on dopaminergic amacrine cell morphology

In contrast to the effects of myopia, defocus-induced hyperopia produced very consistent decreases in staining intensity, dendritic branching, and field size (Figure 20) of all dopaminergic amacrine cells in chick retina. High magnification comparisons of individual cells showed there were substantially fewer dendrites in the first, third, and fourth sublayers of the IPL (Figure 21). These correspond to synaptic connections in both "OFF" and "ON" functional sublayers of the IPL. The reduction in staining intensity may reflect various changes in cellular properties as a result of

treatment. For example, the dopaminergic amacrine cells may produce or store less dopamine than normal. Another possibility is that hyperopia provokes change in cell membrane permeability. Once again, it is difficult to extrapolate a functional meaning for the observed alterations in synaptic morphology, due to the lack of information about the particular synaptic connections between avian dopaminergic amacrines and other cell types.

9.6.2 Serotonergic amacrine cell morphology

The extremely dense branching patterns of serotonergic amacrine dendrites (Figure 14) makes it impossible to examine the individual morphology of these cells using regular immunohistochemical staining. In order to do so, it would be necessary to utilize techniques beyond the scope of this thesis. Suggested procedures include single cell dye injections into living retinal preparations (Vaney 1986), or more recently developed protocols, such as the targeted visualization technique for amacrine cells described by MacNeil and Masland (1998).

It was still useful, however, to create an overlay from optical confocal sections recorded along the z-axis of immunohistochemically stained serotonergic amacrine neurons. This provided a different viewpoint of dendritic lamination within the IPL retinal sublayers (Figure 14), confirming previous studies where frozen transverse cross-sections of chick retina were immunohistochemically labelled to reveal the synaptic layering of serotonergic amacrine cells (Floren 1979, Osborne 1982b).

9.7 Quantitative assessment of serotonin and dopamine levels by HPLC

9.7.1 Effects of ametropias on dopamine and DOPAC

The effects of FDM on retinal dopamine and DOPAC confirm what has been found previously by other workers (Stone et al. 1989, Ohngemach et al. 1997). In treated versus control eyes, there was a consistent overall decrease in dopamine and DOPAC quantities, and also a decrease in the DOPAC/DA ratios. Similar to previous reports, the effects on DOPAC levels were more pronounced, with a decrease for DOPAC that was two-fold in magnitude compared to dopamine. In addition, this study found that myopia caused localized changes in catecholamine quantities between specific portions of the treated and control retinae, with the most consistent decreases observed within the central retina. These results indicate that alterations in dopamine metabolism resulting from FDM may start centrally and extend peripherally during the course of ocular development.

Defocus-induced hyperopia (DIH) also provoked decreased levels of dopamine and DOPAC in a comparable manner to that produced by FDM. These observations differ from what was reported by Guo et al. (1995), apparently the only other comparable study, who found increased amounts of dopamine and DOPAC during lens-induced hyperopia. Ohngemach et al. (1997) remark that perhaps a change in cell volume to tissue volume may account for the results observed by Guo and colleagues, assuming that dopaminergic cell number remains constant after treatment (Teakle et al. 1993). In other words, the decrease in retinal volume may falsely translate into increased measurements of catecholamines, even if the actual levels of dopamine and DOPAC remain the same. This explanation does not account for the changes observed in the current study. Similar to what is reported by Teakle et al. (1993), cell count data from this thesis showed that dopaminergic cell numbers remained constant despite induced myopia or hyperopia. There were

no significant differences in axial length or vitreous chamber depth, although the former was slightly increased while the latter, which ultimately represents retinal surface area, was reduced (Table 13B). This study showed that decreased levels of dopamine and DOPAC occurred despite minimal changes in retinal dimensions. These decreases were very similar to what was observed in the case of myopia in terms of magnitude and distribution, namely within the temporal and central regions, and also when considering the whole eye by pooling all retinal segments together. Discrepancies between studies may be explained by differences in the magnitudes of induced refractive error, and differences in the protocols for the HPLC assays.

9.7.2 Effects of ametropias on serotonin and 5-HIAA

Despite optimization of the HPLC assay for measurement of indoleamines, assay variability was higher for serotonin and 5-HIAA measurements due to the extremely small quantities of these compounds, and the use of an external standard curve. The external standard curve was required in this assay due to lack of an appropriate internal standard (i.e. one that has a similar retention time, but which also elutes as a sharp and identifiable peak that is distinct from the indoleamine peaks). Despite these drawbacks, the HPLC assay performed in this study was better than what has been previously attempted by other researchers (Stone et al. 1989, Ohngemach et al. 1997) who used assay parameters that were optimized for catecholamines in order to measure indoleamines. For the current indoleamine-specific HPLC assay, the elution order of compounds was reversed. This provided a significant advantage because the shorter retention times allowed serotonin and 5-HIAA to pass through the column at a faster rate, and thus minimize possible degradation.

General trends were still noticeable from the data. Myopia caused slight decreases in serotonin and 5-HIAA quantities, while hyperopia caused slight increases. Hyperopia did cause

a very significant localized increase in the amount of 5-HIAA within the nasal retinal area. It is difficult to draw any firm conclusions from this data due to its inherent variability. However, these results do correlate with what was observed in the serotonergic cell count data presented earlier in this thesis, where myopia caused significant decreases in localized serotonergic cell counts, while hyperopia prompted increased cell counts. Since these preliminary HPLC experiments were conducted during the light phase when serotonin levels are normally low (Siuciak 1992), it would be worthwhile to pursue further studies about how ametropias affect retinal serotonin (both number of cells and amount of monoamine) in the middle of the dark cycle when indoleamine levels peak.

10.0 GENERAL DISCUSSION

10.1 Retinal neuron growth and plasticity

Changes in neural structure reflect changes in neural function. Change in neuron morphology is regulated by several factors, including the particular developmental stage, initial and final location of the cell, and the surrounding neural circuitry (Jessell 1991). The growth cone is the principle structure which regulates neural morphology and guides axonal development. The involvement of the growth cone in neural morphogenesis was first suggested by Cajal (1892), who noted that axons in the developing retina appeared to be guided by specific chemotaxic cues. The growth cone begins as an enlargement of the axonal shaft from which several finger-like filopodia emerge. Assembly and disassembly of actin and microtubule subunits within the leading edge of these filopodia allow the growth cone to both advance and retract.

The normal growth processes within any organism require remodeling of the nervous system, particularly during the early stages of development when most species rapidly increase in overall size and body weight. Within the retina, neurogenesis during embryological development

occurs in an organized and sequential manner, with neural connections being physically and chemically guided by one another (Jessell 1991). However, even when retinal neuron populations undergo their final round of cell division, giving rise to post-mitotic cells, there are many recorded instances where retinal cells exhibit further morphological change. In goldfish, Hitchcock (1987) has characterized the scaled enlargement of ganglion cells, which maintain constant coverage of the retina as the size of the fish eye increases due to normal growth. Retinal arborization of ganglion cells in older, larger fish show the same dendritic pattern, on a much bigger scale, as smaller versions of these cells in younger fish. This field expansion results from the addition of new dendrites, along with interstitial growth of existing dendrites. In cat, intercellular distance between retinal cells increases due to passive towing, but the amount of retinal stretch does not fully account for the expanded size of the cells (Mastronarde et al. 1984). It was concluded that active growth of new dendrites must also occur to supplement the passive stretching of dendritic arbours. In rat retina, differentiation and dendritic growth of catecholamine neurons continues post-natally for at least 15 days (Nguyen-Legros et al. 1983). Similar cases of neural plasticity reportedly occur in the retinae of other vertebrate species including birds.

10.2 Effects of serotonin on neural morphology

Previous studies show that serotonin may participate in neural growth, inhibition, and the development of functional neural circuitry. *Helisoma* is a snail species which is commonly used in neurobiological studies because its relatively simple nervous system contains easily identifiable serotonergic neurons associated with specific feeding and motor activities. These include buccal neurons 5, 19, and P5, each having distinct morphologies and characterized functions. Using elegant *in vitro* experiments, Haydon and Kater (1987) showed that each of these three neurons

have unique growth responses to the application of serotonin and dopamine in the culture medium. The growth cone development of neuron 19 was inhibited by separate applications of serotonin and dopamine, but was unaffected by serotonin precursors or metabolites such as 5-HTP and 5-HIAA. This shows that serotonin by itself has specific inhibitory actions on neural growth. On the other hand, growth of neuron P5 was inhibited by serotonin alone but not dopamine, while neuron 5 was unaffected by either monoamine.

There are many other reports of how serotonin affects neuronal architecture. For instance, serotonin enhances synapse formation within the young and adult chicken spinal cord (Chen et al. 1997). In kittens, neural plasticity of the visual cortex is reduced when serotonin transmission is blocked by antagonists such as 5,7-dihydroxytryptamine, ketanserin, and methysergide (Gu and Singer 1995). Hence serotonin acts in roles extending beyond its classical neurotransmitter functions, which involve neuron-specific regulation of dendritic morphology and connectivity.

10.3 Possible roles of dopamine and serotonin in refractive error development

The data from this study indicate that dopamine and serotonin may be involved in the mechanisms which control the development of refractive errors. The dramatic effects of induced myopia and hyperopia on dopaminergic cell dendritic morphology may perhaps be mediated by serotonin. This idea is consistent with numerous previous reports about the role of indoleamines in mediating plastic changes in synaptic architecture. In other species, serotonin has also been noted to facilitate dopamine release (Kato et al. 1983) and provide direct excitatory input to dopaminergic interplexiform cells (Massey and Redburn 1987). These proposed functional activities of serotonin would be compatible with the observed changes in dendritic appearance of dopaminergic amacrine cells in chick retina.

The link between the development of refractive errors and mediating compounds is not clear. Numerous studies suggest the participation of various substances which, among many others, include dopamine (Stone et al. 1989, Ohngemach 1997), vasoactive intestinal polypeptide (Stone et al. 1988), acetylcholine (Fischer et al. 1998a), fibroblast growth factor (Rohrer et al. 1994 and 1997), and retinoic acid (Mertz et al. 1998). A definitive causal link has not been found between any of these compounds and the abnormal growth mechanisms which characterize myopia and hyperopia. However, it is likely that multiple factors are involved. Schaeffel et al. (1995) found that application of 5,7-dihydroxytryptamine, a selective neurotoxin for serotonergic cells, enhances form deprivation myopia. Furthermore, Fischer and colleagues (1998b) noted that excitotoxic amino acids such as NMDA and quisqualic acid would produce myopia, after damage to various amacrine cell populations including those which contain serotonin. Their findings substantiate results in this study which suggest that indoleamines play a regulatory role in ocular growth, where decreased amounts of serotonin provoke myopia, and increased levels of serotonin produce hyperopia.

11.0 SUMMARY AND CONCLUSIONS

1. Form deprived retinae showed fewer serotonergic amacrine cells relative to control. Hyperopia caused higher numbers of serotonergic amacrine cells in treated eyes. Changes in serotonergic amacrine cell number displayed a near-linear correlation with the magnitude of induced refractive error. These findings suggest that indoleamines may play a role in ocular growth and the development of refractive errors. A possible hypothesis might be that abnormally low amounts of serotonin causes myopia, while high levels produce hyperopia.

2. Form deprivation myopia prompted increases in dendritic field spread and amount of dendritic branching of dopaminergic amacrine cells, most notably in the first sublayer of the inner plexiform layer. Conversely, hyperopia caused striking decreases in staining intensity, field size, and dendritic branching of dopaminergic amacrine cells relative to control. These decreases in the amount of dendrites were seen in the first, third, and fourth sublayers of the inner plexiform layer.

3. HPLC assays showed reduced quantities of retinal dopamine and DOPAC in form deprived retinae relative to control. Hyperopia evoked similar decreases in retinal dopamine and DOPAC levels within treated retinae. In both myopia and hyperopia, decreased retinal DOPAC/dopamine ratios indicated pronounced changes in catecholamine synthetic activity and release.

4. These results demonstrate that a high degree of neural plasticity exists within the young retina.

5. Changes in serotonergic amacrine cell numbers, dopaminergic dendritic morphology, and catecholamine levels, resulting from induced ametropias, appeared to be localized within the central retina. It is possible this reflects a faster rate of development in the posterior pole of the eye, and these changes may later progress to the peripheral retinal regions.

6. Confocal microscopy is a valuable technique that allows high-resolution and non-invasive examination of cell distribution and morphology, without disturbing the complex spatial relationships within wholemount retina specimens.

12.0 REFERENCES

Adler R and Farber D, editors (1986). The Retina: A Model for Cell Biology Studies, Part I. Cellular Neurobiology: A Series (Series editor: Sergey Federoff). Orlando: Academic Press, Inc., Harcourt Brace Jovanovich, Publishers.

Anderson DH, Williams DS, Deitz J, Fariss RN, and Fliesler SJ (1988). Tunicamycin-induced degeneration in cone photoreceptors. Visual Neuroscience, Vol. 1: 153-158.

Arlt F (1856). Die Krankheiten des Auges. Prague: Creder & Kleinbub, Vol. 3.

Baquis E (1890). La retina della faina. Anatomischer Anzeiger, Vol. 5: 366-371.

Barrington M, Sattayasai J, Zappia J, and Ehrlich D (1989). Differential effects of excitatory amino acids on eye growth in the posthatch chick. Current Eye Research, Vol. 8: 781-789.

Bartmann M, Schaeffel F, Hagel G, and Zrenner E (1994). Constant light affects retinal dopamine levels and blocks deprivation myopia but not lens-induced refractive errors in chickens. Visual Neuroscience, Vol. 11: 199-208.

Belkin M, Yinin N, and Rose L (1977). Effect of visual environment on refractive error of cats. Doc. Ophthalmologica, Vol. 42: 433.

Bennett AG and Rabbetts RB (1984). Clinical Visual Optics. London: Butterworths.

Binkley S, Macbride S, Klein D, and Ralph C (1973). Pineal enzymes: Regulation of avian melatonin synthesis. Science, Vol. 181: 273-274.

Bock G and Widdows K, editors (1990). Myopia and the Control of Eye Growth, Ciba Foundation Symposium, Volume 155. Chichester: John-Wiley & Sons.

Bodis-Wollner I and Piccolino M, editors (1988). Neurology and Neurobiology: Dopaminergic Mechanisms in Vision, Vol. 43. New York: Alan R. Liss, Inc.

Boelen MK, Wellard J, Dowton M, and Morgan IG (1994). Endogenous dopamine inhibits the release of enkephalin-like immunoreactivity from amacrine cells of the chicken retina in the light. Brain Research, Vol. 645: 240-246.

Boelen MK, Dowton M, and Morgan IG (1993). [Leu5]-enkephalin-like immunoreactive amacrine cells are under nicotinic excitatory control during darkness in chicken retina. Brain Research, Vol. 624: 137-142.

Boelen MK, Wellard J, Dowton M, Chubb IW, and Morgan IG (1991). Glycinergic control of [Leu5]-enkephalin levels in chicken retina. Brain research, Vol. 23: 221-226.

Borish IM. Chapters 1-5 in Clinical Refraction. 3rd edition. Chicago: Professional Press.

Bowmaker JK and Knowles A (1977). The visual pigments and oil droplets of the chicken retina. Vision Research, Vol. 17: 755-764.

Brecha NC (1983). Retinal neurotransmitters: Histochemical and biochemical studies. Chemical Neuroanatomy (Editor: PC Emson). New York: Raven Press. Pages 85-129.

Brunken WJ, Jin XT, and Pis-Lopez AM (1993). The properties of the serotoninergic system in the retina. Chapter 4 in Progress in Retinal Research, Vol. 12: 75-99.

Burnside N and Dearry A (1986). Cell motility in the retina. In The Retina: A Model for Cell Biology Studies, Part I. Cellular Neurobiology: A Series (Editors: R Adler and D Farber. Series editor: Sergey Federoff). Orlando: Academic Press, Inc., Harcourt Brace Jovanovich, Publishers.

Cajal, Santiago Ramon Y (1892). The Structure of the Retina. Springfield, Illinois: Charles C. Thomas Publishers (Compiled and translated by Sylvia A. Thorpe and Mitchell Glickstein, 1972).

Cavanaugh HD, Petroll WM, and Jester JV (1995). Confocal microscopy: Uses in measurement of cellular structure and function. Chapter 8 in Progress in Retinal and Eye Research (formerly Progress in Retinal Research), Vol. 14 (2): 527-565. Oxford: Pergamon Press.

Chen L, Hamaguchi K, Hamada S, and Okado N (1997). Regional differences of serotonin-mediated synaptic plasticity in the chicken spinal cord with development and aging. Journal of Transplantation and Neural Plasticity, Vol. 6 (1): 41-48.

Clark BJ (1985). The role of dopamine in the periphery. In The Dopaminergic System: Basic and Clinical Aspects of Neuroscience (Editors: E Fluckiger, EE Muller, MO Thorner). Berlin, Heidelberg: Springer Sandoz Advanced Texts, Springer-Verlag.

Cohn H (1866). Unter der Augen con 10060 Schulkindern nebst Vorsehlangen zur Verbesserung der Augen Nachteilligin Schuleinrichtungen. Leipzig: Eine Atiologische Studie.

Corrodi H and Jonsson G (1967). The formaldehyde fluorescence method for the histochemical demonstration of biogenic monoamines. A review on the methodology. Journal of Histochemistry and Cytochemistry, Vol. 15: 67-78.

Cottriall CL and McBrien NA (1996). The M1 muscarinic antagonist pirenzipine reduces myopia and eye enlargement in the tree shrew. Investigative Ophthalmology and Visual Science, Vol. 37 (7): 1368-1379.

Cronly-Dillon JR. editor (1991). Vision and Visual Dysfunction. Development and Plasticity of the Visual System. Vol. 11. Boca Raton: CRC Press.

Curtin BJ (1985). The Myopias: Basic Science and Clinical Management. Philadelphia: Harper & Row. Publishers.

Dearry A and Burnside B (1988). Dopamine induces light-adaptive retinomotor movements in teleost photoreceptors and retinal pigment epithelium. In Neurology and Neurobiology: Dopaminergic Mechanisms in Vision, Vol. 43 (Editors: I Bodis-Wollner and M Piccolino). New York: Alan R. Liss. Inc.

Demandolx D. Barois N. and Davoust J (1997). Guidelines for multifluorescence confocal imaging: Acquisition, processing and display. USA Microscopy and Analysis, Issue 25, July 1997. Surrey. England: Rolston Gordon Communications.

Diether S and Schaeffel F (1997). Local changes in eye growth induced by imposed local refractive error despite active accommodation. Vision Research, Vol. 37 (6): 659-668.

Djamgoz MBA and Wagner H-J (1992). Localization and function of dopamine in the adult vertebrate retina (Invited Review). Neurochemistry International, Vol 20 (2): 139-191.

Dogiel A (1883). Die Retina der Ganoiden. Arch. f. mikrosk. Anat., Vol. 22: 419-472.

Dogiel A (1891). Uber die nervosen Elemente in der Retina des Menschen. Arch. f. mikrosk. Anat., Vol. 38: 317-344.

Donders FC (1864). On the Anomalies of Accommodation and Refraction of the Eye. Translated by WD Moore. New Sydenham Society. Reprinted in 1979 by the Robert E. Krieger Publishing Company.

Dong CJ and McReynolds JS (1992). Comparison of the effects of flickering and steady light on dopamine release and horizontal cell coupling in the mudpuppy retina. Journal of Neurophysiology, Vol. 67: 354-372.

Dowling JE (1987) The Retina: An Approachable Part of the Brain. Cambridge, Massachusetts: The Belknap Press of Harvard University Press.

Duke-Elder S and Abrams D (1970). Chapter 7 in Ophthalmic Optics and Refraction, System of Ophthalmology, Vol. 5. St. Louis: C.V. Mosby.

Duke-Elder S and Cook C (1963). Normal and abnormal development, Part I: Embryology. System of Ophthalmology. London: Henry Kimpton Publishing.

Edith CGMH, Vaney DI, and Weiler R (1992). Dopaminergic modulation of gap junction permeability between amacrine cells in mammalian retina. The Journal of Neuroscience. Vol. 12 (12): 4911-4922.

Egger MD and Petran M (1967). New reflected-light microscope for viewing unstained brain and ganglion cells. Science, Vol. 157: 305-307.

Ehinger B, Hansson C, and Tornqvist K (1981). 5-hydroxytryptamine in the retina of some mammals. Experimental Eye Research, Vol. 33: 663-672.

Ehrlich D, Sattayasai J, Zappia J, and Barrington M (1990). Effects of selective neurotoxins on eye growth in the young chick. In Myopia and the Control of Eye Growth (Editors: G Bock, K Widdows), CIBA Foundation Symposium, Vol. 155. Chichester: John Wiley & Sons.

Ehrlich P (1886). Uber die Methyleneblaureaktion der lebenden Nerven-substanz. Deutsche medicinische Wodchenschrift, Vol. 12: 49-52. Berlin: Georg Reimer.

Enroth-Cugell C and Robson JG (1966). The contrast sensitivity of retinal ganglion cells of the cat. Journal of Physiology (London), Vol. 187: 517-552.

Famiglietti EV and Kolb H (1976). Structural basis for ON- and OFF-center responses in retinal ganglion cells. Science, Vol. 194: 193-195.

Fischer AJ, Miethke P, Morgan IG, and Stell WK (1998a). Retinal sources of acetylcholine (Ach) do not participate in visually guided ocular growth or atropine-mediated suppression of form deprivation myopia. Investigative Ophthalmology and Visual Science, Vol. 39 (4): S717.

Fischer AJ, Seltner RL, Poon J, and Stell WK (1998b). Immunocytochemical characterization of quisqualic acid- and N-methyl-D-aspartate-induced excitotoxicity in the retina of chicks. Journal of Comparative Neurology, Vol. 393 (1): 1-15.

Fischer AJ, Seltner RL, and Stell WK (1997). N-methyl-D-aspartate-induced excitotoxicity causes myopia in hatched chicks. Canadian Journal of Ophthalmology, Vol. 32 (6): 373-377.

Fliesler SJ, Rapp LM, and Hollyfield JG (1984). Photoreceptor-specific degeneration caused by tunicamycin. Nature, Vol. 311: 575-577.

Floren I and Hansson HC (1980). Investigations into whether 5-hydroxytryptamine is a neurotransmitter in the retina of rabbit and chicken. Investigative Ophthalmology and Visual Science, Vol. 19 (2): 117- 125.

Floren I (1979). Indoleamine accumulating neurons in the retina of chicken and pigeon. Acta Ophthalmologica, Vol. 57: 198-210.

Gabriel R, Zhu B, and Straznicky C (1992). Synaptic contacts of tyrosine hydroxylase-immunoreactive elements in the inner plexiform layer of the retina of *Bufo marinus*. Cell and Tissue Research, Vol. 267: 525-534.

Gardino PF, Ronal MDS, and Hokoc JN (1993). Histogenesis and topographical distribution of tyrosine hydroxylase immunoreactive amacrine cells in the developing chick retina. Developmental Brain Research, Vol. 72: 226-236.

Glasener G, Schmidt C, and Himstedt W (1988). Two populations of serotonin-immunoreactive neurons in the frog (*Rana esculenta*) retina. Neuroscience Letters, Vol. 84: 251-254.

Goodman GA, Rall TW, Nies AS, and Taylor P, editors (1991). Goodman and Gilman's: The Pharmacological Basis of Therapeutics. New York: Pergamon Press.

Gottlieb MD, Nickla DL, and Wallman J (1992). The effects of abnormal light/dark cycles in the development of form deprivation myopia. Investigative Ophthalmology and Visual Science, Vol. 33 (supplement): 1052.

Gottlieb MD, Fugate-Wentzek LA, and Wallman J (1987). Different visual deprivations produce different ametropias and different eye shapes. Investigative Ophthalmology and Visual Science, Vol. 28 (8): 1225-1234.

Grosvenor T and Flom MC, editors (1991). Refractive Anomalies: Research and Clinical Applications. Stoneham, MA: Butterworth-Heinemann.

Gu Q and Singer W (1995). Involvement of serotonin in developmental plasticity of kitten visual cortex. European Journal of Neuroscience, Vol. 7 (6): 1146-1153.

Guo SS, Sivak JG, Callender MG, and Diehl-Jones B (1995). Retinal dopamine and lens-induced refractive errors in chicks. Current Eye Research, Vol. 14: 385-389.

Hauschild DC and Laties AM (1973). An indoleamine-containing cell in chick retina. Investigative Ophthalmology, Vol. 12 (7): 537-540.

Haydon PG and Kater SB (1987). Novel roles for neurotransmitters: the regulation of neurite outgrowth, growth cone motility and synaptogenesis. Chapter 1 in Growth and Plasticity of Neural Connections (Editors: W Winlow, CR McCrohan). Manchester: Manchester University Press.

Haydon PG, McCobb DP, and Kater SB (1984). Serotonin selectively inhibits growth cone motility and synaptogenesis of specific identified neurons. Science, Vol. 226: 561-564.

Helmholtz HV (1856). Treatise on Physiological Optics, Vol. 1. English translation: Optical Society of America, New York, 1924.

Hirsch MJ and Weymouth FW (1991). Changes in optical elements: Hypothesis for the genesis of refractive errors. Chapter 3 in Refractive Anomalies: Research and Clinical Applications. Editors: T Grosvenor, C. Flom. Stoneham, MA: Butterworth-Heinemann.

Hitchcock PF (1987). Constant dendritic coverage by ganglion cells with growth of the goldfish's retina. Vision Research, Vol. 27 (1): 17-22.

Horton JM (1992). The central visual pathways. Chapter 23 in Adler's Physiology of the Eye, 9th edition. (Editor: William M. Hart, Jr.). St. Louis, Missouri: Mosby-Year Book, Inc.

Hubel DH, Wiesel TN, and Levoy S (1975). Functional architecture of area 17 in normal and monocularly deprived macaque monkeys. Cold Spring Harbor Laboratoy, Symposia on Quantitative Biology, Vol. 40: 581-589.

Hurd LB II and Eldred WD (1993). Synaptic microcircuitry of bipolar and amacrine cells with serotonin-like immunoreactivity in the retina of the turtle, *Pseudemys scripta elegans*. Visual Neuroscience, Vol. 10: 455-472.

Ingham CA and Morgan IG (1983). Dose-dependent effects of intravitreal kainic acid on specific cell types in chicken retina. Neuroscience, Vol. 9: 165-181.

Inoue S (1995). Foundations of confocal scanned imaging in light microscopy. Chapter 1 in Handbook of Biological Confocal Microscopy, 2nd edition (Editor: James B. Pawley). New York and London: Plenum Press.

Irving EL, Sivak JG, Curry TA, and Callender MG (1996). Chick eye optics: Zero to fourteen days. Journal of Comparative Physiology, Vol. 179: 185-194.

Irving EL (1993). Optically induced ametropia in young chickens. Doctoral dissertation, School of Optometry, University of Waterloo, Waterloo, Ontario, Canada.

Irving EL, Sivak JG, and Callender MG (1992). Refractive plasticity of the developing chick eye. Ophthalmic and Physiological Optics, Vol. 12: 448-456.

Irving EL, Callender MG, and Sivak JG (1991). Inducing myopia, hyperopia, and astigmatism in chicks. Optometry and Vision Science, Vol. 68 (5): 364-368.

Iuvone PM (1988). Dopamine: A light-adaptive modulator of melatonin synthesis in the frog retina. In Dopaminergic Mechanisms in Vision (Editors: I Bodis-Wollner, M Piccolino). New York: Alan R. Liss, Inc.

Iuvone PM, Galli CL, Garrison-Gund CK, and Neff NH (1978). Light stimulates tyrosine hydroxylase activity and dopamine synthesis in retinal amacrine cells. Science, Vol. 202: 901-902.

Jessell TM (1991). Cell migration and axon guidance. Chapter 58 in Principles of Neural Science, 3rd edition (Editors: ER Kandel, JH Schwartz, TM Jessell). New York: Elsevier Science Publishing.

Kandel ER, Schwartz JH, and Jessell TM, editors (1991). Principles of Neural Science, 3rd edition. New York: Elsevier Science Publishing, Co., Inc.

Kato S, Negishi K, and Teranishi T (1984). Embryonic development of monoaminergic neurones in the chick retina. Journal of Comparative Neurology, Vol. 224: 437-444.

Kato S, Negishi K, Teranishi T, and Sugawara K (1983). 5-hydroxytryptamine: Its facilitative action on [^{3}H] dopamine release from the retina. Vision Research, Vol. 23 (4) suppl.: 445-449.

Kee CS, Marzani D, and Wallman J (1998). Lens-compensation is not the same as form deprivation myopia. Investigative Ophthalmology and Visual Science, Vol. 39 (4): S715.

Kepler J (1611). Dioptrics. Ausburg: David Franke. As cited in Refractive Anomalies: Research and Clinical Applications (1991). Editors: T Grosvenor and MC Flom. Stoneham, MA: Butterworth-Heinemann).

King AS and McLelland J (1975). Special sense organs: Eye. Chapter 15 in Outlines of Avian Anatomy. New York: The Macmillan Publishing Company, Inc.

Kirsch M and Wagner H-J (1989). Release pattern of endogenous dopamine in teleost retinae during light adaptation and pharmacological stimulation. Vision Research, Vol 29: 147-154.

Kiyama H, Katayama-Kumoi Y, Kimmel J, Steinbusch H, Powell JF, Smith AD, and Tohyama M (1985). Three dimensional analysis of retinal neuropeptides and amine in the chick. Brain Research Bulletin, Vol. 15: 155-165.

Koch T (1973). Eye, *Organus visus*. Chapter 6 in Anatomy of the Chicken and Domestic Birds. Ames, Iowa: The Iowa State University Press (Edited and translated from German by Bernard H Skold and Louis DeVries).

Kramer SC (1971). Dopamine: A retina neurotransmitter I. Retinal uptake, storage, and light-stimulated release of H3-dopamine in vivo. Investigative Ophthalmology, Vol. 10 (6): 438-452.

Kuffler SW (1953). Discharge patterns and functional organization of mammalian retina. Journal of Neurophysiology, Vol. 16: 37-68.

Lauber JK and Kinnear A (1979). Eye enlargement in birds induced by dim light. Canadian Journal of Ophthalmology, Vol. 14: 265-269.

Lauber JK, Shutze JV, and McGinnis J (1961). Effects of exposure to continuous light on the eye of the growing chick. Proceedings of the Society for Experimental Biology and Medicine, Vol. 106: 871-872.

Laufer M, Negishi K, and Drujan BD (1981). Pharmacological manipulation of spatial properties of S-potentials. Vision Research, Vol. 21: 1657-1660.

Li T, Troilo D, Glasser A, and Howland HC (1995). Constant light produces severe corneal flattening and hyperopia in chickens. Vision Research, Vol. 35 (9): 1203-1209.

Li X-X, Schaeffel F, Kohler K, and Zrenner E (1992). Dose-dependent effects of 6-hydroxy dopamine on deprivation myopia, electroretinograms, and dopaminergic amacrine cells in chickens. Visual Neuroscience, Vol. 9: 483-492.

Lowry OH, Rosebrough NR, Farr LF, and Randall RS (1951). Protein measurement with the folin phenol reagent. Journal of Biological Chemistry, Vol. 193: 265-275.

MacNeil MA and Masland RH (1998). Extreme diversity among amacrine cells: implications for function. Neuron, Vol. 20: 971-982.

Malmfors T (1963). Evidence of adrenergic neurons with synaptic terminals in the retina of rats demonstrated with fluorescence and electron microscopy. Acta Physiologica Scandinavia, Vol. 58: 99-100.

Mann I (1969). The Development of the Human Eye. New York: Grune and Stratton, Inc.

Marc RE, Liu W-LS, Scholz K, and Muller JF (1988). Serotonergic and serotonin-accumulating neurons in the goldfish retina. Journal of Neuroscience, Vol. 8: 3427-3450.

Masland RH (1988). Amacrine cells. Trends in Neuroscience, Vol. 11 (9): 405-410.

Massey SC and Redburn DA (1987). Transmitter circuits in the vertebrate retina. Progress in Neurobiology, Vol. 28: 55-96.

Masters BR (1990). Confocal microscopy of ocular tissue. Chapter 11 in Confocal Microscopy (Editor: T. Wilson). London: Academic Press Limited.

Mastronarde DN, Thibeault MA, and Dubin M (1984). Non-uniform postnatal growth of the cat retina. Journal of Comparative Neurology, Vol. 228: 598-608.

May J and Thanos S (1992). Development of the visual system of the chick - A review. Journal fur Hirnforschung (Berlin), Vol. 6: 673-702.

McBrien NA, Moghaddam HO, Cottriall CL, Leech EM, and Cornell LM (1995). The effects of blockage of retinal cell action potentials on ocular growth, emmetropization and form deprivation myopia in young chicks. Vision Research, Vol. 35 (9): 1141-1152.

McBrien NA, Moghaddam HO, and Reeder AP (1993). Atropine reduces experimental myopia and eye enlargement via a nonaccommodative mechanism. Investigative Ophthalmology and Visual Science, Vol. 34 (1): 205-215.

Mertz JR, Nickla DL, Marzani D, and Wallman J (1998). Visual conditions alter choroidal retinoic acid synthesis potentially altering eye growth. Investigative Ophthalmology and Visual Science, Vol. 39 (4): S868.

Minsky M (1988). Memoir on inventing the confocal scanning microscope. Scanning, Vol. 10: 128-138.

Morgan IG and Boelen MK (1996). A retinal dark-light switch: A review of the evidence. Visual Neuroscience, Vol. 13: 399-409.

Morgan IG (1992). What do amacrine cells do? Progress in Retinal Research (Editors: Neville Osborne and Gerald Chader), Vol. 11: 193-214. Oxford: Pergamon Press.

Morgan WW and Kamp CW (1983). Effect of strychnine and of bicuculline on dopamine synthesis in retinas of dark-maintained rats. Brain research, Vol. 278: 362-365.

Morgan WW and Kamp CW (1980). A GABAergic influence on the light-induced increase in dopamine turnover in the dark-adapted rate retina *in vivo*. Journal of Neurochemistry, Vol. 34: 1082-1086.

Napper GA, Brennan NA, Barrington M, Squires MA, Vessey GA, and Vingrys AJ (1997). The effect of an interrupted daily period of normal visual stimulation on form deprivation myopia on chicks. Vision Research, Vol. 37 (12): 1557-1564.

Napper GA, Brennan NA, Barrington M, Squires MA, Vessey GA, and Vingrys AJ (1995). The duration of normal visual exposure necessary to prevent form deprivation myopia in chicks. Vision Research, Vol. 35 (9): 1337-1344.

Negishi K, Teranishi T, and Kato S (1985). Retinal growth in carp of the same age: density and number of dopamine neurons. Brain Research, Vol. 350(1-2): 125-131.

Nguyen-Legros J (1996). Retinal dopamine: Basic mechanisms and clinical implications. Chapter 14 in CNS Neurotransmitters and Neuromodulators: Dopamine. (Editor: Trevor W. Stone). Boca Raton, Florida: CRC Press.

Nguyen-Legros J and Savy C (1988). Dopamine innervation of the vertebrate retina: Morphological Studies. In Neurology and Neurobiology: Dopaminergic Mechanisms in Vision, Vol. 43. (Editors: Ivan Bodis-Wollner and Marco Piccolino). New York: Alan R. Liss, Inc.

Nguyen-Legros J, Vigny A, and Gay M (1983). Post-natal development of TH-like immunoreactivity in the rat retina. Experimental Eye Research, Vol. 37: 23-32.

Nichols CW, Jacobowitz D. and Hottenstein M (1967). The influence of light and dark on the catecholamine content of the retina and choroid. Investigative Ophthalmology, Vol. 6 (6): 642-646.

Norton TT and Rada JA (1995). Reduced extracellular matrix in mammalian sclera with induced myopia. Vision Research, Vol. 35 (9): 1271-1281.

Norton TT (1990). Experimental myopia in tree shrews. In Myopia and the Control of Eye Growth, Ciba Foundation Symposium, Volume 155 (Editors: G Bock and K Widdows). Chichester: John-Wiley & Sons.

Ohngemach S, Hagel G, and Schaeffel F (1997). Concentrations of biogenic amines in fundal layers in chickens with normal visual experience, deprivation, and after reserpine application. Visual Neuroscience, Vol. 14: 493-505.

Oishi T and Lauber JK (1988). Chicks blinded by formoguanamine do not develop lid suture myopia. Current Eye Research, Vol. 7 (1): 69-73.

Osborne NN (1984). Indoleamines in the eye with special reference to the serotonergic neurones of the retina. Chapter 3 in Progress in Retinal Research, Vol. 3: 61-103. (Editors: Neville Osborne and Gerald Chader). Oxford: Pergamon Press.

Osborne NN (1982a). Evidence for serotonin being a neurotransmitter in the retina. Chapter 16 in Biology of Serotonergic Transmission (Editor: NN Osborne). John Wiley & Sons.

Osborne NN (1982b). Uptake, localization and release of serotonin in the chick retina. Journal of Physiology, Vol. 331: 469-479.

Over R and Moore D (1981). Spatial acuity of the chicken. Brain Research, Vol. 211: 424-426.

Oyster CW, Takahashi ES, and Brecha NC (1988). Morphology of retinal dopaminergic neurons. In Neurology and Neurobiology: Dopaminergic Mechanisms in Vision, Vol. 43. (Editors: Ivan Bodis-Wollner and Marco Piccolino). New York: Alan R. Liss, Inc.

Parkinson D and Rando RR (1983). Effects of light on dopamine metabolism in the chick retina. Journal of Neurochemistry, Vol. 40: 39-46.

Parkinson D and Rando RR (1981). Evidence for a neurotransmitter role for 5-hydroxytryptamine in chick retina. The Journal of Neuroscience, Vol. 1 (11): 1211-1217.

Parnas I and Bowling D (1978). Killing of single neurons by intracellular injection of proteolytic enzymes. Nature, Vol. 270: 626-628.

Pawley JB, editor (1995). Handbook of Biological Confocal Microscopy. 2nd edition. New York: Plenum Press.

Piccolino M and Demontis G (1988). Dopaminergic system and modulation of electrical transmission between horizontal cells in the turtle retina. In Neurology and Neurobiology: Dopaminergic Mechanisms in Vision, Vol. 43 (Editors: I Bodis-Wollner M Piccolino). New York: Alan R. Liss, Inc.

Pickett Seltner RL and Stell WK (1995). The effect of vasoactive intestinal peptide on development of form deprivation myopia in the chick: A pharmacological and immunocytochemical study. Vision Research, Vol. 35 (9): 1265-1270.

Rapport MM, Green AA, and Page IH (1948). Serum vasoconstrictor (serotonin). IV. Isolation and characterization. Journal of Biological Chemistry, Vol. 176: 1243-1251.

Raviola E, Wiesel TN, Reichlim S, Lam KSI, and Chetri A (1991). Increase in retinal vasoactive intestinal peptide (VIP) after neonatal lid-fusion in the rhesus macaque. Investigative Ophthalmology and Visual Science, Vol. 32: 1203.

Raviola E and Wiesel TN (1978). Effect of dark-rearing on experimental myopia in monkeys. Investigative Ophthalmology and Visual Science, Vol. 17 (6): 485-488.

Redburn DA (1985). Serotonin neurotransmitter systems in vertebrate retina. Chapter 5 in Retina Transmitters and Modulators: Models for the Brain. Vol. II. (Editor: W.W. Morgan). Boca Raton. Florida: CRC Press.

Remington LA (1998). Clinical Anatomy of the Visual System. Boston: Butterworth-Heinmann.

Rohrer B. Tao J. and Stell WK (1997). Basic fibroblast growth factor, its high- and low-affinity receptors. and their relationship to form deprivation myopia in the chick. Neuroscience, Vol. 79 (3): 775-787.

Rohrer B. Iuvone PM. and Stell WK (1995). Stimulation of dopaminergic amacrine cells by stroboscopic illumination or fibroblast growth factor (bFGF, FGF-2) injections: possible roles in prevention of form-deprivation myopia in the chick. Brain Research, Vol. 686: 169-181.

Rohrer B and Stell WK (1994). Basic fibroblast growth factor (bFGF) and transforming growth factor beta (TGF-B) act as stop and go signals to modulate postnatal ocular growth in the chick. Experimental Eye Research, Vol. 58: 553-562.

Rohrer B. Spira AW. and Stell WK (1993). Apomorphine blocks form-deprivation myopia in chickens by a dopamine D_2-receptor mechanism acting in retina or pigmented epithelium. Visual Neuroscience, Vol. 10: 447-453.

Rose L, Yinon U, and Belkin M (1974). Myopia induced in cats deprived of distance vision during development. Vision Research, Vol. 14: 1029-1032.

Roth RH (1979). Tyrosine hydroxylase. Chapter 9 in The Neurobiology of Dopamine. (Editors: AS Horn, J Korf, BHC Westerink). London: Academic Press.

Sandell JH and Masland RH (1986). A system of indoleamine-accumulating neurons in the rabbit retina. Journal of Neuroscience, Vol. 6 (11): 3331-3347.

Schaeffel F, Bartmann M, Hagel G, and Zrenner E (1995). Studies on the role of the retinal dopamine/melatonin system in experimental refractive errors in chickens. Vision Research, Vol. 35 (9): 1247-1264.

Schaeffel F, Hagel G, Bartmann M, Kohler K, and Zrenner E (1994). 6-Hydroxy dopamine does not affect lens-induced refractive errors but suppresses deprivation myopia. Vision Research, Vol. 34 (2): 143-149.

Schaeffel F, Troilo D, Wallman J, and Howland HC (1990). Developing eyes that lack accommodation grow to compensate for imposed defocus. Visual Neuroscience, Vol. 4: 177-183.

Schaeffel F, Glasser A, and Howland HC (1988). Accommodation, refractive error and eye growth in chickens. Vision Research, Vol. 28 (5): 639-657.

Schaeffel F and Howland HC (1988). Mathematical model of emmetropization in the chicken. Journal of the Optical Society of America A, Vol. 5 (12): 2080-2086.

Schaeffel F, Howland HC, and Farkas L (1986). Natural accommodation in the growing chicken. Vision Research, Vol. 26: 1977-1993.

Schwahn HN and Schaeffel F (1997). Flicker parameters are different for suppression of myopia and hyperopia. Vision Research, Vol. 37 (19): 2661-2673.

Shaskan EG and Snyder SH (1970). Kinetics of serotonin accumulation into slices from rat brain: relationship to catecholamine uptake. Journal of Pharmacology and Experimental Therapeutics, Vol. 175: 404-418.

Sheppard CJR and Choudhury A (1977). Image formation in the scanning microscope. Optica, Vol. 24: 1051.

Sherman SM, Norton TT, and Casagrande VA (1977). Myopia in the lid-sutured tree shrew. Brain Research, Vol. 124: 154-157.

Siuciak JA, Gamache PA, and Dubocovich ML (1992). Monoamines and their precursors and metabolites in the chicken brain, pineal, and retina: Regional distribution and day/night variations. Journal of Neurochemistry, Vol. 58: 722-729.

Sivak JG, Barrie DL, Callender MG, Doughty MJ, Seltner RL, and West JA (1990). Optical causes of experimental myopia. In Myopia and the Control of Eye Growth (Editors: G Bock, K Widdows), CIBA Foundation Symposium, Vol. 155. Chichester: John Wiley & Sons.

Steiger A (1913). Die Entstehung der spharischen Refracktionen des menschilichen Auges. Berlin: S Karger.

Stell WK (1972). The morphological organization of the vertebrate retina. Chapter 3 in Handbook of Sensory Physiology, Vol. VII/2 Physiology of Photoreceptor Organs (Editor: MGF Fuortes). Berlin, Heidelberg: Springer-Verlag.

Stone RA, Lin T, Desai D, and Capehart C (1995). Photoperiod, early post-natal eye growth, and visual deprivation. Vision Research, Vol. 35 (9): 1195-1202.

Stone RA, Lin T, and Laties AM (1991). Muscarinic antagonist effects on experimental chick myopia. Experimental Eye Research, Vol. 52: 755-758.

Stone RA, Lin T, Iuvone PM, and Laties AM (1990). Postnatal control of ocular growth: Dopaminergic mechanisms. In Myopia and the Control of Eye Growth (Editors: G Bock, K Widdows). CIBA Foundation Symposium, Vol. 155. Chichester: John Wiley & Sons.

Stone RA, Lin T, Laties AM, and Iuvone PM (1989). Retinal dopamine and form-deprivation myopia. Proceedings of the National Academy of Science USA, Vol. 86: 704-706.

Stone RA, Laties AM, Raviola E, and Wiesel TN (1988). Increase in vasoactive intestinal polypeptide after eyelid fusion in primates. Proceedings of the National Academy of Sciences USA, Vol. 85 (1): 257-260.

Stone T, editor (1996). CNS neurotransmitters and neuromodulators: Dopamine. Boca Raton, Florida: CRC Press, Inc.

Su YY and Watt CB (1987). Interaction between enkephalin and dopamine in the avian retina. Brain Research, Vol. 423 (1-2): 63-70.

Suzuki E, Noguchi E, Miyake S, and Yagi K (1976). Occurrence of 5-hydroxytryptamine in chick retina. Experientia, Vol. 33: 927-928.

Teakle E, Wildsoet CF, and Vaney DI (1993). The spatial organization of tyrosine immunoreactive amacrine cells in the chicken retina and the consequences of myopia. Vision Research, Vol. 33 (17): 2383-2396.

Teranishi T, Negishi K, and Kato S (1984). Regulatory effect of dopamine on spatial properties of horizontal cells in carp retina. Journal of Neuroscience, Vol. 4: 1271.

Troilo D, Tong L, Glasser A, and Howland HC (1995). Differences in eye growth and the response to visual deprivation in different strains of chicken. Vision Research, Vol. 35 (9): 1211-1216.

Troilo D and Wallman J (1991). The regulation of eye growth and refractive state: An experimental study of emmetropization. Vision Research, Vol. 31 (7/8): 1237-1250.

Troilo D, Gottlieb MD, and Wallman J (1987). Visual deprivation causes myopia in chicks with optic nerve section. Current Eye Research, Vol. 6 (8): 993-999.

Twarog BM and Page IH (1953). Serotonin content of some mammalian tissues and amine and a method for its determination. American Journal of Physiology, Vol. 174: 157-161.

Vaney DI (1994). Patterns of neuronal coupling in the retina. Chapter 12 in Progress in Retinal and Eye Research (Formerly Progress in Retinal Research. Editors: Neville Osborne and Gerald Chader). Vol. 13 (1): 301-355. Oxford: Pergamon Press.

Vaney DI (1986). Morphological identification of serotonin-accumulating neurons in the living retina. Science. Vol. 233: 444-446.

Vogt M (1973). Functional aspects of the role of catecholamines in the central nervous system. British Medical Bulletin. Vol. 29: 168-172.

Von Graefe A (1857). Beitrage zur Physiologie und Pathologie der scheifen Augenmuskeln. Albrecht Con Graefes Arch Ophthlamol, Vol. 28: 163.

Walker RJ (1986). Biosynthesis, storage and release of dopamine. In The Neurobiology of Dopamine Systems (Editors: W Winlow, R Markstein). Manchester, U.K.: Manchester University Press.

Wallman J, Wildsoet C, Xu A, Gottlieb MD, Nickla DL, Marran L, Krebs W, and Christensen AM (1995). Moving the retina: Choroidal modulation of refractive state. Vision Research, Vol. 35 (1): 37-50.

Wallman J and Adams JA (1987). Developmental aspects of experimental myopia in chicks: Susceptibility, recovery and relation to emmetropization. Vision Research, Vol. 27 (7): 1139-1163.

Wallman J, Gottlieb MD, Rajaram V, and Fugate-Wentzek LA (1987). Local retinal regions control local eye growth and myopia. Science, Vol. 237: 73-77.

Wallman J, Turkel J, and Trachtman J (1978). Extreme myopia produced by modest change in early visual experience. Science, Vol. 201: 1249-1251.

Walls, GL (1942). The Vertebrate Eye and Its Adaptive Radiation. New York: Hafner Publishing Company (reprinted 1963).

Weiss S and Schaeffel F (1993). Diurnal growth rhythms in the chicken eye: Relation to myopia development and retinal dopamine levels. Journal of Comparative Physiology A, Vol. 172: 263-270.

White JG, Amos WB, and Fordham M (1987). An evaluation of confocal versus conventional imaging of biological structures by fluorescence light microscopy. The Journal of Cell Biology, Vol. 105: 41-48.

Wiesel TN and Raviola E (1979). Increase in axial length of the macaque monkey eye after corneal opacification. Investigative Ophthalmology and Visual Science, Vol. 18 (12): 1232-1236.

Wildsoet CF and Wallman J (1995). Choroidal and scleral mechanisms of compensation for spectacle lenses in chicks. Vision Research, Vol. 35 (9): 1175-1194.

Wildsoet CF and Pettigrew JD (1988a). Experimental myopia and anomalous eye growth patterns unaffected by optic nerve section in chickens: Evidence for local control of eye growth. Clinical Vision Sciences, Vol. 3 (2): 99-107.

Wildsoet CF and Pettigrew JD (1988b). Kainic acid-induced eye enlargement in chickens: Differential effects on anterior and posterior segments. Investigative Ophthalmology and Visual Science, Vol. 29 (2): 311-319.

Wilhelm M, Zhu B, Gabriel R, and Straznicky C (1993). Immunocytochemical identification of serotonin-synthesizing neurons in the vertebrate retina: A comparative study. Experimental Eye Research, Vol. 56: 231-240.

Wilson KT, Sivak JG, and Callender MG (1997). Induced refractive anomalies affect chick orbital bone structure. Experimental Eye Research, Vol. 64: 675-682.

Wilson T, editor (1990). Confocal Microscopy. London: Academic Press Limited.

Witkovsky P and Dearry A (1991). Functional roles of dopamine in the vertebrate retina. Chapter 10 in Progress in Retinal Research, Vol. 11: 247-291. (Editors: Neville Osborne and Gerald Chader). Oxford: Pergamon Press.

Witkovsky P. Stone S. and Besharse J (1987). Dopamine mimics light-adaptation in horizontal cells of the Xenopus retina. Society of Neuroscience Abstracts, Vol. 13: 24.

Yinon U and Koslowe KC (1986). Hypermetropia in dark reared chicks and the effect of lid suture. Vision Research, Vol. 26 (6): 999-1005.

Young FA and Leary GA (1991). Refractive error in relation to the development of the eye. Chapter 2 in Vision and Visual Dysfunction, Visual Optics and Instrumentation, pages 29-44. (Series editor: W Neil Charman. General editor: JR Cronly-Dillon). Boca Raton: CRC Press.

Young RW (1985). Cell proliferation during postnatal development of the retina in the mouse. Brain Research, Vol. 353 (2): 229-239.

IMAGE EVALUATION
TEST TARGET (QA-3)

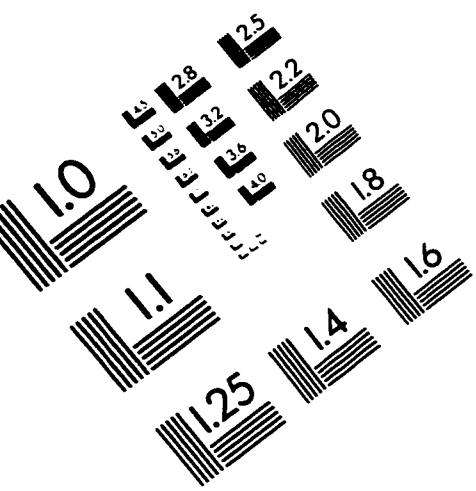

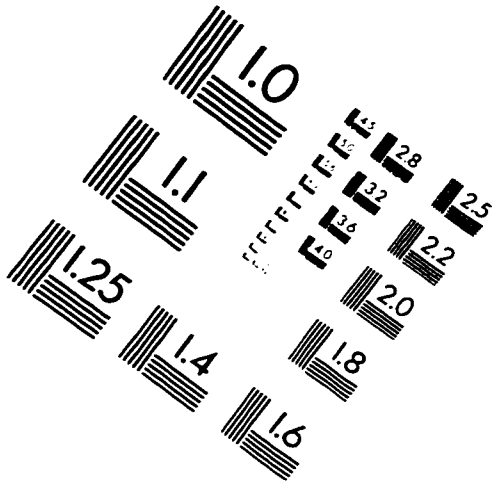

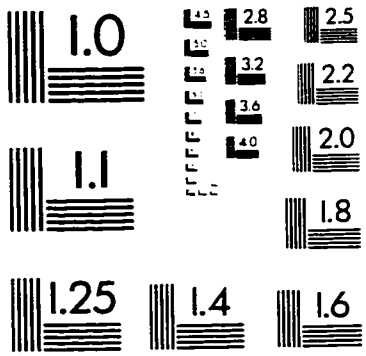

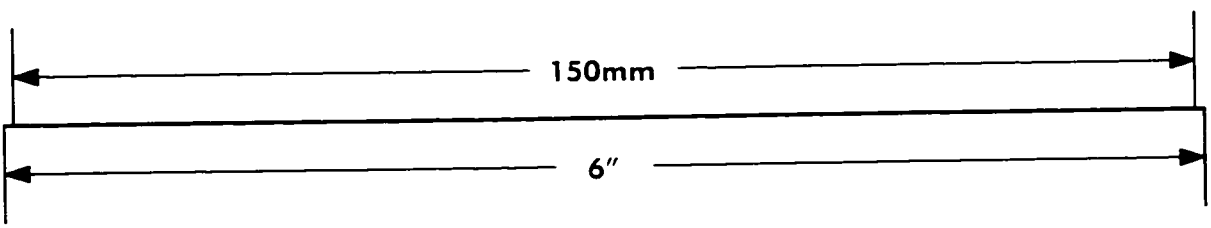

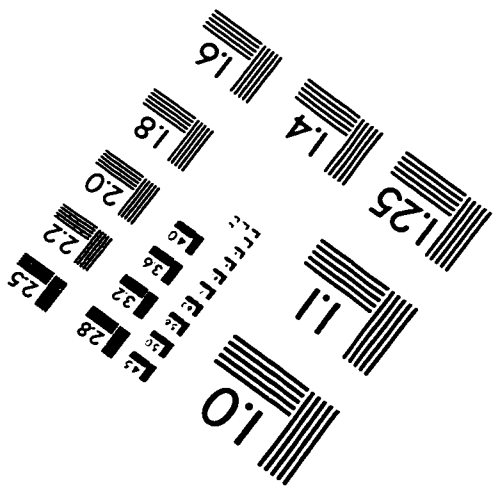

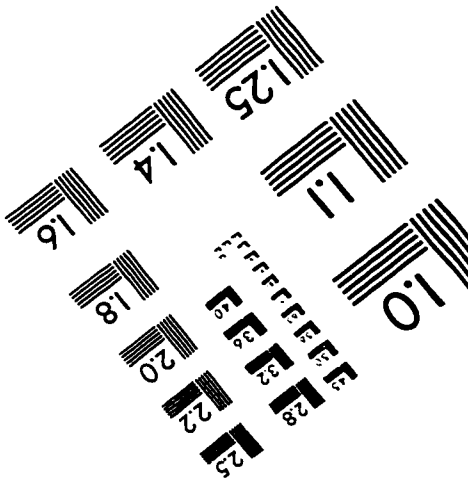

APPLIED IMAGE, Inc
1653 East Main Street
Rochester, NY 14609 USA
Phone: 716/482-0300
Fax: 716/288-5989